UNIVERSITY OF
KWAZULU-NATAL
INYUVESI
YAKWAZULU-NATALI

LIQUID-LIQUID EXTRACTION OF NEODYMIUM

by

Thulani Bayeni

BSc. Eng.

Submitted in fulfilment of the academic requirements of

Master of Science in Engineering

School of Engineering, Chemical Engineering

College of Agriculture, Engineering and Science

University of KwaZulu-Natal

Durban

South Africa

January 2022

Preface

The research contained in this thesis was completed by the candidate while based in the Discipline of Chemical Engineering, School of Engineering of the College of Agriculture, Engineering and Science, University of KwaZulu-Natal, Howard College, South Africa.

The contents of this work have not been submitted in any form to another university and, except where the work of others is acknowledged in the text, the results reported are due to investigations by the candidate.

_____

Signed: Professor P. Naidoo

Date:

_____

Signed: Dr. M. Williams-Wynn

Date:

_____

Signed: Dr. K. Moodley

Date:

Statement of Authorship

I, Thulani Bayeni, declare that:

(i) The research reported in this dissertation, except where otherwise indicated, is my original work.

(ii) This dissertation has not been submitted for any degree or examination at any other university.

(iii) This dissertation does not contain other persons' data, pictures, graphs or other information, unless specifically acknowledged as being sourced from other persons.

(iv) This dissertation does not contain other persons' writing, unless specifically acknowledged as being sourced from other researchers. Where other written sources have been quoted, then:

a. Their words have been re-written but the general information attributed to them has been referenced;

b. Where their exact words have been used, their writing has been placed inside quotation marks, and referenced.

(v) This dissertation does not contain text, graphics or tables copied and pasted from the internet, unless specifically acknowledged, and the source being detailed in the thesis and in the references sections.

_____

Signed: Thulani Bayeni

Date: January 2022

Declaration

The following paper that has a link with this dissertation is in the process of being written:

- Bayeni, T., Williams-Wynn*, M., Naidoo, P., Durski, M. and Moodley, K., n.d. The Distribution coefficients of Nd^{3+} between HNO_3 and HDEHP. Unpublished

Acknowledgements

I would like to acknowledge and give thanks to the following:

Prof P. Naidoo, Dr. M. Williams-Wynn, for their constant guidance throughout this project; ever-present and ready to impart the knowledge and wisdom to improve the quality of the work presented in this dissertation and Dr K. Moodley for his invaluable inputs to bring this work to completion.

The technical staff of the Discipline of Chemical Engineering for their assistance in and training in the use of laboratory equipment.

My parents, whose academic paths and personal lives have been an example worth following. My brother and sister, for their support and also my family for their steadfast emotional guidance before and during the duration of this degree.

My colleagues N. Khosa and N. Siwela for their encouragement through word and deed.

And most importantly to the God through whom all things exist and under whose instruction all principles, scientific and otherwise, stand.

Abstract

Neodymium is classified as a rare earth element (REE). These elements possess a unique set of optical, electrochemical and magnetic properties that allow for their use in electronics manufacturing, medicine, catalysis and clean technologies. The global neodymium supply from primary source mining is isolated to a few countries, therefore developing technologies to recover neodymium and other rare earth elements from electronic waste is an emerging research area with economic incentive. The readiness of these technologies for industrial implementation is dependent on data for the extraction of neodymium from aqueous acidic solution into an organic phase for recovery. The available literature on these processes is limited.

To address the gaps in the available literature, in this study, the distribution coefficient of neodymium in liquid-liquid equilibrium systems was measured across a range of nitric acid concentrations (0.1 – 2.9 M). The distribution coefficient is a measure of the affinity of a solute for the organic solvent to the aqueous phase. The extractant solutions used were composed of various concentrations of phosphorous acid diluted with n-dodecane. The tested extractant solutions are 0.1, 0.5 and 1 M of di(-2-ethylhexyl)phosphoric acid in n-dodecane. To investigate possible enhancements to the performance of the extractant, trace amounts of the ionic liquids (ILs) 1-butyl-3-methylimidazolium bis(trifluoromethylsulfonyl)imide (at concentrations of 0.019 and 0.19 M) and tributylmethylphosphonium methyl sulfate (at concentrations of 0.01, 0.1 and 0.25 M) were added to the organic extractant (0.5 M HDEHP in n-dodecane). The distribution coefficient data obtained for an extractant concentration of 0.5 M HDEHP was also used to determine its performance in a liquid-liquid extraction column by way of elementary mass balance calculations.

The experiments performed in this study were undertaken using a bank of 6 stirred equilibrium cells immersed in a water bath maintained at a temperature of 298.15 K. Each vessel was filled with 5 ml of the aqueous and the organic solutions and mixed vigorously for 12 hours before being allowed to gravimetrically settle for 8 hours. Samples of the aqueous phase were withdrawn from the vessels, diluted using de-ionised water and analysed by way of inductively coupled plasma optical emission spectroscopy (ICP- OES). The equilibrium acid concentration of these samples was measured using acid-base titrations with 0.1 M sodium hydroxide solution. In this work the distribution coefficient data of 10 unique systems are presented, 2

test systems to validate the experimental method and 8 unique configurations of nitric acid concentration and extractant composition.

The analysis of the distribution coefficient of neodymium showed that neodymium has an inversely proportional relationship to the aqueous [H^+] concentration, established by the nitric acid concentration. For the HDEHP in n-dodecane extractant, the maximum distribution coefficient calculated was 274.26 at a nitric acid concentration of 0.2701 M with the 1.0 M HDEHP in n-dodecane. In the ionic liquid doped systems the maximum calculated distribution coefficients were 158.70 at a nitric acid [H^+] concentration of 0.1161 M 1-butyl-3-methylimidazolium bis(trifluoromethylsulfonyl)imide doped extractant and 23.454 at an aqueous acid concentration of 0.0974 M when neodymium was extracted with the 1-butyl-3-methylimidazolium bis(trifluoromethylsulfonyl)imide doped extractant. The degree of extraction achievable by the addition of ILs is either decreased or increased, based on the concentration and species of ionic liquid. It was found that when ILs are used to enhance phosphorus acid extractant solutions, phase separation within the extractant occurs readily, decreasing the precision of measurements by more than 10%.

The calculations for a liquid-liquid extraction column were performed based on a solution of neodymium and iron in nitric acid media extracted using 0.5 M HDEHP in n-dodecane. The results showed that neodymium with a solvent free purity of 96.75% by mass could be obtained using a column in which the extractant to volumetric feed flow ratio is 3.2. It is recommended that further distribution coefficient studies be undertaken to provide insight into the distribution behaviour of multiple ion-containing systems when extracted with IL containing synergistic extractant solutions.

Nomenclature

Names and Abbreviations

$18C_6$	18-crown-6
[A336][CA-100]	[Trialkylmethyl- ammonium][Sec-nonylphenoxyacetate]
Bu_2Et_2	Dibutyl(diethylcarbamoylmethyl)phosphine Oxide
$BMImNTf_2$	1-butyl-3-methylimidazolium Bis(trifluoromethylsulfonyl)imide
CMPO	Octyl(phenyl)-N,N-diisobutylcarbamoylmethyl Phosphine Oxide
Cyanex 272	Di (2,4,4-trimethylpentyl)phosphinic Acid
Cyanex 925	Bis(2,4,4-trimethylpentyl)octylphosphine Oxide
Cyphos IL 104	Trihexyl(tetradecyl)phosphonium Bis(2,4,4-trimethylpentyl)phosphinate
D_2EHPA	Di(2-ethylhexyl)phosphoric Acid
$DB_{18}C_6$	Dibenzo-18-crown-6, $15C_5$: 15-crown-5
$DC_{18}C_6$	Cis-dicyclohexano- 18-crown-6
DEHP	Thiamine Triphosphate
DMDOHEMA	N,N'-dimethyl-N,N'-dioctylhexylethoxymalonamide
DODGAA	N, N-dioctyldiglycolamic Acid
EHEHPA	2-ethylhexyl Phosphonic Acid Mono-2-ethylhexyl
HCl	Hydrochloric Acid
HDEHP	Di-(2-ethylhexyl)phosphoric Acid
HNO_3	Nitric Acid
Htta	2-thenoyltrifluoroacetone
HYD	1-hydroxy-2,5-pyrrolidinedione
LLE	Liquid-Liquid Equilibium
NfO	Nonafluorobutanesulfonate
NiMH	Nickel Metal Hydride
PAN	1-(2-pyridyl- azo)-2-naphthol

Names and Abbreviations

PC-88A	2-ethylhexyl Phosphonic Acid-mono-2-ethylhexyl ester
Ph_2Et_2	Diphenyl(diethylcar- bamoylmethyl)phosphine Oxide
REE	Rare Earth Element
REM	Rare Earth Metal
REO	Rare Earth Oxide
SOFC	Solid Oxide Fuel Cell
TALSPEAK	Trivalent Actinide Lanthanide Separation with Phosphorus-Reagent Extraction from Aqueous Komplexes
TBP	Tributyl Phosphate
THTP	Thiamine Triphosphate
TODGA	N,N,N',N'-tetra(n-octyl)diglycolamide
TPEN	N,N,N’,N’-tetrakis(2-pyridylmethyl)ethylenediamine
TPMDPO	Tetraphenylmethylenediphosphine Dioxide
TRUEX	Transuranium Extraction
TSIL	Task-specific Ionic Liquids
UN	United Nations
USA	United States of America
VPE	Vibrating Plate Extraction Column

Symbols

A	Organic Ion
$\overline{A}$	Aggregate Molecule
β	Separation Factor
D_M	Distribution Coefficient of species M
E	Extractant Feed Flow Rate
g	Gram
ε_i	Noise
F	Aqueous Feed Flow Rate
j	Ion Transfer Flux
k_B	Boltzmann Constant

Symbols

κ^*	Generalised Bending Constant of a Molecule
$\overline{LH}$	Monomeric Form of the Extractant Molecule
$\overline{LH_2}$	Dimeric Form of the Extractant Molecule
Ln	Any Rare Earth Element
[M]	Mass Concentration of M in the Aqueous Phase
$[\bar{M}]$	Mass Concentration of M in the Organic Phase
N	Stoichiometric Coefficient
NO_3^-	Nitrate Anion
p_0	Intrinsic Spontaneous Packing Parameter
R	Aggregation Number
R^2	Coefficient of Determination
R_a^2	Adjusted Coefficient of Determination
θ_0	Regression Equation Intercept
θ_i	Regression Equation Gradient
μ°_{Agg}	Standard Chemical Potentials of Aggregate
X	Aqueous Solution Flow Rate
χ_{LH,L^-}	Exchange Parameter

Subscripts and Superscripts

n	LLE Separation Column Stage Number
w	Stripping Solution
-	Anionic Species
+	Cationic Species

Table of Contents

List of Figures

List of Tables

Chapter 1: Introduction

Rare earth elements (REEs) refer to the lanthanoid series in the third row of the periodic table of the elements. This includes scandium (Sc), yttrium (Y), lanthanum (La) and the 14 elements following La (Xie *et al.*, 2014). REEs are generally claimed to be some of the most important chemical elements, used in elemental form, due to their unique set of optical, electronic and magnetic properties that allow for their application in electronics manufacturing, medicine, catalysis and numerous clean technologies. Their place in the advancement of these spheres has been investigated and documented in reports by the European Commission (2011), UN Environment Programme and UN University (2009), and US Department of Energy (2011). In 2014 the European Commission highlighted REEs as having the highest supply risk among 41 different raw materials (European Commission, 2014; Tunsu *et al.*, 2015).

The critical designation assigned to REEs availability is linked primarily to their high demand which increases alongside the fast expansion of their applications. In some cases, these applications require specific components, e.g., cerium oxide as a polishing agent for glass, terbium for use in laser repeaters (USGS, 2002), or neodymium used in permanent magnets. In 2015 the five most in-demand REEs for green energy applications were neodymium, dysprosium, europium, yttrium and terbium (Ronda et al., 1998; Tunsu et al., 2015); a situation which likely will remain unchanged in the future (see Figure 1.1). The future of renewable technologies hinges upon the availability of REEs for their use in wind turbine magnets, smartphone components and electric vehicle cells.

The 'rare' in the name *rare earth elements* is somewhat misleading as it implies a scarcity in the natural abundance of the elements but, ore deposits containing multiple lanthanoids are fairly abundant in the earth's crust. Lead, whose abundance in the earth's crust is 0.0016%, is in fact less common than light REEs (lanthanum, cerium, and neodymium) (Fleischer, 1954). Even thulium and lutetium, considered the less abundant REEs, are 100 times more abundant in the earth's crust than gold (USGS, 2002; Tunsu *et al.*, 2015). However, REE ore deposits are dispersed, sparsely located and rarely found in concentrations that can be economically exploited (Xie *et al.*, 2000).

Lanthanoids occurring in nature together often exhibit similar chemical properties increasing the complexity of the processes required for their separation. Hence, they are often, categorised

into four groups of similar physiochemical properties (La-Ce-Pr-Nd, Pm-Sm-Eu-Gd, Gd-Tb-Dy-Ho and Er– Tm–Yb–Lu), (Jones, Wall and Williams, 1996; Wang, Pranolo and Cheng, 2011).

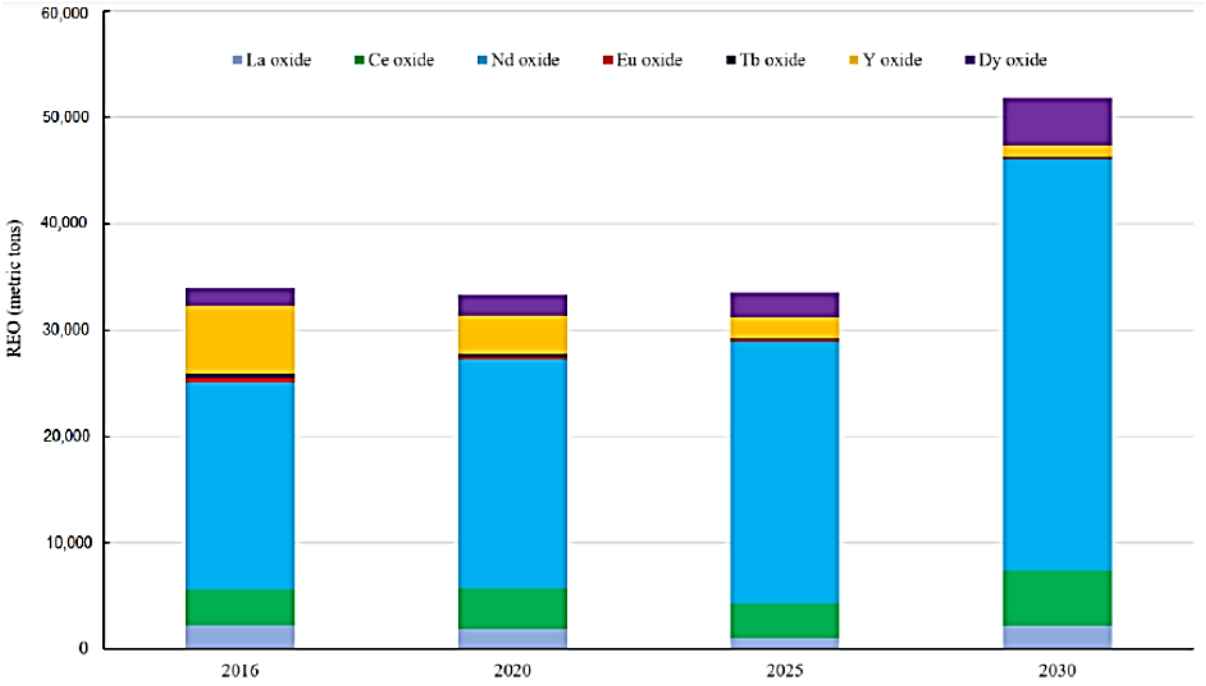

Figure 1.1 Demand for Rare Earth Oxides (REO) in 2016, 2020, 2025 and 2030 (Zhou, Li and Chen, 2017)

The degree of dispersion of REEs in the earth's crust raises multiple challenges in so far as their virgin extraction and processing are concerned:

1. Firstly, the mining of rare earth metals for single-use products is unsustainable as the naturally occurring reserves of these metals are finite.
2. The undesirable environmental and social impacts of mining activity would become intensified with the 700% predicted increase in the demand for neodymium over the next 25 years (Alonso *et al.*, 2012; Atwood, 2013).
3. The occurrence of multiple REEs together in the same deposits introduces complexity into processes aimed at separating the elements. In addition to REEs occurring as groups, they often exist alongside uranium or thorium decay chains, which can potentially cause radiotoxicity necessitating additional regulations that could accompany the processing of such materials (Kilbourn, 1994; Tunsu *et al.*, 2015).

Nevertheless, a variety of processing routes are available for the recovery of REEs from mined ore. Subsequent to mining and communition, ores can be beneficiated by floatation, magnetic or gravimetric methods. These methods produce rare earth concentrates which are subsequently processed using hydrometallurgical methods to recover the REEs. (Xie *et al.*, 2014; Krishnamurthy and Gupta, 2016).

Europium, yttrium and terbium are used in conjunction with lanthanum, cerium and gadolinium in phosphors to produce low-energy fluorescent lamps (Davris *et al.*, 2016). Neodymium, yttrium, cerium, lanthanum and praseodymium are used in the manufacture of nickel-metal hydride (NiMH) batteries used in hybrid vehicles. Scandium possesses significant economic value, particularly with its prominent use in solid oxide fuel cells (SOFCs). Yttrium-scandium garnets are used in solid-state lasers and the range of use of Al-Sc alloys span from the aerospace industry to sports equipment (Ahmad, 2003, Davris *et al.*, 2016).

Neodymium is also used for the manufacturing of permanent magnets. These magnets are used in cellphones, wind turbines, hard disk drives (HDDs), magnetic resonance imaging equipment and hybrid cars (Atwood, 2013; Tunsu *et al.*, 2015; Millsaps, 2018). The magnets contain mainly neodymium, iron and boron but dysprosium, praseodymium, gadolinium and terbium can also be found in them (Gergoric, Barrier and Retegan, 2018). The price of neodymium was USD66200 per metric ton by the end 2021, but in the past fifteen years it has reached a low of USD15427 in 2009 and a high of USD250574 in 2011 (Statista, 2022).

The world's supply of neodymium comes primarily from China, which provides 90-95% of global demand, making the cost and availability of the resource particularly vulnerable to political events (Gergoric *et al.*, 2018).

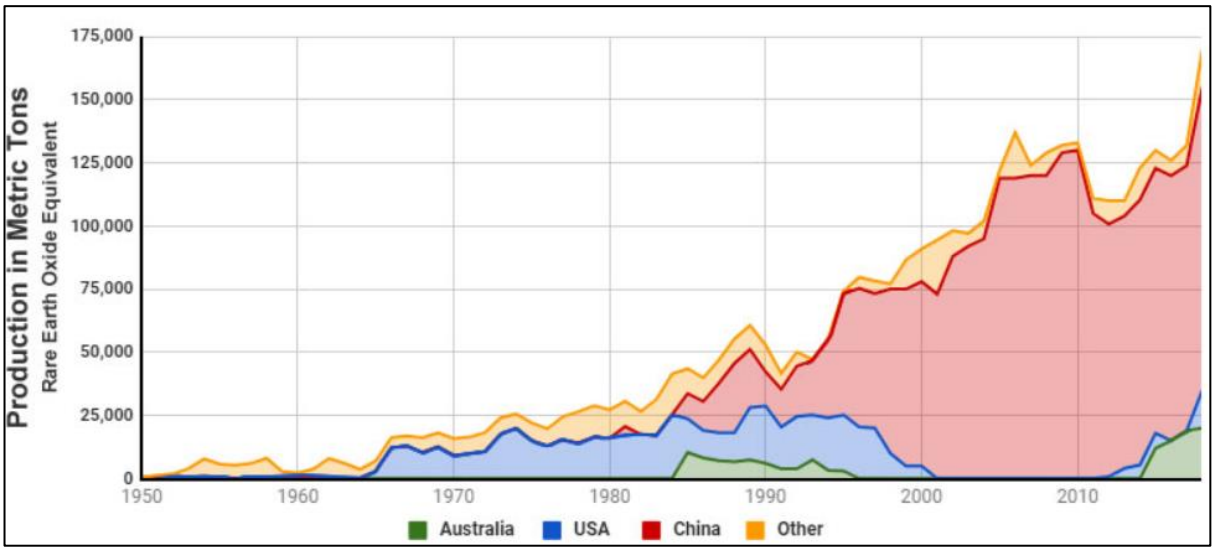

Figure 1.2 The Global production of REEs by country from 1950 (King, 2020)

Mines operating for the purpose of extracting REE containing ores from deposits have been operating since the 1950s (King, 2020). In the 1990s, China began producing cheaper REEs on a considerable scale, as seen in Figure 1.2. The producers in the rest of the world were unable to compete in the market with depressed prices, making them unprofitable and leading to their closure in the 1990s. The near-monopolistic control over the REE market by China has resulted in significant price fluctuations. This monopoly has driven a search for new deposits of REEs and has fast-tracked plans to exploit other known deposits including the re-opening of Mountain Pass mine (Nevada, USA) in 2012 (Chen, 2010; Tunsu *et al.*, 2015).

Urban mining, the "*management of anthropogenic resources stocks and waste (products and buildings), in the view of long-term environmental protection, resource conservation, and economic benefits*" is a concept that is beginning to gain traction (Cossu, 2013; Tunsu *et al.*, 2015). Waste from electronic and electrical equipment (WEEE) along with other waste streams (e.g., construction, demolition and landfilled wastes; exhaust oils; combustion and industrial residues; sludges, and others) are the targets of urban mining to obtain a range of materials (Tunsu *et al.*, 2015). Processing these waste streams for the recovery of the REEs they contain, could prove to be a new exploitable deposit of metals. However, urban mining cannot be expected to entirely replace the extraction and processing of virgin minerals (Tunsu *et al.*, 2015). The imbalance between the demand for raw materials and the availability of recyclable streams, as well as the difficulty of processing waste material, is a leading cause of this. Urban mining, however, can be a tool in the arsenal of the environmental conservation effort to

prevent excessive mining. The widespread adoption of urban mining could also contribute to the mitigation of some of traditional mining's drawbacks particularly in the time it takes to discover and exploit new/already existing deposits (Tunsu *et al.*, 2015). Furthermore, the recovery of REEs from waste electronics can help stabilise markets and possibly lower the cost of the material for countries in which REEs are not indigenous (Binnemans *et al.*, 2013).

It is expected that waste containing neodymium-based magnets will increase in the future, making the recovery of REEs from this waste an attractive prospect. In 2011 less than 1% of REEs were recycled and as of 2019, 12% of electronic waste was being recycled (Binnemans *et al.*, 2013; Balaram, 2019). REE products produced from mining are at purities greater than 99%. Solvent extraction methods for the recovery of these REEs have been shown to produce products with purities of up to 99.9% (Haque *et al.*, 2014; Gruber and Carsky, 2020).

Neodymium magnets can be reused if they have been made to standard sizes at the point of production or if the magnets are large and easily accessible (Binnemans *et al.*, 2013). Direct reuse is the least investigated method of recycling rare earth magnets (Hogberg *et al.*, 2017). Should standardised size magnets be available, direct reuse would require that the magnets first be demagnetised through high energy input. The magnet assembly would also be required to withstand the thermal expansion coefficients of the different materials (Hogberg *et al.*, 2017). Magnets of the reusable persuasion are not readily available as the design of equipment, in many cases, is not suited for their use (Binnemans *et al.*, 2013).

The demand for permanent magnets has increased significantly in the past few decades. This increase in demand is due to the development of novel technological devices, such as green energy production via wind turbines, and alterations in existing ones (HDDs, mobile phones, headphones, speakers). Neodymium-iron-boron (NdFeB) magnets are the most common REE-based magnets (Coey, 2012). These contain primarily neodymium, iron and boron alongside small amounts of dysprosium, praseodymium, gadolinium, or terbium as shown in in parts per million along with the uncertainties as provided by Xu *et al.*, *(*2000). The elements within these magnets form molecules in a tetragonal crystalline structure, with oxides on the grain boundary layers.

Table 1.1 Compositions of NdFeB magnets.[1]

Nd (wt %)	Fe (wt %)	B (wt %)	Pr (wt %)	Dy (wt %)	C (ppm)	N (ppm)	O (ppm)
18.00[2]	72.40[3]	0.90	1.82	5.30	0.0336	29.00	343.0

[1] (Xu *et al.*, 2000); Uncertainties: [2] (±1.00); [3] (±0.70)

Hard disk drives (HDDs) are a vital source of REEs from waste electronic and electrical equipment (WEEE) recycling due to their abundance. Six hundred million HDDs were manufactured in the year 2008. Each HDD contained in the region of 20g sintered NdFeB (Tunsu *et al.*, 2015). HDDs accounted for only 25% of the global production of sintered NdFeB magnets in 2018. Taking the lifespan of an HDD to be 5 years as well as the trend of hardware upgrading, the availability of end-of-life products as a primary material for REE recovery is not a concern in the near future (Tunsu *et al.*, 2015).

For the recovery of REEs from magnets, pyrometallurgical and hydrometallurgical routes can be considered, with the latter being the most common. Previous studies (Xu, Chumbley and Laabs, 2000; Gruber and Carsky, 2020) focused on relatively clean magnets and not magnets from end-of-life consumer products mixed with materials such as shredder residues. The magnet alloys were dissolved in strong mineral acids, and REEs are selectively precipitated as sulphates, oxalates or fluorides. This method requires large volumes of chemicals. Even with the use of selective leaching methods, the leaching of materials other than the intended REE occurs, necessitating a separation step prior to the leachate entering a REE separation plant (Binnemans *et al.*, 2013).

Pyrometallurgical routes for the processing of REE magnets are more energy-intensive, although they use less chemicals than hydrometallurgical routes. The pyrometallurgical routes include liquid metal extraction, electro-slag refining and the glass slag method (Binnemans *et al.*, 2013). Ionic liquids however, offer an attractive potential to make hydrometallurgical solvent extraction methods more efficient. Ionic liquids could replace the organic phase in liquid-liquid extractions resulting in safer systems due to their low volatility (Baba *et al.*, 2011). However, data on the degree of improvement achievable is not readily available in the openly published literature.

The original scope of this work proposed experimental work on the recovery of REEs from permanent magnets as the factors affecting this recovery is not well established in the literature. However, due to the constraints placed on research activities by the COVID-19 pandemic in 2020, many changes were made to the work plan. The decision was made to evaluate the distribution coefficients of REEs from solutions prepared from synthetic rare earth oxides instead of the dissolution of permanent neodymium magnets, and investigate the parameters that affect the distribution. Neodymium (the primary constituent of NdFeB permanent magnets, see Table 1.1) in the powered form of neodymium oxide is the primary REE used in the experiments carried out in this work. These tests were then used to design extraction experiments based on REE magnets in subsequent work within the broader project scope conducted by other members of the research team.

1.1 Aim and objectives

The aim of this study is to measure the distribution coefficients at equilibrium of neodymium from an aqueous nitric acid phase to an organic phase. These measurements can then be used to assess the performance of the extractant solutions extraction systems. The objectives of the study are:

1. Perform the distribution coefficient measurements of a test system with europium oxide at nitric acid concentrations of 0.1-2.0 M and an organic phase concentration of 0.25 M HDEHP in n-dodecane to validate the experimental method.
2. To measure the distribution coefficients for yttrium between varying nitric acid solutions (0.2-3.0 M) and an organic extractant with a concentration of 1.0 M HDEHP in n-dodecane as a further test system.
3. To measure the distribution coefficients for neodymium at varying nitric acid solutions (0.1-2.9 M) and varying organic extractant concentrations (0.1 M, 0.5 M, 1.0 M HDEHP in n-dodecane).
4. Investigate the effect of the addition of the ionic liquids, (1-butyl-3-methylimidazolium bis(trifluoromethylsulfonyl)imide and tributylphosphonium methyl sulfate) at trace concentrations (< 0.25 M) on the distribution coefficient.
5. To predict the separation behaviour of a neodymium and iron containing feed in an LLE separation column and investigate the effect of the number of extraction stages, the number of stripping stages and the ratio of the organic extractant to feed ratio on the purity of neodymium obtainable.

This thesis comprises 7 chapters. The literature review presented in chapter 2 discusses investigations into hydrometallurgical processes on the recovery of REEs and the thermodynamic relations that govern these processes. Chapter 3 discusses the experimental methodology applied by other researchers. The experimental method employed in this study is covered in Chapter 4 with the results and discussion following in the 5th chapter. The thesis concludes with conclusions and recommendations in Chapters 6 and 7, respectively.

Chapter 2: Review of the Thermodynamic Principles (REE Separation and Recovery)

This chapter presents a review of the available literature with details of the chemical components and the theoretical principles that govern their behaviour in systems where the separation and recovery of REEs are concerned. The recovery of REEs using hydrometallurgical techniques (particularly those exploiting liquid-liquid equilibria (LLE)) is the primary focus of this review due to its relevance to this study. The thermodynamic principles that govern the LLE for phosphorous acids (the focus of this thesis) are discussed while presenting the models that can be used to describe the process and subsequently predicting its behaviour. The categories of solvents investigated in literature to achieve similar separations as this study are also presented and discussed. The models describing processes using solvation and anion exchanging extractants are not discussed in detail as a part of this work. The reader may refer to Xie *et al.*, (2014) for more information on this topic.

2.1 Hydrometallurgical separation

The process of REE solvent extraction refers to the separation of the different groups of REE from the leachate. The similar physical and chemical properties of REE clusters make them difficult to separate from each other (Xie *et al.*, 2014). Separation processes with the ability to yield high purity REE solutions and compounds continue to be developed based on ion exchange and solvent extraction techniques. Prior to the introduction of large-scale solvent extraction in the 1960s, the only practical method for the separation of REEs in large quantities was ion exchange technology (Reddy *et al.*, 2009). However, recent use of ion exchange technology has been reserved for applications in which small quantities of high purity REE are required. Consensus exists in that solvent extraction is the most feasible technology for separating REEs in commercial settings due to the large volumes of dilute REE-containing liquors that require handling (Peppard *et al.*, 1953; Peppard *et al.*, 1957a; Peppard and Wason, 1958; Xie *et al.*, 2014).

Several physical and chemical phenomena can be exploited to achieve the separation of similar REEs from each other. The most prominent of these factors is the lanthanide contraction, which can be described as the decrease in the ionic radii of the REEs along the lanthanide series (McLennan, 1994). This decrease in ionic radii affects the strength of the complexes that

REEs form in aqueous solutions. The chemical characteristics displayed by the sub-structures of REEs enable the recovery of REEs in groups of adjacent elements. This behaviour is called the *tetrad-effect* and was first discussed by Peppard *et al., (*1969). Even when taking these differences in chemical behaviour into account, complete separation of adjacent elements on a large scale has remained economically challenging and would require many separation stages (Tunsu *et al.*, 2015).

2.2 Extractants

Reddy *et al.*, (1995) reviewed solvent extraction methods for the purpose of separating and purifying REEs. The authors discussed the considerable work done in the 1990s investigating the effect of the variation of the extractant species on the separation and purification of REEs. Three major classes of extractants: cation exchangers (or acidic extractants), solvation extractants (or neutral extractants), and anion exchangers (or basic extractants) have been proposed for REE separation applications (Xie *et al.*, 2014). A summary of the studied commercial extractants is presented in Table 2.1 (Xie *et. al*, 2014). Table 2.1 also shows the relative costs of these extractants. In Table 2.1, multiple abbreviations are used for the sake of conciseness. The complete chemical names of abbreviations used in tables can be found in the nomenclature as well as where they appear in the sections discussed thereafter.

Table 2.1 Types of Reagents based upon the work of Xie et al.[1]

Reagents class	Structure	Extractants	Cost
Carboxylic acids	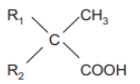	Versatic acids: R1 + R2 = C_7, Versatic 10; R1 + R2 = C_6–C_8, Versatic 911	USD367,09 /kg[a] .
	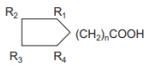	Naphthenic acids: R1-R4: varied alkyl groups	USD119,12 /kg[b]
Phosphorous acids	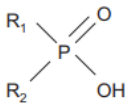	Phosphoric acids: R1 = R2 = $C_4H_9CH(C_2H_5)CH_2O$–, (HDEHP) Phosphonic acids: R1 = $C_4H_9CH(C_2H_5)CH_2O$–, R2 = $C_4H_9CH(C_2H_5)CH_2$–, (EHEHPA, HEHEHP, P507, PC88A) Phosphinic acids: R1 = R2 = $C_4H_9CH(C_2H_5)CH_2$–, (P229) R1 = R2 = $CH_3(CH_2)_3CH_2CH(CH_3)CH_2$–, (Cyanex 272)	USD372.32 /kg[c]
	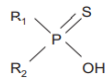	Monothiophosphorous acids R1 = R2 = $CH_3(CH_2)_3CH_2CH(CH_3)CH_2$–, (Cyanex 302)	USD55.13 /kg[d]
	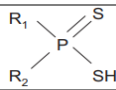	Dithiophosphorous acids R1 = R2 = $CH_3(CH_2)_3CH_2CH(CH_3)CH_2$–, (Cyanex 301)	USD1.10 /kg[e]
Solvating extractants	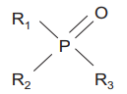	Phosphorous ester: R1 = R2 = R3 = $CH_2(CH_2)_2CH_2O$–, (TBP) R1 = R2 = $CH_2(CH_2)_2CH_2O$–, R3 = $CH_2(CH_2)_2CH_2$–, (DBBP) Phosphine oxides: R1 = R2 = R3 = $CH_2(CH_2)_6CH_2$–, (TOPO, Cyanex 921)	USD1244,45 /kg[f]
Anion exchanger	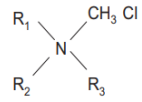	Primary amines: R = $(CH_3)_3C(CH)_2C(CH_3)_2)_4$ (Primene JMT, N1923) Quaternary amines: R1 = R2 = R3 = C_8–C_{10} mixture (Aliquat 336, Adogen 464)	USD257.83 /kg[g]

[a](Molbase.com, 2020), [b](TCI Chemical, 2020), [c](Sigmaaldrich.com, 2020a), [d](Xie, 2020), [e](Chemicalbook.com, 2020), [f](Sigmaaldrich.com, 2020b), [g](Sigma-Aldrich, 2020c). [1](Xie *et al*., 2014)

Table 2.2 presents information to gain insight into extractants used for the recovery of REEs. Futher details are expanded in Table 3.1 (see Chapter 3) which is an extensive summary of relevant published works reviewed. The details of the selected process in the table are discussed in Chapter 3.1.2 and in Appendix A The studies displayed are ordered primarily by the process used to study the REEs and subsequently according to their chronology. Wherever "(-)" appears in the table, it indicates that this information was not reported in the published work.

Table 2.2 Summary of selected articles on the extraction/recovery of REEs

	REE	Source	Recovery Process	Chemicals	
				Extractant	***REE Solvent***
a	Nd	NdFeB magnets	Liquid metal Extraction	Molten Mg (99.8%)	(-)
b	Eu and La	$Eu(NO_3)_3$ $La(NO_3)_3{\cdot}6H_2O$	TREUEX, TALSPEAK	HDEHP, CMPO	HNO_3
c	La, Ce, Pr, Nd, Sm, Eu, Gd, Tb, Dy, Ho, Er, Tm, Yb and Lu	Chlorides or nitrates	LLE	DEHPA, EHEHPA	(-)
d	Pr, Nd, Yb and Er	(-)	LLE	HDEHP (97 wt.%)	(-)
e	Yb and Lu	Yb_2O_3	LLE	HDEHP+ cyclohexane	(-)
f	La, Ce, Pr, Nd and Eu	Nitrate forms	LLE	D2EHPA (0.05M)	HNO_3
g	Am, Cm, Cf and Fm	10 ppm standard solutions	LLE	HDEHP in benzene (0.08 – 1.0M)	HNO_3
h	La, Ce, Pr, Nd, Sm, Gd, Tb, Dy, Ho, Yb, Lu and Eu	Nitrate Salts	LLE	TOMA, THTP, DEHP, HDEHP	(-)
i	Y, La, Ce and Eu	Waste Fluorescent Lamps	LLE	DODGAA	HCl, H_2SO_4 (50mM)
j	Th and U	(-)	LLE	CMPO	HNO_3 (0.1 – 7.0M)
k	Am, Eu	Pure radioactive tracer	LLE	TODGA (1M), HDEHP (0.25M) in n-Dodecane	HNO_3 (various)
l	Ce, La, Y, Sc, Pr, Nd, Sm, Gd, Er, Dy and Yb	Bauxite residue	LLE	$HbetTf_2N$ (97%)	(-)
m	Eu	$Eu(NO_3)_3{\cdot}6H_2O$ salts	LLE	DMDOHEMA (varying) HDEHP (varying)	HNO_3
n	Y, La, Ce, Pr, Nd, Sm, Eu, Gd, Tb, Dy, Ho, Er, Tm, Yb and Lu	REE ore	LLE	HEH(EHP) HDEHP	H_2SO_4
o	Y and Eu	Oxides	LLE	HDEHP (varying)	HNO_3
p	Dy, Nd and Pr	NdFeB magnets	LLE	HDEHP	H_2SO_4 (1.5-2M)

[a]Xu, Chumbley and Laabs (2000), [b]Tkac *et al., (*2012), [c]Sato (1989), [d]Hino *et al., (*1997), [e]Lahari *et al., (*1998), [f]Geist *et al.* 1999, [g]Takayama *et al., (*2011), [h]Sun *et al.*, (2012), [i]Yang *et al., (*2013), [j]Turanov *et al., (*2013), [k]Nayak *et al., (*2014), [l]Davris *et al., (*2016), [m]Rey *et al., (*2016), [n]Huang *et al., (*2017), [o]Williams-Wynn *et al.*, (2020), [p]Gruber and Carsky (2020)

2.2.1 Carboxylic and Phosphoric Acid Extractants

Carboxylic and phosphoric acids are both classified as cation exchangers (Xie *et al.* 2014). Systems that employ the use of carboxylic acids as extractants (see Table 2.1) have been investigated by the U.S. Department of Energy (1963), Korpusov *et al., (*1974) and Zheng *et al.*, (1991). Versatic acids are highly branched non-polar alkyl group natural intermediates used in the production of polymers, displaying excellent hydrolytic stability and resistance to heat. Versatic acids have exceptional solubility characteristics in non-polar compounds, for example, solvents, organic polymers and plastics (Hexion, 2015). Carboxylic acids are particularly useful in the selective extraction of Y^{3+} from other REEs (Zheng *et al.*, 1991). The market for carboxylic acids is stated to be healthy and sustained, making them an attractive prospect for use in industrial processes that might require large volumes of these components (Parker *et al.*, 2020).

The extraction potential of phospho-acidic extractants, have been investigated by Geist *et al., (*1999), Takayama *et al., (*2011), Nayak *et al., (*2014), Williams-Wynn *et al.*, (2020) and others in optimized concentration ranges as described in Table 2.2. The most widely used phosphor-acidic extractants are di-(2-ethylhexyl)phosphoric acid (HDEHP) and 2-ethylhexyl ester (HEHEHP) (Xie *et al.*, 2014). The molecular structures of these extractants are shown in Table 2.1. The onset of saturation effects occurs at heavier loadings for HEHEHP than HDEHP. This increases the extraction efficiency (Xie *et al.,* 2014). The immiscibility that phosphorous acids display with HCl, HNO_3 and H_2O make them suitable candidates for LLE with aqueous mixtures. When this property is considered along with the solute solubility and separation factor displayed for various REEs in this medium it strengthens the case for their suitability for application in LLE systems (Korkisch, 1969; Nilsson and Nash, 2007). The supply chain necessary to produce phosphorus acids is currently stable, however concerns over phosphorous reserves have arisen in the past and if proven significant could pose a threat to the long-term stability of the phosphorous acid markets (Carrington, 2019; Foskor - Home, 2020).

Peppard *et al.,* (1957a) noted that the distribution coefficients exhibited by tracer ions of REEs between HDEHP in aqueous chloride solutions and toluene solutions displayed an inverse third-power dependency on the HCl concentration in the aqueous phase and a third-power dependency on the HDEHP concentration in the organic phase. This indicates the dissociation and participation of a single acid group in an HDEHP dimer in the organic phase of the extraction reaction. Gelatinous substances were observed to form in the organic

phase at the conditions of high metal loadings and low acidities. The formation of these gelatinous substances is undesirable due to the viscosity and phase separation considerations introduced by their presence (Xie *et al.*, 2014).

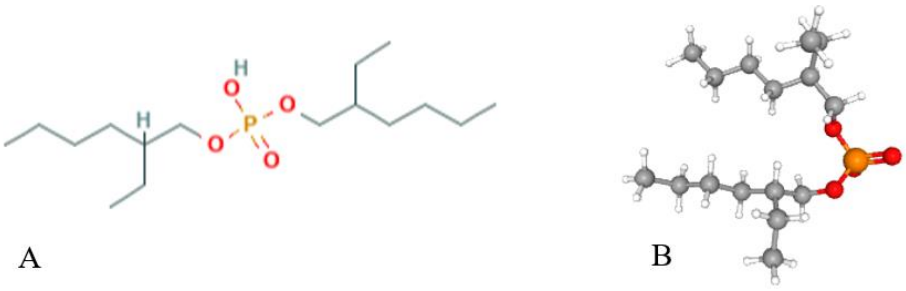

Figure 2.1 A-Chemical Structure depiction of HDEHP, B-Ball and stick model depiction of HDEHP (National Center For Biotechnology Information (Pubchem), 2021).

HDEHP (shown in Figure 2.1) is a phosphorous acid used as an extractant in this work. The chemical formula of HDEHP is $C_{16}H_{35}O_4P$. It has a formal charge of zero and a molecular weight of 322.42g/mol (Ma *et al.*, 2013). It has a hydrogen bond donor and acceptor sites of 1 and 4 respectively. HDEHP presents as a light yellow, odourless and moderately viscous liquid at room temperature.

2.2.2 Solvation Extractants

Complexation, also known as solvation, is a theory of solvent extraction that is described by the extraction of a metal ion by acidic extractants. The theory states that the molecules within an extracting mixture 'compete' with each other for the metal ion based on the degree of their affinity for association (Kislik, 2002). Multiple types of solvation extractants have been investigated for the separation of REEs (Peppard *et al.*, 1957a; Peppard *et al.*, 1957b; Sherrington, 1983; Lu *et al.* 1998). The ability for the extraction of lanthanides using tributyl phosphate (TBP) was observed to increase proportionally with the increase in atomic number. However, the distribution coefficient proved to be much lower when TBP was investigated in chloride solutions than in nitric acid media. When solvation extractants are used in combination with nitric acid, the extraction systems yield satisfactory results for REEs lighter than samarium (Xie *et al.*, 2014). TBP is amongst the most investigated of the solvation

extractants, as its immiscibility with HNO_3 and H_2O is a characteristic that is required for use as an extractant for LLE extraction (Xie *et al.*, 2014).

2.2.3 Anion exchanger Extractants

Anion exchangers extract metal ions from the solvent as anionic complexes. This causes their range of efficacy to be limited to conditions in which strong anionic ligands are present in. When anionic exchangers with primary or tertiary amines were used, the separation factors for adjacent rare earth elements were shown to be poor in chloride media as opposed to sulphate media wherein the result was found to be more satisfactory (Rice and Stone, 1962; Bauer, 1966). Chelation with ethylenediaminetetraacetic acid (EDTA) improves the extraction and separation of rare earth pairs. In nitrate media the characteristics of aliquot 336 allow it to extract light REEs more readily than their heavier counterparts. This behaviour contrasts with that of most cation exchange and solvating extractants, for which the extraction of rare earth metals increases steadily with increasing atomic number (Xie *et al.*, 2014).

Lanthanoids which naturally occur together often exhibit similar chemical properties and the categorisation of lanthanides into four groups (La-Ce-Pr-Nd, Pm-Sm-Eu-Gd, Gd-Tb-Dy-Ho and Er– Tm–Yb–Lu) becomes evident when the logarithm of their physical-chemical parameters in the context of extraction systems are plotted against their atomic numbers. Breakpoints occur in these plots, and these are dependent upon the stabilisation energies related to the interelectron repulsion energy of the 4f electrons. The relative stabilisation as a function of the interelectron repulsion energy enables separation (Nash, 1993). In cases where the separation and recovery of multiple REEs were investigated a correlation to the groups defined by the aforementioned criteria could not be discerned. However, research in which the studied groups of REEs mirror those occurring in natural ore deposits or within particular types of electronic waste proves to be a wise choice with respect to the applicability to industrial separation or handling (Tunsu *et al.*, 2014).

2.2.4 Synergistic Extractant effect

The synergistic effect is the phenomenon displayed by the degree of extraction in a system of mixed extractants. More particularly it can be described as a situation in which the degree of

extraction exhibited by systems in which the blend of mixed extractants is used, is greater than the sum of the degree of extraction for the individual extractants under the same conditions (Zhao *et al.*, 2019). Synergistic extraction does not only improve the extraction efficiency and selectivity of the resultant blend. It also enhances the stability of extracted complexes, can improve the solubility of extracted complexes in the organic phase, assist in the elimination of the emulsification, prevent the formation of the third phase, and increase the rate of extraction (Zhao *et al.*, 2019). There are several types of synergistic solvent extraction processes that have been investigated for the extraction and separation of REEs. These include mixtures of acidic extractants (e.g., organophosphorus or carboxylic acids), various mixtures of neutral extractants (e.g., TBP and trioctylphosphine oxide (TOPO)), and blends of these extractants (Santhi *et al.*, 1991; Wang *et al.*, 2011).

2.2.5 Ionic liquids

Ionic liquids (ILs) are molten salts at room temperature. They are also referred to as liquid electrolytes or ionic melts. They are composed purely of ions which are often asymmetric organic cations and polyatomic organic or inorganic anions (Cevasco and Chiappe, 2014). Of late ILs have garnered attention for use in extraction systems for the separation of inorganic and organic compounds in water-immiscible phases (Baba *et al.*, 2011; Turanov *et al.*, 2013). They are usually treated as diluents, but also possess characteristics that enable them to act as extractants. Their appeal lies in their novelty and ecologically friendly characteristics. ILs also possess physicochemical characteristics that can be varied to a desired set of specifications by the combination of cationic and anionic partners (Baba *et al*., 2014) ILs that are immiscible in water are produced by the extension of the alkyl-chain of the cationic moiety or by introducing hydrophobic anions such as $(CF_3SO_2)_2N^-$, commonly abbreviated as Tf_2N^-.

Imidazolium and pyridinium-based ILs have shown promising results in terms of the extraction ability in cyclohexane/cyclohexene separation (Delgado-Mellado *et al.*, 2019). The optimal extractive ability using imidazolium- and pyridinium-based ILs in extractive systems was found to be at a temperature of 298.2 K by Delgado-Mellado *et al.*, (2019). Dicationic ILs have been proven to have lower levels of recovery than monocationic ILs. Mono-imidazolium ILs with butyl groups at N-1 and N-3 sites have the capacity to yield the best recovery. The extraction efficiency order of triazoles (compounds containing a 5 membered ring with two carbons and 3 nitrogens) from high to low were reported as [BBMIm][Br], [BPMIm][Br],

[BHMIm][Br], [BMIm][Br] (1-butyl-3-methylimidazolium bromide), $[C_4(BMIm)_2]Br_2$, $[C_4(MIm)_2]Br_2$ (Yang *et al*., 2018).

The use of ILs as extractants in LLE systems for rare earth metals has been reported in literature, and a list of these studies is presented in Table 2.3. For systems in which octyl(phenyl)-n,n-diisobutylcarbonylmethylphosphone oxide (CMPO) is blended with ILs, the overall extraction ability of the system was increased considerably as opposed to conventional organic sol vent extraction systems. This indicated the possibility of far more efficacious extraction processes where ILs are used. The degree to which the addition of ILs to LLE increases the extraction ability is heavily dependent on the judicious selection of the organic extractant.

Ionic liquids such as betainium bis(trifluoromethylsulfonyl)imide have been used in the investigation by Stoy *et al., (*2021) for the selective recovery of REEs from coal fly ash. Stoy *et al., (*2021) developed a new valorization process based on the ionic liquid. The extraction efficiency of this process relied on the the thermomorphic behaviour of the ionic liquid with water at the instance at which they were heated and formed a singular liquid phase. This singular phase was used for the leaching from the coal fly ash which occurred via a proton-exchange mechanism. When the leaching was complete, the singular phase was cooled causing the ionic liquid and water to separate. The REEs were then recovered from the ionic liquid phase by stripping in a mild acid.

Turanov *et al., (*2013) found that generally low concentrations of IL in an organic solvent containing CMPO were adequate for the proficient recovery of REEs from HNO_3 and HCl solutions. The extraction of components with a CMPO containing extractant increased with increments in the hydrophobicity of the anionic moiety and with a decrease in the hydrophobicity of the cationic moiety. As a result, the effect of IL addition to extractants can be categorised as synergistic extraction.

Referring to Table 2.3 it can be seen that a large proportion of studies on the use of ionic liquids in extractant solutions include the imidazolium functional group. Their use to enhance the extractive performance has been well documented. The binding energies between these molecules and the ion targeted for extraction has been explained by the employment of density functional theory. It is therefore expected that for a well-documented anion such as

imidazolium, there exists a large body of work to provide insight into the factors that could affect the extractive ability of the solutions in which they are contained (Yu *et al*., 2021).

Table 2.3 Ionic liquid LLE extractant studies as summarised by Baba et al.[1]

REE	Synergistic Extractant		Reference
	Organic	***Ionic Liquid***	
Lanthanides, Y	CMPO	[C_4mim][PF_6]	Nakashima *et al.* 2003
Nd, Eu	Htta	[C_4mim][Tf_2N]	Jensen *et al.* 2003
U, Am, Nd, Eu	HDEHP, Cyanex 272	[C_{10}mim][Tf_2N]	Cocalia *et al.* 2005
Lanthanides, Y	CMPO	[C_4mim][PF_6], [C_4mim][Tf_2N]	Nakashima *et al.* 2005
Eu, La	Htta	[C_4mim][Tf_2N]	Mekki *et al.* 2006
Eu	TPEN	[C_6mim][Tf_2N]	Shimojo *et al.* 2006
La, Sr, Ca, Li, Na, Cs	(-)	[C_4mim][NfO]	Kozonoi and Ikeda 2007
Sc, Y, La, Yb	Cyanex 925	[C_8mim][PF_6]	Sun *et al.* 2007
Lanthanides, Y	TPMDPO, Ph2Et2, Bu2Et2	[C_4mim][PF_6], [C_4mim][Tf_2N]	Turanov *et al.* 2008
Y, Eu, Ce, La	PC-88A	[C*n*mim][Tf_2N] (*n* = 8, 12)	Kubota *et al.* 2008
La, Eu, Lu	Htta-18C6 (synergistic extraction)	[C_4mim][Tf_2N]	Hirayama *et al.* 2008
Lanthanides	TODGA	[C*n*mim][Tf_2N] (*n* = 2, 4, 6)	Shimojo *et al.* 2008
Ce, Th, Gd, Yb	(-)	[C_8mim][PF_6]	Zuo *et al.* 2008a
Th/Rare earths	primary amine N1923	[C_8mim][PF_6]	Zuo *et al.* 2008b
Lanthanides, Sc, Y, Th	D2EHPA	[C_8mim][PF_6]	Zuo *et al.* 2009
Sm, Eu, Gd, Dy	HYD	[C][Tf_2N] (*n* = 4, 6)	Mallah *et al.* 2009
Sc, Y, Eu, Ce	[A336][CA-100] (TSIL)	[A336][CA-100] (TSIL)	Sun *et al.* 2009
Y, Dy, Ho, Er, Yb	Cyphos IL 104 (TSIL)	[$C_n$mim][PF_6] (*n* = 4, 8), Cyphos IL 104 (TSIL)	Liu *et al.* 2009
Sm, Eu, Gd, Dy	PAN-HYD (synergistic extraction)	[C_6mim][Tf_2N]	Mallah *et al.* 2010
Y, Eu	DODGAA	[$C_n$mim][Tf_2N] (*n* = 4, 8, 12)	Kubota *et al.* 2010
U, Pu, Eu, Am	CMPO-modified IL (TSIL)	CMPO-modified IL (TSIL)	Odinets *et al.* 2010
Ce, Nd, Sm, Dy, Yb	HDEHP	[$C_n$mim][PF_6] (*n* = 2, 4), [C_4mpy][PF_6]	Yoon *et al.* 2010
Lanthanides	Htta, Htta-18C6, Htta-DC18C6, Htta-DB18C6, Htta-15C5	[C_4mim][Tf_2N]	Okamura *et al.* 2010

[1] Baba *et al., (*2014)

2.2.6 Solvents

Among the parameters that affect the extent to which REEs can be recovered, is the selection of the acid in which the precursor material will be dissolved. Nitric acid and sulphuric acid are amongst the most widely studied. The adsorption characteristics of REEs in sulphuric acid

solutions can be likened to their behaviour in hydrochloric acid solutions, with higher distribution coefficients in the former. The exception to this is scandium, where the effect is reversed (Korkisch, 1969). Investigations conducted into the comparison between nitric acid and sulphuric acid have shown that leaching of a given batch of sludge with nitric acid was more effective than with sulphuric acid under comparable conditions. The use of nitric acid also negates the need for agitation of pulp mixtures when processing times of 24-48 hours are employed (Qi, 2018). Should nitric acid be used as a solvent in industrial applications the nitrates formed upon neutralization have the potential to be an environmental pollutant. Ecological and amenity damage to rivers, lakes and costs contribute to high water treatments costs as well as long-term health impacts on humans consuming nitrate contaminated water sources (Bian *et al.*, 2020).

Studies considering the direct leaching of bauxite mud using dilute mineral acids nitric, hydrochloric and sulfuric acid have been widely carried out for the selective dissolution of REE with subsequent enrichment or purification of the REE-containing solution by the use of ion-exchange or solvent extraction (Ochsenkühn-Petropulu *et al.*, 1996; Borra *et al.*, 2015; Davris *et al.*, 2016). Sulfurous acid leaching (Rio Tinto Alcan International Ltd, 1989), carbonisation, bioleaching and employment of highly acidic ionic liquids (Davris *et al.*, 2016) have been shown to yield adequate results for selective leaching of Sc and other REEs. The ionic liquid $HbetTf_2N$ possesses a switching thermomorphic behaviour, namely, it is hydrophobic at temperatures below 55 °C, but at temperatures above 55 °C forms an aqueous solution. Metals that are dissolved into $HbetTf_2N$ are often extracted by employing a subsequent stripping step utilising an acidic solution at ambient temperatures. This regenerates the IL which can be separated from the aqueous solution for reuse due to the hydrophobicity it displays at ambient conditions. The employment of this leaching strategy has been studied for phosphor lamps and neodymium magnet wastes (Dupont and Binnemans, 2015; Davris *et al.*, 2016).

2.3 Quantitative and Qualitative Models

2.3.1 Distribution coefficient

To appropriately consider the classes of extractants, the separation factor and the distribution coefficient must be clearly identified. These provide a quantitative description of the solvent extraction (Xie *et al.*, 2014). The distribution coefficient, D_M, with M referring to the metal ion, is defined by:

$$\mathbf{D_M} = \frac{[\mathbf{M_{org}}]}{[\mathbf{M}]} \tag{2.1}$$

where $[M_{org}]$ is defined as the mass concentration of M in the organic phase, and [M] is defined as the mass concentration of M concentration in the aqueous phase. The distribution coefficient can be used to predict the partitioning behaviour of a particular chemical species within two phases. The separation factor, β, for two different metal ions, namely M_1 and M_2, is defined by:

$$\beta_{M_1/M_2} = \frac{\mathbf{D_{M_1}}}{\mathbf{D_{M_2}}} \tag{2.2}$$

Both the distribution coefficient and the separation factor are optimized at their maximum values, under a set of comparable chemical conditions, with the same metal ion species to be isolated.

2.3.2 Thermodynamic Predictive Models

For extractants classified as 'cation exchanger', the mechanism can be described with Ln defined as any rare earth element, A, denoting the organic ion, H, denoting the hydronium ion denoting and overscoring denoting a species present in the organic phase. The extraction of REEs from aqueous media using cation exchange extractants in the acidic form is expressed by Peppard *et al., (*1958) as follows:

$$\mathbf{Ln^{3+} + 3\overline{HA} \leftrightharpoons \overline{LnA_3} + 3H^+} \tag{2.3}$$

The process is more complex than can be expressed in equation 2.3 as the acidic extractants are usually aggregated as dimers or larger oligomers in non-polar organic solutions. This has a dampening effect on the polarity of the REEs, and the REE complexes formed in the process of extraction may be present along with undissociated organic acid. Therefore, a form that more acutely describes the reaction occurring during the process of extraction was described by Mason *et al., (*1978) in the following manner:

$$\mathrm{Ln^{3+}} + 3\overline{\mathrm{H_2A_2}} \leftrightharpoons \overline{\mathrm{Ln(HA_2)_3}} + 3\mathrm{H^+} \tag{2.4}$$

where H_2A_2 denotes the dimeric form of the organic acid. When one inspects equation (2.4) it becomes apparent that the extraction can be stimulated by increasing the pH of the aqueous phase. Whereas increasing the acidity of the aqueous solution will reverse the extraction and promote stripping of the solution (Xie *et al.*, 2014).

Spadina *et al., (*2019) modelled an extraction system in which an aqueous phase ($HNO_3 + Eu(NO_3)_3$) and organic phase (dodecane + HDEHP) were in contact. The aqueous phase contained multiple ionic species, whereas the organic phase (solvent) comprised of monomers and dimers of the extractant, and aggregates. The aggregates were assumed to be spherically shaped on average, differing in size (Spadina *et al.* 2019). This model was applied for systems wherein spherical aggregates were experimentally observed. The reactions occurring in the system were described by Spadina *et al., (*2019) as follows:

$$2\overline{\mathrm{LH}} \leftrightharpoons \overline{\mathrm{LH_2}} \tag{2.5}$$

$$\mathrm{N_{H_2O}} \cdot \mathrm{H_2O} + \mathrm{N_{LH}} \cdot \overline{\mathrm{LH}} \leftrightharpoons \overline{\mathrm{A_{N_{H_2O};N_{LH}}}} \tag{2.6}$$

$$\mathrm{N_{H_2O}} \cdot \mathrm{H_2O} + \mathrm{N_{H^+}} \cdot \mathrm{H^+} + \mathrm{N_{NO_3^-}} \cdot \mathrm{NO_3^-} + \mathrm{N_{LH}} \cdot \overline{\mathrm{LH}} \leftrightharpoons \overline{\mathrm{A_{N_{H_2O;};N_{H^+};N_{NO_3^-};N_{LH}}}} \tag{2.7}$$

$$\mathrm{N_{H_2O}} \cdot \mathrm{H_2O} + \mathrm{N_{Eu^{3+}}} \cdot \mathrm{Eu^{3+}} + \mathrm{N_{NO_3^-}} \cdot \mathrm{NO_3^-} + \mathrm{N_{LH}} \cdot \overline{\mathrm{LH}} \leftrightharpoons \overline{\mathrm{A_{N_{H_2O;};N_{H^+};N_{NO_3^-};N_{LH,R};N_{Eu^{3+}}}}} + \mathrm{N_{L^-}} \cdot \mathrm{H^+} \tag{2.8}$$

$$N_{H_2O} \cdot H_2O + N_{Eu^{3+}} \cdot Eu^{3+} + N_{H^+} \cdot H^+ + N_{NO_3^-} \cdot NO_3^- + N_{LH} \cdot \overline{LH} \leftrightharpoons \overline{A_{N_{H_2O};N_{H^+};N_{L^-};N_{NO_3^-};N_{LH,R};N_{Eu^{3+}}}} + N_{L^-} \cdot H^+ \quad (2.9)$$

where H_2O, Eu^{3+}, H^+, NO_3^-, $\overline{LH}$, $\overline{LH_2}$ and $\overline{A_{N_{H_2O};N_{H^+};N_{NO_3^-};N_{LH}}}$ are the symbols for the water, Eu cation, proton, nitrate anion, monomeric form of the extractant, the dimeric form of the extractant, and aggregate of a particular composition, respectively. N with a subscript represents the stoichiometric numbers of the subscripted species. R (present in equation 2.11) represents the dissociated state of the extractant molecule, while over-scoring denotes the species present in the solvent.

The model was developed firstly by the quantification of the free energy of the aggregate using the standard chemical potentials of aggregate (μ°_{Agg}), generalised bending constant of the molecule in the extractant film (κ^*), intrinsic spontaneous packing parameter (p_0), Boltzmann constant (k_B), the exchange parameter (χ_{LH,L^-}), Gibbs-Duhem relation and combinatorics (Spadina *et al.* 2019). This is followed by the calculation of equilibrium aggregate concentrations using the chemical potentials, standard chemical potentials, molal ion concentration, the activity of the dissociated extractant head groups and the Gibbs energy. This yielded a model of the following form:

$$\beta = \frac{1}{k_B T} \quad (2.10)$$

$$B_{Agg,x} = \exp\left(-\beta\mu^{\circ''}_{Agg,x} + \sum_j N_j \ln\left(\frac{m_j^{aq}}{m_j^{org}}\right) + N_{H_2O}\left(\frac{\sum_j x_j^{org}}{x_{H_2O}^{org}} - \frac{\sum_j x_j^{aq}}{x_{H_2O}^{aq}}\right) + -N_L - \ln(10)(pK_a^{\circ} - pH) + \beta N_{LH,R}\mu^{\circ}_{LH} \right) \quad (2.11)$$

$$\mu^{o''}_{Agg,x} = -k_B T \ln N_{complex} - \sum_i N_{Cat,i} N_{bond,i} E_{0,Cat,i} + k_B T \ln\left(N_{H_2O}! \prod_j N_j!\right) + k_B T\left(H_2O \ln N_{H_2O} + \sum_j N_j \ln N_j - N_{H_2O} - \sum_j N_j\right) + \frac{N_{LH}}{2}\kappa^*\left(1 + \frac{l_{chain}}{R_{core}} + \frac{1}{3}\frac{{l_{chain}}^2}{{R_{core}}^2} - p_{0,eff}\right) + k_B T \chi_{LH,L^-}\frac{N_{LH,R} N_{L^-}}{N_{LH}} - k_B T \ln\left(\frac{1}{N_L - 1}\right) \quad (2.12)$$

where *j* accounts for the ions in the core and *i*, the number of cations in the core.

Figure 2.2 below shows the distribution coefficients measured in Spadina *et al., (*2019). It is these distribution coefficients on which the aforementioned model is based.

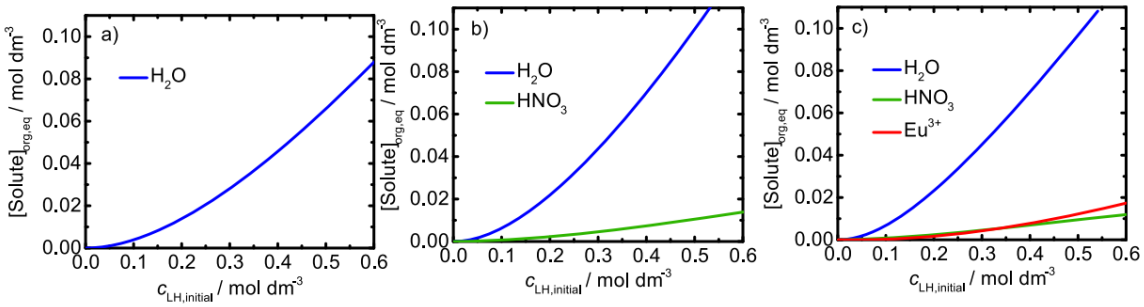

Figure 2.2 The concentrations of the solute as they appear in the organic extractant, HDEHP, as a function of the initial concentration $c_{LH,initial}$. A- Pure water, B- HNO_3 aqueous solution, $m(HNO_3)_{aq,eg} = 1$ mol.kg^{-1}, C-$Eu(NO_3)_3$, HNO_3 aqueous solution, $m(HNO_3)_{aq,eq} = 1$ mol.kg^{-1} and $m(Eu^{3+})_{aq,eq} = 0.032$ mol.kg^{-1} (Spadina *et al.*, 2019).

The distribution coefficients of REE containing LLE systems is the measurement focus of this study. The conceptual elements and modelling by Spadina *et al., (*2019) are presented for the purpose of gaining an in-depth appreciation for the chemical phenomena occurring in LLE systems and how the results of this thesis could be used to predict the behaviour of similar systems outside of the scope of this work.

2.3.3 Mathematical Predictive Models

An alternative to the specialised thermodynamic models used to predict the extraction behaviour is a purely mathematical approach. Regression analysis is one such method that considers the independent variables measured and categorises the degree of their impact on the dependent variable. Apart from the degree of impact of each independent variable mathematical regression provides insight into the relevance of particular independent variables measured, their interaction, and the certainty of the relationship between the variables (Ranganathan *et al.*, 2019). Discussed below are the concepts of Single Linear Regression and Multivariate Regression.

Simple Linear regression

Simple linear regression is a form of a statistical model that can be utilised for the study of the relationship between an independent variable x and a dependent variable Y. This statistical model assumes that the relationship can be described by a straight line and yields the equation of the line of best fit (also referred to as the trend line) by estimating the coefficients of the gradient and the intercept of said line. The model also quantifies the uncertainty associated with the aforementioned estimate. These estimated coefficients can be subsequently used to predict the values of the dependent variable (Ranganathan *et al.*, 2019). In mathematical terms this means that when presented with the set of independent variables X (constituted of values from x_i to x_n) and associated dependent variables Y (constituted of values Y_i to Y_n) in matrix form, the application of simple linear regression will yield a model of the following form:

$$Y_i = \theta_0 + \varepsilon_i + x_i\theta_1 \tag{2.13}$$

Where θ_0 represents the intercept, θ_i the gradient and ε_i the 'noise' or error. The matrix form is given as:

$$Y = \theta X + \varepsilon \tag{2.14}$$

To evaluate the coefficients that provide the best fit for the observed data the ordinary least squares approach is used which can be ultimately expressed as follows:

$$\widehat{\theta_0} = \overline{Y} - \widehat{\theta_1}\overline{x} \tag{2.15}$$

Where $\bar{\theta} = \frac{\sum_{i=1}^{n}\theta_i}{n}$ and $\bar{x} = \frac{\sum_{i=1}^{n}x_i}{n}$ denote the sample mean of θ and x, respectively. These parameters can be used to estimate the response of Y wherein the Gauss-Markov conditions

are satisfied. Further algebraic manipulation as outlined in (Ranganathan *et al*., 2019) yields an expression for the coefficient of determination (R^2) as follows:

$$R^2 = \frac{\sum_{i=1}^{n}\left(\hat{Y}_i - \overline{Y}\right)^2}{\sum_{i=1}^{n}(Y_i - \overline{Y})^2} \tag{2.16}$$

R^2 varies from a value of 0 to a value of 1. A value close to zero indicates that the model is not capable of describing (or predicting) any of the variability around its mean whereas an R^2 value of 1 indicates that the model is a perfect fit, with no deviation in the measured data from the line fitted to it.

Multivariate Regression

Multiple linear regression or multivariate linear regression is a generalised form of the concepts presented above in the section on linear variable regression. The primary difference between linear variable regression and multivariate linear regression is the number of independent variables (also referred to as predictors) from which the relationship between they and the dependent variable is quantified. This is mathematically expressed in the increase in the dimensions of the matrix of variables X presented in equation 2.14 above. Following mathematical manipulations, as discussed by Ranganathan *et al., (*2019) equation 2.16 can be derived to describe *the goodness of fit* subject to the Gauss-Markov conditions holding. The number of independent variables used to evaluate the coefficient of determination is denoted by the letter p, due to the nature of the R^2 value a greater value of p will directly relate to an increased value of R^2. Ideally, when presenting a model for a system in which multiple independent variables are inputs, the relative robustness of the independent variable's impact on the dependent variables should be taken into account (Ranganathan *et al.*, 2019). Considering this influence would make the particular model proposed parsimonious, that the ability to predict the dependent variable with the greatest precision with the minimum number of variables. To adjudicate the parsimonious nature of a model the adjusted coefficient of determination (R_a^2) can be computed utilising the equation 2.17 of the following form:

$$\mathbf{R_a^2 = 1 - \frac{\sum_{i=1}^{n}\frac{\left(Y_i - \hat{Y}_i\right)^2}{(n-p-1)}}{\sum_{i=1}^{n}\frac{(Y_i - \overline{Y})^2}{(n-1)}}} \tag{2.17}$$

Where n represents the number of observations (ie. number of dependent variables given a unique set of independent variables) made. The R_a^2 value ranges from 0 to 1, which outputs

closer to representing a greater level of parsimoniousness (Ranganathan *et al.,* 2019). Therefore, this suggests that the most apt multivariate model is that which displays the greatest value for both R^2 and R_a^2. The linearity of multivariate linear regression refers to the linearity of the modelled parameters. To improve the fit of the model the matrix of independent variables can be expanded by including multiples of the independent variables by themselves. This approach may appear to increase the matrix size without increasing the number of truly independent parameters, however, the model coefficients obtained from this approach shall be independent.

2.3.4 Liquid Extraction Equipment

The study of the distribution coefficients does not only inform the understanding of the distribution behaviour of ions in LLE systems, but also their eventual applicability in the liquid-liquid extraction separation units. The purpose of liquid-liquid extraction separation systems is to separate species existing in a solution by exploiting the abundance of the species in each phase. The exploitation of the miscibility behaviour finds its quantitative expression in the distribution coefficient (see Section 2.3.1). The goal of separation is to achieve high purity of the targeted species (Gruber and Carsky, 2020).

There is a wide range of liquid extraction equipment available to achieve the separation of chemical species in solutions. This equipment generally uses a combination of gravitational or centrifugal force along with agitation to effect separation. The reciprocating plate column (RPC) and the vibrating plate extraction (VPE) column are amongst those which employ agitation (Rathilal, 2010). As presented by Hino *et al., (*1997) the results of equilibrium studies can be utilised to simulate the operation of counter-current mixer-settler cascades. The VPE column can be modelled as a mixer-settler cascade.

The contacting of the target species REE-containing solution with an immiscible extractant is known as extraction. Mixer-settler cascades, and by extension VPE columns, can consist of solely the extraction process (Hino *et al.*, 1997). However, the degree of separation of the target species from the other species in solution can be enhanced using a stripping process. In the stripping process, the extractant which was used to extract the target species from the initial solution is contacted with a stripping solution/ wash acid to increase the purity of the target species. Hino *et al., (*1997) found the use of a stripping solution to be beneficial in the separation of Pr/Nd and Y/Er using PIA-226 as the extractant. In the investigation conducted

by Gruber and Carsky (2020) the use of a stripping stage in the VPE column was found to improve the purity of the product (no indication was given by authors as to the degree of improvement). Figure 2.3 presented below is a schematic diagram of a mixer-settler cascade which includes a set of extraction stages as well as stripping stages. Where the E represents the extractant solution, Y represents the organic solution flow rate, X represents the aqueous solution flowrate, W and F denoting the wash acid (also known as stripping solution) and feed aqueous solution categorisations respectively, M denoting the metal ion in solution, whereas q and n represent the number of stripping and extraction equilibrium stages respectively.

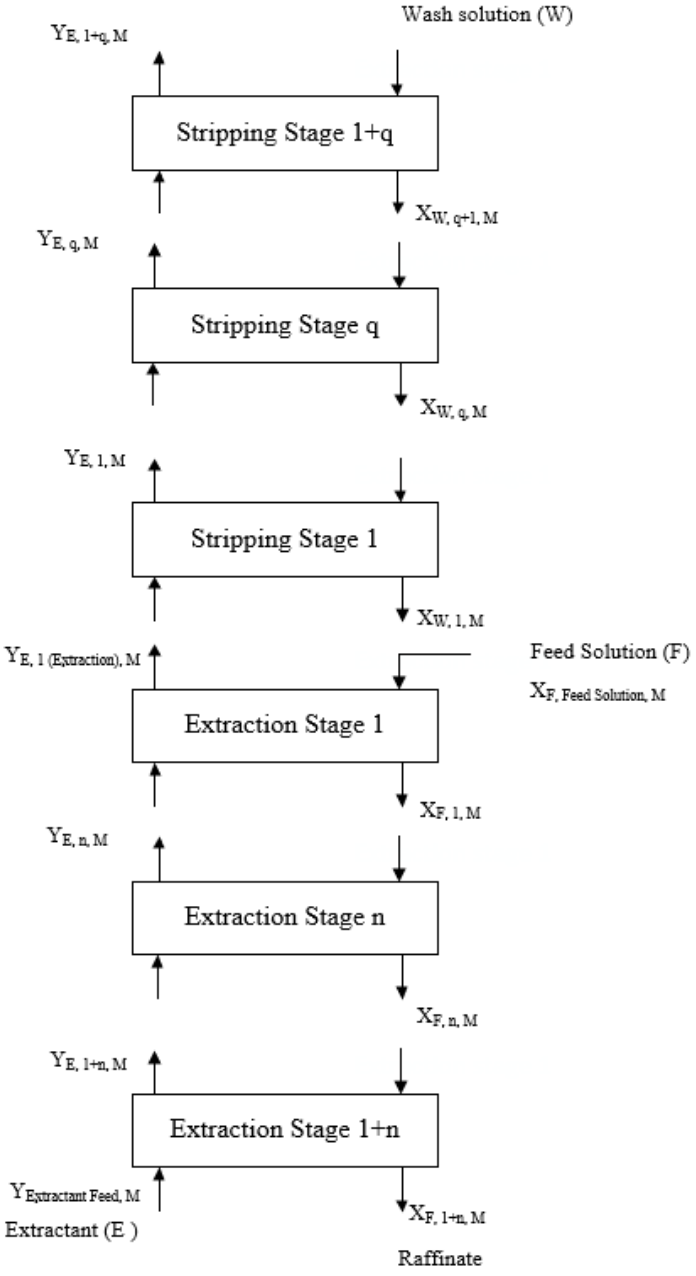

Figure 2.3 Flow Schematic for LLE extraction and stripping stages (This work).

The interaction of the feed, stripping solution, extractant flow rates and the dissolved ions they contain can be quantified by equations 2.18 and 2.19 presented by Hino *et al., (*1997). Each of the equations is applied to each equilibrium stage in a sequential manner. These equations are a modified form of mass balance manipulated to readily fit the schematic as presented in Figure 2.3. Although equations 2.18 and 2.19 below bear the extraction stage demarcation of:

$$Y_{E,n,M} = X_{E,n,M} \cdot D_{n,M} \tag{2.18}$$

The calculation of the composition of intermediate streams between the in the mixer-settler cascade are performed using the combination of equation 2.18 and 2.19 below. Equation 2.19 is derived using the model in Figure 2.3 and a mass balance.

$$F \cdot X_{F,1,M} + E \cdot Y_{E,1+n,M} = F \cdot X_{F,n,M} + E \cdot Y_{E,n,M} \tag{2.19}$$

From equation 2.19 above it can be seen that the number of extraction equilibrium stages and the number of equilibrium stripping stages are parameters that can be varied to affect the amount of target species in each stream. This implied that this variation also affects the purity of the purity of the target species in the organic and extractant flows. Relative to one another one variable, a ratio, is used to relatethe organic to aqueous flows. This ratio is specific to either the extraction section or the stripping section and is represented in equation 2.20 as follows:

$$\text{Organic to Aqueous ratio} = \frac{E}{F} \equiv \frac{E}{W} \tag{2.20}$$

The equations listed above were utilised in the simulation investigation performed by Hino *et al., (*1997) to obtain trends that describe the effect of the aforementioned parameters on the separation equipment presented in Figure 2.4 below.

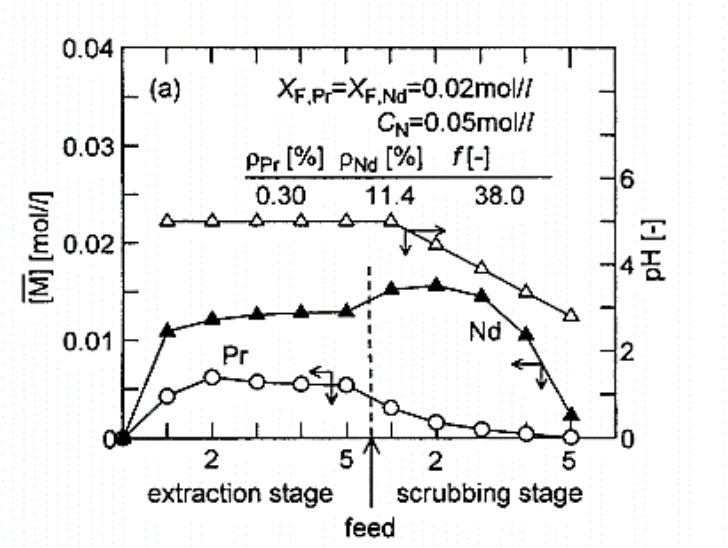

Figure 2.4 Results of the simulation of the Pr/Nd simulation extracted with PIA-226/kerosene in counter-current cascades of 5 extraction and 5 scrubbing stages at flow rate ratios equal to 1 l/min in extraction and stripping stages (Hino *et al.*, 1997).

From Figure 2.4 it can be seen that the bulk of the ion transfer between the organic and the aqueous phase occurs in the first stage of the extraction section with a marginal degree of extraction occurring thereafter. Then in the stripping stages it can be seen that for Pr the degree of re-extraction is relatively constant in each stage whereas for Nd the bulk of the re-extraction occurs in the fifth scrubbing stage.

Gruber and Carsky (2020) on the other hand varied the organic to aqueous flowrate to reach a neodymium target purity of 0.99. The result was achieved with the initial feed solution at a concentration of 1.5 – 2.0 M sulphuric acid (H_2SO_4), extracted with 1.2 M HDEHP in n-dodecane. The stripping solution used to re-extract the metal ion from the solution was a H_2SO_4 solution of 4.0 M. The VPE column used was specified to have an internal diameter of 50 mm. The number of plates or theoretical equilibrium stages in the VPE column used in Gruber and Carsky (2020) was not mentioned. It is worth noting that to obtain a neodymium purity of 0.99 the pregnant solution was put through the column twice with a crystallisation of the target ions into crystal sulphates and their redissolution occurring between each extraction. At the end of the first extraction and stripping stages the neodymium purity was 0.7451. The ratio of organic to aqueous in the extraction section used to obtain this purity was a value of 10.

The focus of this work was primarily on determining the distribution coefficients of neodymium. The distribution coefficients were then used to calculate the number of extraction stages, the number of stripping stages and the neodymium purity for various organic extractant

to aqueous feed ratios in an LLE separation column. The results of these calculations can be found in section 5.7.

In summary, the thermodynamic predictive models reviewed in this chapter provide a qualitative basis that can be used to closely link the extraction mechanics of the LLE extraction to quantitative analyses. In this work the thermodynamic predictive models are presented for the purpose of gaining insight into the thermodynamic basis of LLE extraction systems without their rigour that their application would demand. The mathematical predictive models however, are a more useful method for data trend analysis in the context of a limited amount of laboratory measurements. The mathematical predictive models are therefore the method chosen to analyse the data contained in this study. The rigorous thermodynamic dynamic models lend their use to studies in which robust predictive capabilities are required. This work is limited to the analysis of the LLE measurements within the chemical parameters outlined in the objectives and subsequently their expression in a theoretical liquid-liquid extraction separation unit.

Chapter 3:Review of Experimental Techniques

This chapter covers a review of the experimental techniques used by various researchers in investigating the separation and recovery of REEs using hydrometallurgical processes. The review considers systems in which the REE is recovered from aqueous media (synthesized solutions or the solutions which are a product of leaching from waste). The aqueous media contains either a single species of metal ion or various species. The choices made by the researchers, and the implications of these choices on the behaviour of LLE systems, are expounded upon in cases that have a direct bearing on the experimental choices made in this work. The exposition detailing the experimental parameters in various published works is initially presented as Table 3.1. This is followed by a discussion of the effect of the various experimental parameters on the results. In the final part of this chapter, the selection of the LLE systems used to validate the equipment and to inform the choice of operating conditions for the experimental method used in this work are presented and discussed.

3.1 Review of LLE experiments with REEs

Table 3.1 describes the commonalities and differences in the methods used in the published literature for the separation and recovery of REEs. The studies are ordered primarily by the process used to study the extraction of REEs and subsequently according to their chronology. Wherever "(-)" appears in the table, it indicates information not published in that work. The sections which follow in this chapter expand on the details in Table 3.1.

Table 3.1 Summary of extraction studies reviewed showing the experimental techniques and conditions

	REE	Source	Recovery Process	Chemicals		Vessel Type	Agitation	Temperature (K)	Extraction Time (hr)	Analytical techniques	Result Uncertainty
				Extractant	*Solvent*						
a	Nd	NdFeB magnets	Liquid metal Extraction	Molten Mg (99.8%)	(-)	Stainless steel crucible	(-)	948-978	2-8	Scanning electron microscopy, x-ray diffraction, and energy dispersive spectroscopy	(-)
b	Eu and La	$Eu(NO_3)_3$ $La(NO_3)_3{\cdot}6H_2O$	TREUEX TALSPEAK	HDEHP CMPO	HNO_3	(-)	Vortex mixer	295 ± 2	0.067	ICP-MS	±10%
c	La, Ce, Pr, Nd, Sm, Eu, Gd, Tb, Dy, Ho, Er, Tm, Yb and Lu	Chlorides or nitrates	LLE	DEHPA EHEHPA	(-)	Conical Flask	Shaking	293	0.16	EDTA titration	(-)
d	Pr, Nd, Yb and Er	(-)	LLE	HDEHP (97 wt%)	(-)	(-)	(-)	298	(-)	(-)	(-)
e	Yb and Lu	Yb_2O_3	LLE	HDEHP+ cyclohexane	(-)	(-)	(-)	(-)	(-)	HGPe detector	(-)
f	La, Ce, Pr, Nd and Eu	Nitrate forms	LLE	D2EHPA (0.05M)	HNO_3	Stirred Cell	(-)	293	6	ICP-OES	±3%
g	Am, Cm, Cf and Fm	10 ppm standard solutions	LLE	HDEHP in benzene (0.08 – 1.0 M)	HNO_3	Polypropylene Tube	Centrifuging	301 ± 1	0.16	ICP-MS	(-)
h	La, Ce, Pr, Nd, Sm, Gd, Tb, Dy, Ho, Yb, Lu and Eu	Nitrate Salts	LLE	TOMA, DEHP, THTP, DEHP, HDEHP	(-)	Glass Cells	Vibrating mixture	343	1	ICP-AES	(-)

Table 3.1 Summary of extraction studies reviewed showing the experimental techniques and conditions continued

	REE	Source	Recovery Process	Chemicals		Vessel Type	Agitation	Temperature (K)	Extraction Time (hr)	Analytical techniques	Result Uncertainty
				Extractant	***Solvent***						
i	Y, La, Ce and Eu	Waste Fluorescent Lamps	LLE	DODGAA	HCL, H_2SO_4 (50mM)	(-)	(-)	303	12	ICP-AES	(-)
j	Th and U	(-)	LLE	CMPO	HNO_3 (0.1 – 7.0M)	Test tubes	Stirring (60rpm)	293 ± 2	1	ICP-MS	<5%
k	Am, Eu	Pure radioactive tracer	Combined Solvent Extraction	TODGA (1M) HDEHP (0.25M) in n-Dodecane	HNO_3 (various)	Equilibrium Tube	(-)	298	(-)	Well type NaI (TI) detector	±5%
l	Ce, La, Y, Sc, Pr, Nd, Sm, Gd, Er, Dy and Yb	Bauxite residue	LLE	HbetTf2N (97%)	(-)	Mini reactor	Mechanical stirrer	298	(-)	ICP-MS	(-)
m	Eu	$Eu(NO_3)_3 \cdot 6H_2O$ salts	LLE	DMDOHEMA (varying) HDEHP (varying)	HNO_3	Test tubes	Mixing	Ambient	1	ICP-OES	(-)
n	Y, La, Ce, Pr, Nd, Sm, Eu, Gd, Tb, Dy, Ho, Er, Tm, Yb and Lu	REE ore	LLE	HEH(EHP) HDEHP	H_2SO_4	Separating Funnell	Mechanical Thermostatic Oscillator	298 ± 1	0.16	ICP-AES	±3%
o	Y and Eu	Oxides	LLE	HDEHP (varying)	HNO_3	Jacketed Glass Vessel	PTFE coated stirrer	298	12	ICP-OES	Various
p	Dy, Nd and Pr	NdFeB magnets	LLE	HDEHP	H_2SO_4 (1.5-2M)	Extraction Column	Vibrating plate	(-)	(-)	(-)	(-)

[a]Xu *et al.*, (2000), [b]Tkac *et al.*, (2012), [c]Sato (1989), [d]Hino *et al.*, (1997), [e]Lahari *et al.*, (1998), [f]Geist *et al.*, (1999), [g]Takayama *et al.*, (2011), [h]Sun, Luo and Dai (2012), [i]Yang *et al.*, (2013), [j]Turanov *et al.*, (2013), [k]Nayak *et al.*, (2014), [l]Davris *et al.*, (2016), [m]Rey *et al.*, (2016), [n]Huang *et al.*, (2017), [o]Williams-Wynn *et al.*, (2020), [p]Gruber and Carsky (2020)

3.1.1 REE Sources

The ‘raw material’ from which the REE-containing solutions are synthesized has a bearing on the amount of energy required to prepare the raw material (i.e., cleaning, comminution, preliminary separation) prior to it being made into a solution that can be introduced into the LLE system of interest. As mentioned in the introduction, the original scope of this work included the leaching of REEs from permanent NdFeB magnets. To this end, the preparation of REE-containing solutions from recycled materials is reviewed in Appendix A. In the main body of this section the preparation of acidic aqueous solutions from rare earth oxides (REOs) is discussed.

Tkac *et al., (*2012) and Rey *et al., (*2016) employed the use of nitrate salts in the synthesis of their REE solutions. Tkac *et al., (*2012) formed these by using the salts and diluting them directly with nitric acid to concentrations of ≈ 0.1 M. The use of REOs for solution synthesis reported by Williams-Wynn *et al., (*2020) requires that REO first be diluted with concentrated nitric oxide and then subsequent dilution to the desired acidic concentration. On the other hand, Rey *et al., (*2016) contacted the salts with dilute solutions of 0.05 M or 1.0 M nitric acid. Hino *et al., (*1997) prepared the solutions by dissolving the REOs in a heated HCl solution followed by a removal of the excess acid by evaporation. For cases in which the dissolution of the REO is not readily achievable at ambient temperatures, the application of heat is often required. In the solution preparation process by Hino *et al., (*1997) the ionic strength was kept stable by the addition of 0.5 M (Na, H)Cl. The aqueous phases used in the investigations by Geist *et al., (*1999) produced a solution of 10 mg/l (REE content). The pH of 2.1 was formulated by the addition of nitric acid either on its own, or with ammonium thiocyanate with a concentration of 1.0 M; or a mixture of formic acid (0.975 M), sodium formate (0.025 M) and sodium nitrate (0.008 M).

Gruber and Carsky (2020) reported the dissolution of magnets for LLE extraction. This dissolution was achieved by the mixing of sulphuric acid (1.5 – 2.0 M) and the magnets at a temperature of 353 K until dissolution could be visually confirmed. This required relatively large acid volumes of 7.5 - 8 litres for every 1000 g of crushed magnets.

3.1.2 Process

The processing methods from the literature that was reviewed can be arranged into hydro- and pyro-chemical processes. The nature of the stream to be processed, considered alongside its chemical complexities guides the choice of treatment processes. The high energy requirement of pyrometallurgy is not suitable for feeds with a low percentage of REEs or the treatment of small amounts of material (Yoon *et al.*, 2014). In most cases, pyrometallurgical products require additional processing to produce high purity REMs. This is due to the fact that gas-solid pyro-processing of streams containing more than one REE will lead to mixed products (Tunsu *et al.*, 2014). For REE-based end-of-life products, the REEs will be found in the slag phase of the pyro-processing products in low concentrations, making the recovery of the materials difficult to achieve economically (Binnemans *et al.*, 2013).

Electrochemical methods employing the use of molten salts have the advantage of high chemical stability, high reaction rates, low temperature sensitivity and low vapour pressures (Tanaka *et al.*, 2013). The hydrometallurgical processes possess unique advantages in the separation and recovery of individual REEs. The ability of these hydrometallurgical processes to handle lower grade and more complex input streams with multiple contaminants applies equally to the processing of REEs from mineral ores and end-of-life streams (Tunsu *et al.*, 2014). When reclaiming REEs from end-of-life products, three stages can be identified: characterisation, assaying and pre-treatment of the material; leaching and separation of metal ions; and refining of the product (Tunsu *et al.*, 2014). The separation of REM ions in solution can be carried out by the use of solvent extraction and ion exchange (Nash, 1993).

Ionic liquids (discussed in Section 2.2.5) are gaining attention as alternative solvents in the hydrometallurgical separation of metals. Ionic liquids are considered as better substitutes for organic diluents due to their extremely low volatility, adjustable miscibility and polarity, and electrical conductivity. The electrical conductivity of ionic liquids presents the possibility of depositing the separated components as solids from the loaded organic phase, avoiding a stripping step (Kolarik, 2012; Tunsu *et al.*, 2014).

The TRUEX (Transranium Extraction) process is a process that utilises actinide extraction for extracting actinides from acidic nitrate and chloride solutions. The TALSPEAK Process (Trivalent Actinide Lanthanide Separation with Phosphorus-Reagent Extraction from Aqueous Komplexes) is the proposed selective extraction of trivalent lanthanides from the actinides, which are retained in the aqueous phase as aminopolycarboxylate complexes. These processes

are not described as a part of this work, and further and more detailed descriptions can be found in the work by Tkac *et al., (*2012).

3.1.3 Vessel & Vessel loading

The dimensions of the vessel in which experiments are undertaken have a bearing on the results, particularly as they relate to the method and means of agitation including the amount of sample within the vessel . Unfortunately, as with agitation (see Section 3.1.5), the authors of the reviewed literature rarely include the details and dimensions of the experimental vessels used. However, the loading of the liquid-liquid extraction vessels was stated by Sato (1989), Hino *et al., (*1997), Geist *et al., (*1999), Turanov *et al., (*2013), Nayak *et al., (*2014) and Rey *et al., (*2016) to consist of equal volumes of aqueous and organic phase components. The volumes of each phase varied from 1 ml (Tkac *et al.*, 2013; Nayak *et al.*, 2014) in 5 ml vessel volumes (Nayak *et al.*, 2014) to equal 15 ml measures in 50 ml vessels (Sato, 1989).

A cylindrical stainless-steel crucible 5 cm in diameter and 10 cm in height was used in the high-temperature separation method investigated by Xu *et al., (*2000) whereas glass vessels such as conical flasks, test tubes and separating funnels were used by Sato (1989), Rey *et al., (*2016) and Huang *et al., (*2017), respectively.

3.1.4 Temperature

The methods of temperature control employed by the authors of the reviewed literature fall for the most part into two categories. In the first category, the experiments were conducted at ambient temperatures (Tkac *et al.*, 2012; Rey *et al.*, 2016). In the second category, the temperature was controlled by means of submerging the extraction vessels into a bath of fluid (Sato, 1989; Takayama *et al.*, 2011). It is worth noting that most authors do not specify the means of temperature control, however, the balance of the stated temperatures falls in the range of 293-298 K (see Table 3.1). The exceptions to the two aforementioned methods of temperature control were the use of a jacketed cell employed by Williams-Wynn *et al., (*2020), whereas an atmosphere-controlled chamber was used by Xu *et al., (*2020).

For the cases in which the temperature of the extraction vessel was not actively controlled (i.e., ambient temperature) consideration must be given to the impact of the action on the ease with

which the results can be compared to others and also their reproducibility given the potential for the lack of temperature stability over the period of time in which extraction takes place. The extraction temperature can influence the distribution ratios and separation factors in the LLE processes involving REEs. In the investigation carried out by Xu *et al., (*1995) using P204 for the extraction of REEs, the distribution ratio was shown to decrease with an increase in temperature. Between (10 and 50) °C, the distribution ratios of La, Ce, Pr, Eu and Gd were maximised at 10°C while the separation factors for the light REE couples (Ce/La, Pr/Ce, and Nd/Pr) increased with the increase of temperature. However, for REEs with an atomic number larger than 60 (e.g., europium, terbium, dysprosium etc.) and the adjacent elements, the separation factor decreases with increasing temperature (Qi, 2018). When monitoring the effect of temperature increase on the concentration of neodymium in equilibrium in the processing of sludge leached with 2.0 M nitric acid, a decrease in the concentration and recovery of neodymium was observed. While this previous result, obtained by Xu *et al., (*1995), might lead one to pursue an optimum distribution ratio by increasing or decreasing the temperature of some extractions far beyond the ambient region, this decision must be made factoring in the additional energy for heating/cooling (and subsequent cost implications) should this methodology be applied to industrial-scale operations.

3.1.5 Agitation

In systems where the immiscibility of liquids is exploited to induce mass transfer phenomena; the degree of mass transfer and degree of separation of the desired components achievable is proportional to the contact area between the fluids. The finer dispersions of one fluid in another induced by agitation is the source of the increased contact area. It is worth noting that in most cases where immiscibility has been exploited (see Table 3.1), agitation of the system has been employed and declared by the author(s). Most of the works presented in the table do not specifically mention the degree of agitation achieved by the method chosen. However, the manner of stirring along with its advantages and disadvantages must be considered.

When relatively small amounts of liquid require mixing, an option available to ensure a high degree of mixing is the vortex mixer as employed by Tkac *et al.*, (2012). The ill-defined method of "shaking" is by far the most mentioned by authors in the description of investigations (Sato, 1989; Hino *et al.*, 1997; Takayama *et al.*, 2011; Yang *et al.*, 2013). Huang *et al., (*2017) provides a more detailed account of the shaking employed by the use of a thermostatic

oscillator at 150 rpm, the main advantage of which is the combined automated control of the temperature and mixing provided by the instrument.

Stirring of vessel contents was the other commonly used method of agitation. Given the immiscibility of the phases within the vessel, there are a few considerations to be made when this method of agitation is chosen. Chief amongst them is the placement of the stirring mechanism within the cell (and naturally the position in the vessel contents). Should the stirring mechanism be submerged in too low or too high a position in the cell along with a slow to moderate rate of stirring, it is conceivable that only the mixing of a single phase in the cell will be achieved. This mixing of a single phase (with a single low/high submerged mechanism) or the mixing of both phases without disruption of the miscibility boundary (where two stirring mechanisms are placed both high and low in the vessel to effect stirring of vessel content phases) may be desired by the investigator for the purpose of maintaining a quantifiable contact area between the phases, as described by Geist *et al., (*2013) and by Turanov *et al., (*2013) at 60 rpm. A single stirring mechanism can be used to induce mixing of the cell contents with a disruption of the miscibility boundary. This is an agitation strategy suited to investigations wherein the quantification of equilibrium constants is the objective as mentioned by Davris *et al., (*2016), Rey *et al., (*2016) and, Williams-Wynn *et al., (*2020). In these cases, the speed of the stirring and the placement of the stirrer within the vessel are vital in ensuring that adequate mixing occurs.

3.1.6 Time

The length of time for which the experiments are conducted shows a wide distribution from 0.067 to 12 hours (see Table 3.1). The lack of kinetic studies in REE LLE systems makes it difficult to comment with a high degree of certainty on the effect of these decisions on the results. However, when systems of a similar constitution are observed (in so far as chemical species and concentrations are concerned), the observer can expect to see a proportional relationship between the distribution coefficient and the extraction time when considering systems that have not yet reached equilibrium.

3.1.7 Separation & Sampling

The allowance for separation of immiscible phases is only a requirement in agitation schemes wherein the miscibility boundary is disrupted. This separation can be allowed to occur by gravity-induced settling as described by Williams-Wynn *et al., (*2020) or by the use of a centrifuge as detailed by Sato (1989) and Takayama *et al., (*2011). The method of sampling that is chosen is dictated by the limitations and specifications of the particular analytical technique (see Section 3.1.8). In the cases where ICP (Inductively Coupled Plasma) techniques were employed, a sample of the aqueous phase was withdrawn from the LLE vessel (Geist *et al.*, 1999; Tkac *et al.*, 2012; Williams-Wynn *et al.*, 2020). The specifics of the sampling method (syringes, sampling taps, etc.) were not described in any of the reviewed literature. Sampling of the aqueous and/organic phases occurred after the extraction vessel contents had been allowed to settle without further mixing and agitation. The amount of sample withdrawn from the system by Geist *et al., (*1999) was 1 ml in volume. No further sample volumes were reported in the literature reviewed.

3.1.8 Analytical Techniques

In recent decades, various experimental methods for the determination of metal species in complex matrices of uncertain composition, such as environmental waters, have been proposed. The techniques are based on the identification of individual species or classes of species. Anodic stripping voltammetry (ASV) and competing ligand exchange with adsorption cathodic stripping voltammetry (CLE-AdCSV) are two electrochemical procedures used for metal distribution tests in aqueous media. Electrochemical techniques such as stripping chronopotentiometry are novel methods of metal concentration analysis that show much promise. The nonelectrical techniques (ion exchange, complexing resins, the Donnan membrane technique, diffusive gradients in thin-film gels and the permeation liquid membrane) are amongst the techniques used for metal ion concentration measurement (Pesavento *et al.*, 2008).

Inductively Coupled Plasma (ICP) analysis is the most common method used for the purpose of analysing samples from the hydrometallurgical processing of REEs. The ICP analyses used fall into the three main types: mass spectroscopy (MS), atomic emission spectroscopy (AES) and optical emission spectroscopy (OES). In the field of this analysis, plasma refers to a gaseous mixture containing cations and electrons with the ability to retain electrical

conductance. The governing concept in the use of plasma for elemental analysis is based on the interaction of molecules with electromagnetic radiation (Tyler, 1992). Acid digestion and hydride generation are methods of preparation of samples for elemental analysis. In ICP-OES and ICP-AES, the sample solution enters a spray chamber wherein argon gas carries it to an ionisation setup. The ionised gaseous mixture then emits photons that are collected by a lens or concave mirror to be analysed (Date and Gray, 1989).

ICP-OES is generally used for samples that contain a high degree of total dissolved solids (TDS) or solids in suspension. This method has a tolerance of 30% for TDS while ICP-MS has a TDS tolerance of 0.2%. ICP-OES is particularly robust in the analysis of groundwater, wastewater, soil, and solid waste. In more general terms, ICP-OES is used to measure contaminants for environmental safety assessments and elements with a higher regulatory limit (ThermoFisher.com, n.d.). ICP-MS is generally useful in the analysis of samples with low detection limits. Therefore ICP-OES is a more economical option if the elements within the sample do not require the lower detection limits that ICP-MS possesses. ICP-OES analysis has an added advantage in that the operation of the equipment does not require a high level of technical expertise (Date and Gray, 1989; Thompson and Walsh, 1989). These advantages of ICP-OES analysis must be balanced against the drawbacks, the largest of which is the high potential for spectral interference. In the process of passing the positive ICP sample ions through a quadrupole mass filter and then the mass detector, the ICP-MS provides isotopic information and mass data (Thompson and Walsh, 1989). In the instance that a sample contains analytes of a large difference in concentration, ICP-MS has a wider dynamic linear range than ICP-OES therefore the sample may not need to be diluted to detect these elements (ThermoFisher.com, n.d.). The ICP-MS method of analysis has a speciation capacity alongside the ability to perform rapid semi-quantitative analysis, perform isotopic analysis and efficiently remove polyatomic spectral interferences using collision cell technology (Tyler, 1992; Date and Gray, 1989).

The run times for ICP analysis are relatively short, with ICP-MS having the ability to detect most elements in less than one minute. The coating on detectors of ICP-MS equipment is light-sensitive and wears off as ions hit the detector surface. It, therefore, requires an amount of replacement commensurate with its use (Thompson and Walsh, 1989).

3.2 Effect of experimental parameters on results

Although the results from a fair number of literature sources have been reviewed, for the sake of direct relevance only the specific excerpts of results from Sato (1989), Geist *et al., (*1999), Nayak *et al., (*2014) and Williams-Wynn *et al., (*2020) (see Figure 3.1-3.2) are presented and discussed. The data of Sato (1989), Geist *et al., (*1999) and Nayak *et al., (*2014), were reported without any indication of uncertainty or error. The existence or lack of a reported uncertainty related to a particular published work can be observed in the "Uncertainty" column of Table 3.1. The uncertainty in the reported values is a cumulation of the uncertainties related to the experimental parameters and experimental equipment. The concept of uncertainty is explored further in Section 5.1. It is also worth noting that the data in these instances was reproduced from the reading of graphs presented in the works.

Figure 3.1 shows the effect of temperature on the distribution coefficient. The distribution coefficients of the various rare earth elements have been shown to decrease with an increase in temperature. This implies that the extractions proceed in an endothermic reaction. Similar results that describe the effect of temperature on the distribution coefficient were obtained for the heat change in the extractions of rare-earth elements from nitric acid solutions by HDEHP (Sato, 1989).

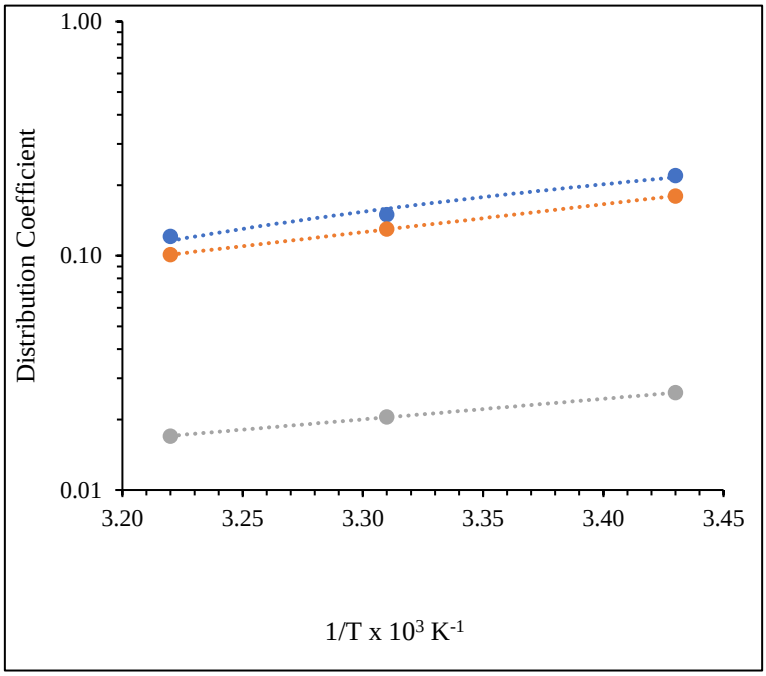

Figure 3.1 Temperature-dependence of distribution coefficient for extraction of rare-earth elements (Nd, Ce and La) from 0.1 M HCl with 0.05 M HDEHP in kerosene (Reproduced from Sato, 1989). ● , Neodymium; ● ,Cerium and ● , Lanthanum.

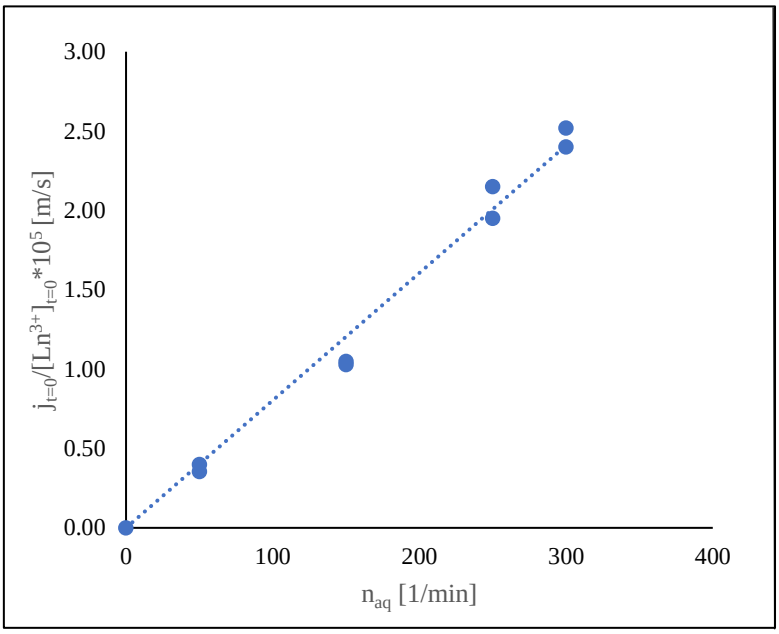

Figure 3.2 The flux dependency on stirring speed for extraction of Pr into HDEHP from nitric acid pH= 2.1 (reproduced from Geist *et al.*, 1999),

Figure 3.2 displays the flux and its dependency on the stirring speed mixing organic and aqueous phases. The agitation regime that yields the above results is that where each phase (aqueous and organic) was stirred separately without the disruption of the miscibility boundary layer. Although these results are indicative of a flux, they have value insofar as the selection of a mixing/stirring speed is concerned. It can be noted from a cursory evaluation of the results presented in Figure 3.2 that the stirring speed is directly proportional to the flux. As the flux is directly related to the distribution coefficient, therefore it can be said that an increase in the mixing speed will result in a decreased time period prior to reaching equilibrium.

The results from Nayak *et al., (*2014) and Williams-Wynn *et al., (*2020) show the effect of the nitric acid aqueous concentration on the distribution coefficient of Eu when contacted with 0.25M HDEHP in n-dodecane (see Figure 3.3).

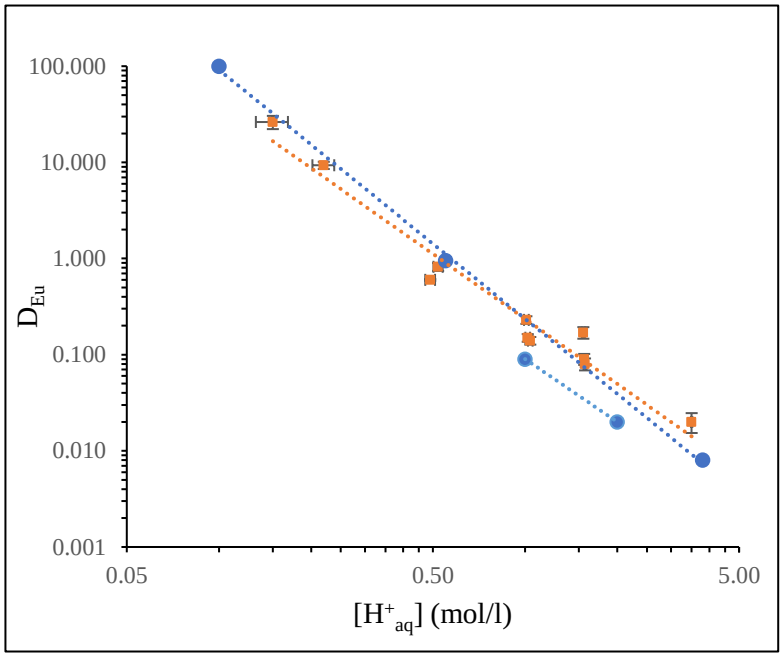

Figure 3.3 Distribution coefficient (D) of Eu in HNO_3, extracted with 0.25 M HDEHP in dodecane. ●, Nayak *et al.* (2014); ■, Williams-Wynn *et al.* (2020).

The results depicted in Figure 3.3 were used to evaluate and verify the validity of the experimental method used in this work. Results published by Qi (2018) for the distribution behaviour of REEs in a P507- kerosene-HNO_3 system display a sharp decrease in the distribution ratio as the concentration of the H^+ ion in the equilibrated phase increases. The distribution ratio in the aqueous phase reaches a minimum value. A similar relationship can be seen in Figure 3.3. in which the distribution coefficients from REE-containing systems appear to exhibit similar characteristics.

The experimental techniques used by Williams-Wynn *et al., (*2020) were employed in the unpublished work of Bridgemohan *et al., (*2020). Bridgemohan *et al., (*2020) investigated the distribution behaviour of iron between varying concentrations of aqueous HNO_3 and organic extractant HDEHP. These results yielded a relationship in which the distribution coefficient of iron was found to be indirectly proportional to the aqueous $[H^+]$. The results obtained by Bridgemohan *et al., (*2021) are displayed in Figure 5.16 (see Section 5.7.1) and will be considered only where they are pertinent to the extraction column is concerned.

Chapter 4:Experimental Method

This chapter provides a detailed description of the experimental setup and methods employed for the distribution coefficient measurements and preparation of samples for analysis. A brief rationale for the selection of the experimental equipment are also discussed. A brief discussion of the calibration procedure undertaken is also discussed.

4.1 Chemicals

Table 4.1 presents a list of the chemicals employed in performing this study. Ultrapure water with an electrical resistivity of 18 MΩ·cm measured at ambient temperature was used. This water was obtained from a Q5 Ultrapure (MilliporeTM) unit located in the Analytical Laboratory, Chemical Engineering building, University of KwaZulu-Natal (UKZN), Howard College Campus. The gases used (argon and nitrogen) were purchased from Afrox South Africa and utilized in the analysis of the metal concentrations using ICP-OES located at UKZN, Pietermaritzburg campus. This ICP-OES is of the Varian type model 720 ES.

Table 4.1 List of chemicals used in the experiment and analysis

Chemical name	Formula	CAS no.	Supplier	Purity*
Argon baseline 5.0	Ar	7440-37-1	Afrox	0.99999 [a]
Di-bis(2-ethylhexyl) phosphate/HDEHP	$C_{16}H_3SO_4P$	298-07-7	Merck	0.95 [b]
Europium (III) oxide	Eu_2O_3	1308-96-9	DLD Scientific	0.9999 [c]
Karl Fischer Calibrant WS0.1	C_7H_8O, $C_4H_6O_3$	100-66-3 108-32-7	Romil	0.999[b], 0.999[b]
Karl Fischer Electrolyte A	$C_3H_4N_2$ SO_2 $C_4H_{11}NO_2$ CH_4OH $C_3H_5IN_2$	67-65-1 111-42-2 288-32-4 7446-09-5 68007-08-9	Romil	0.999[b], 0.999[b], 0.999[b], 0.999[b], 0.999[b]
n-Dodecane	$C_{12}H_{26}$	112-40-3	Merck	0.99 [b]
Neodymium (III) oxide	Nd_2O_3	1313-97-9	Sigma Aldrich	0.9999 [c]
Nitric acid	HNO_3	7697-37-2	Merck	0.55 [c]
Nitrogen baseline 5.0	N_2	7727-37-9	Afrox	0.99999 [a]
Potassium hydrogen phthalate	$C_8H_5KO_4$	877-24-7	Merck	0.9980 [c]
Sodium hydroxide	NaOH	1310-73-2	Sigma-Aldrich	0.98 [c]
Tributylmethylphosphonium methyl sulfate	$C_{14}H_{33}O_4PS$	69056-62-8	Fluka	0.95[b]
Trihexyltetradecylphosphonium bis(trifluoromethylsulfonyl)amide	$C_{34}H_{68}F_6NO_4PS_2$	460092-03-09	Fluka	0.95[b]
Water	H_2O	7732-18-5	Analytical Laboratory /ChemEng UKZN	0.9999[d]
Yttrium (III) oxide	Y_2O_3	1314-36-9	Sigma-Aldrich	0.9999 [c]

[a] Volume basis; [b] Molar basis; [c] Mass basis; [d] Electrical resistivity (18 MΩ·cm);*Supplier stated purity.

4.2 Experimental Equipment

A conceptual drawing of the experimental setup along with a legend of labels describing the components from which it is constituted is presented in Figure 4.1. It should be noted that the drawing depicts only one equilibrium cell, whereas the equipment has 6 such cells as is described below. Table 4.2 presented below lists the manufacturer details and model number of the equipment utilised. Wherever a '-' appears in Table 4.2 the equipment was in existence at the onset of the investigation and further detail could not be retrospectively obtained.

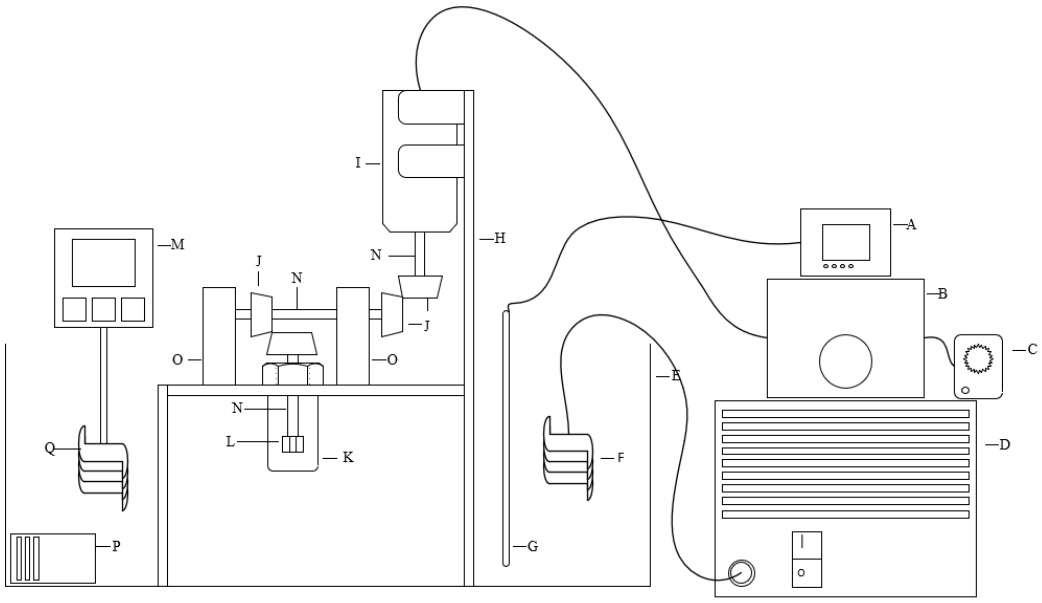

Figure 4.1 Schematic of experimental equipment.

A - Temperature sensor display, B - Variable speed motor controller, C – Timer, D - Chiller. E – Perspex Water Bath, F – Chiller Coil, G – Temperature Sensor, H – Equipment Support Frame, I- Motor, J – Bevel Gear, K – Glass Cell, L – PTFE Mixer, M – Temperature Controller, N – Mixing Shaft, O – Mixing Shaft Support Block, P – Water Circulating Pump, Q - Temperature Controller Coil.

Table 4.2 Equipment details for experimental set up

Label	Equipment Description	Manufacturer and model details
A	Temperature Sensor Display	Shinko ACS-13A-S/M
B	Variable Speed Motor Controller	PWM Variable Speed Motor Controller
C	Timer	Tedelex BND-50/A536
D	Chiller	Chiller, Grant Instruments, Model CIG
E	Perspex Water Bath	-
F	Chiller Coil	-
G	Pt100 Temperature Sensor	-
H	Equipment Support Frame	-

Table 4.2 Equipment details for experimental set up continued

Label	Equipment Description	Manufacturer and model details
I	Motor	Brushed DC Geared Motor
J	Bevel Gear	RS Pro POM 20 Teeth Mitre Gear
K	Glass Cell	25 ml glass sample cell
L	PTFE Mixer	-
M	Temperature Controller	Vivo Itherm, Class 1
N	Mixing Shaft	-
O	Mixing Shaft Support Block	-
P	Water Circulating Pump	DragonFly Pond and Fountain Pump
Q	Temperature Controller Coil	-

A diagram of the experimental apparatus is provided in Figure 4.1. It consists of a bank of 6, 25 ml glass cells, attachable to a frame of 316 stainless steel. This assembly allowed multiple runs at the same temperature conditions, therefore ensuring greater uniformity in the variable parameters of the experiment and the significant diminishing of the time required to carry out experiments over all the required data points. The distribution coefficients of the REEs in this work were determined using three distinct measurements. These were: the equilibrium concentrations of the REEs in the aqueous phase before and after extraction via ICP-OES and the measurement of the H^+ ion concentration using a potentiometric titrator (Metrohm; Titrando 888; readability of 0.0001 $mol.lit^{-1}$).

The cells are attached to the stainless-steel frame using screw caps. The screw caps have two ports in their lids. The first is a large central one that allows for a vertical mixing shaft manufactured of stainless steel tipped with a polytetrafluoroethylene (PTFE) stirrer to be housed within the cell, while the second is a smaller hole allowing for sampling. PTFE was the chosen material for the stirring mechanism owing to its durability and chemical stability in both the organic and aqueous phases used in the experiments. The length of the stainless-steel mixing shaft was designed to allow the PTFE mixer blades to lie between the miscibility boundary. The vertical mixing shaft in each cell is connected by way of bevel gears and a series of rods to a single motor (Brushed DC Geared Motor1), regulated by a speed controller (PWM Variable Speed Motor Controller). The placement of the stirrer mechanism in the equilibrium cell allows for vigorous mixing (at a speed of 721 ± 2 rpm) of the organic and aqueous phases

(completely disrupting the miscibility boundary), maximizing the surface area for mass transfer and minimizing the time required to reach equilibrium (see Chapter 3.1.5).

The steel frame housing the bank of cells as described earlier was submerged in an isothermal water bath. The water bath is fashioned from transparent sheets of polycarbonate which provides a clear view of its contents as well as a measure of thermal insulation. Various operational temperatures (293.15 – 343.15 K) have been reported in literature. The experiments in this work were carried out at a temperature of 298.15 K (close to ambient temperatures) as any benefit on the distribution coefficient derived from operation at a temperature far beyond the ambient would be outweighed by the cost of additional temperature control on large-scale processes.

The temperature of the water in the bath was maintained using a temperature bath controller and circulator (Vivo Itherm, Class 1, stability ± 0.05 °C). A chiller was also used to maintain the temperature setting (Chiller, Grant Instruments, Model CIG). A hydraulic pump (DragonFly Pond Pump) placed in the water bath ensures that any temperature gradients that may form within the bath are eliminated and that any isolated temperature fluctuations that may occur are dampened efficiently by the effect of the convective heat transfer induced by the use of a water pump. The temperature within bath is monitored by a Pt 100 temperature sensor connected to a Shinko controller (Shinko DIC, model ACS-13A Series 1/16 DIN). Although the temperature of the fluid in each of the equilibrium cells is not directly measured, the cells submerged in the water bath as well as the relative masses of the fluid in the cells to the water in the bath (more than 100 times) ensures that any temperature deviations that might have occurred within the equilibrium cells are overcome by heat transfer between the equilibrium cell contents and the water in the bath.

The synthesis of all chemical solutions and measuring of such were carried out on a mass basis with the use of a mass balance (Ohaus, Pioneer, PX224/E, readability of 0.0001g) with a maximum capacity of 210 g. The equilibrium concentration of the hydronium ion in the aqueous phase was measured using a potentiometric titrator (Metrohm; Titrando 888; readability of 0.0001 $mol.lit^{-1}$). The NaOH solution used for the titrations was prepared by the dissolution of NaOH pellets (see Table 4.1) on a mass basis to a concentration of approximately 0.1 M. Due to the hygroscopic nature of the NaOH pellets the concentration of the synthesized NaOH solution was verified by back titration with potassium hydrogen phthalate solution (concentration of approximately 0.2 M). The hygroscopic nature of the ionic liquids used in

this experiment also necessitated an evaluation of their water content by coulometric Karl-Fischer titration. An inductively coupled plasma optical emission spectrometer (Varian ICP-OES, 720 ES) was used to determine the metal concentration in the diluted aqueous samples.

As the density of the aqueous inorganic phase is greater than that of the organic phase, it resides in the lower segment of the cell when mixing is not in effect and the time allowed for the phases to separate has elapsed. Samples from the aqueous phase were withdrawn from each equilibrium cell using a syringe. When the syringe needle was inserted into the equilibrium cell the visibility provided by the polycarbonate water bath into the experimental chamber was vital to ensure that the sample was taken only from the aqueous phase.

4.3 Calibration of sensors

The Pt100 temperature sensor was calibrated against a temperature standard (WIKA; CTH 6500) with a calibration uncertainty of 0.02 K (see Appendix B). The reference thermometer and the temperature probe were attached to one another via the use of cable ties and placed into the calibration bath. The temperature on the calibration device was left to stabilize after each setting temperature and the temperature reported by the temperature on the probe module was recorded for a range of temperatures (288.15 – 308.15 K) in 5 K increments. The calibration of the Pt 100 temperature sensor was carried out twice during the course of the experiments without any hysteresis effects or change in original drift observed in any of the measurements.

4.4 Procedure

4.4.1 Equipment Start-up

1. After the temperature sensor calibration was performed, water was placed into the water bath.
2. The equipment was started up by switching on the temperature sensor, temperature circulator and water bath pump.

4.4.2 Aqueous Phase Preparation

3. The mass of REO required to produce a solution of ≈ 2000 ppm was calculated considering the REO supplier specified purity.
4. The predetermined mass of REO (approximately 0.05 g per 25ml of aqueous solution) was initially weighed out in a weighing boat, placed in the volumetric flask and weighed.
5. The REO was placed in a volumetric flask followed by the predetermined mass of 55% wt. aqueous HNO_3 solution.
6. The contents of the flask were agitated until complete dissolution of REO was achieved.
7. Once the dissolution of the REO was visually confirmed, a predetermined mass of de-ionised water was added to the volumetric flask to yield a solution of the desired H^+ concentration.

4.4.3 Organic Phase Preparation

8. The HDEHP supplier purity was taken into account in the preparation of the organic phase.
9. The organic extractant (HDEHP + n-dodecane in concentration 0.1 M, 0.5 M and 1.0 M) was prepared by measuring predetermined masses of the HDEHP and n-dodecane.
10. A volume of 200 ml of organic extractant phase at each concentration was prepared to ensure the same solution was used for all data points tested.
11. The HDEHP and n-dodecane were mixed to form the organic phase

4.4.4 LLE Experiment

12. The glass cells and stirrers used were thoroughly washed using ethanol and air dried.
13. The cells were numbered from 1-6, and the mass of each vial was measured and recorded.
14. The cells were then loaded with a predetermined measure of the aqueous REE and organic solutions (5 ml of each using an Isolab model 5000 011.05.905, 5000 µl micropipette).
15. The individual cells were attached to the frame, taking care to ensure all seals were watertight.
16. A check was done to ensure all equipment was plugged in and functioning.
17. The temperature of the water bath was checked to ensure minimal temperature deviations were observed.
18. The cells were attached to the frame using the screwcaps as the support and the assembly was lowered into the bath.
19. The mechanical stirrer was switched on and allowed to operate for 12 hours.
20. Once the 12 hours elapsed, the mixture within the cells was allowed to separate. The solution was left for 8 hours.

4.4.5 Sampling

21. Once the mixture separated into two distinct phases, the frame and attached cells were kept in the water bath to avoid any disturbance of the organic and aqueous phases from equilibrium conditions.
22. A syringe was inserted into the cells via the sampling porthole and a sample of approximately 4 ml was drawn from the lower aqueous layer. Care was taken not to disturb the phases.
23. The equipment was shut down by switching off the stirrer, temperature circulator and chiller in the water bath.

4.4.6 Sample Analyses

24. Standard solutions of REE with concentrations of 2, 5, 10, 20, 50 and 100 ppm were prepared via steps 1-4 to use as calibration standards for the ICP-OES.
25. The aqueous phase sample was diluted to a concentration below 100 ppm for the ICP-OES analysis.
26. An aliquot of the aqueous sample (diluted) was titrated against standard 0.1 M NaOH solution to confirm the H^+ concentration at equilibrium.
27. Once the ICP-OES analysis was complete the organic phase concentrations of REE were determined using the mass conservation principle.
28. For the mass balance calculation, the REE concentrations of the aqueous feed prior to loading in the cells and the equilibrium concentration of the REE of the aqueous phase in the cell after extraction and settling were used.

4.4.7 Organic phase preparation with IL doping

29. The organic phase with ionic liquids (0.0018 M, 0.018 1-butyl-3-methylimidazolium bis(trifluoromethylsulfonyl)imide and 0.01 M, 0.1 M, 0.25 M tributylphosphonium methyl sulfate) was prepared at (0.5 M HDEHP in n-Dodecane) in accordance with steps 6-7 above, thereafter steps 8-25 were followed.
30. Two hundred milliliters of the organic phase at each concentration was prepared to ensure all data points tested were constituted from aliquoting a single solution.

Chapter 5:Results & Discussion

This chapter presents the distribution coefficient data measured for 10 unique systems. These are presented along with discussions on their trends and the observed influence of the parameters on the trends. The first 2 systems presented are an evaluation of the distribution coefficients of Eu^{3+} and Y^{3+} at a single concentration of HDEHP in the diluent n-dodecane. The Eu^{3+} system presented was measured previously by both Williams-Wynn *et al., (*2020) and Nayak *et. al* (2014). The Y^{3+} system presented was measured previously by Williams-Wynn *et al., (*2020). Both these systems were used to verify the validity of the experimental method used in this study. The following 3 systems focus on the distribution coefficient of Nd^{3+} with varying concentrations of HDEHP in n-dodecane. In the final five systems, the influence of ionic liquids is presented and discussed. A comparative discussion of the effect of ionic liquid addition on the distribution coefficient is also presented. The chapter concludes with the preliminary investigation and discussion for the performance of a 0.5 M HDEHP in n-dodecane extractant in a liquid-liquid extraction separation unit fed with iron and neodymium in solution at an acid concentration of 0.1 M.

5.1 Materials, Equipment and Uncertainty

All materials and equipment used in the experiments that yielded the results presented and discussed hereunder are documented in Chapter 4. The barometric pressure in the laboratory in which the experiments were conducted and consequently the pressure of the LLE extraction system was 101.3 kPa, with an uncertainty of 1 kPa.

The uncertainty in the data presented in this work ultimately affects the two variables displayed in the tables presented in Sections 5.2 – 5.6 below. These variables are the uncertainty in the measurement of the distribution coefficient and the uncertainty in the measurement of the nitric acid concentration. The uncertainty for both variables is constituted by the uncertainty contributions from the repeatability of the measurements and the use of experimental equipment. The uncertainty in the measurement of the distribution coefficient is evaluated by further considering the uncertainties associated with the sample dilution, the analytical curve from the sample testing and the calibration curve. The uncertainty associated with the measurement of the acid concentration is quantified by considering the uncertainty contributions from the purity of the chemical components (see Table 4.1), the uncertainty

associated with the NaOH consumption as well as the uncertainty associated with the method repeatability.

The classification of each uncertainty contribution and the detailed formulation of the overall uncertainty of the variables presented in Sections 5.2 – 5.6 of this work follow the GUM (BIPM Joint Committee for Guides in Metrology. 2008) and can be found in Appendix C. The work of Faustino *et al., (*2016) is additionally referenced for the purpose of presenting the specific contributions of the various experimental uncertainties to the combined uncertainty in the form of a detailed Ishikawa diagram (see Sections C.1 and C.2). Table 5.1 below outlines the various uncertainty contributions considered in this work.

Table 5.1 Uncertainty contributions for the evaluation of measurement uncertainty

Uncertainty	**Value**	**Units**
Influence in Temperature		
Pt100 Standard Probe	0.02	K
Correlation for T	0.3	K
Shinko DIC Resolution	0.05	K
Repeatability	variable	K
Influence on Pressure		
Mensor CPC 8000 high-pressure calibrator	0.0005	kPa
Repeatability	variable	kPa
Influence on REM distribution		
Ohaus Pioneer, PX224/E	0.0001	g
Correlation for ICP-OES calibration	variable	g/g
Purities of chemicals*	variable	g/g
Repeatability	variable	g/g
Influence on acid concentration		
Ohaus Pioneer, PX224/E	0.0001	G
Volumetric flask uncertainty	0.1	cm^3
Burette uncertainty	0.1	cm^3
Purities of chemicals*	variable	g/g
Repeatability	variable	mol/dm^3

*Refer to Table 4.1

In the reviewed literature that is similar to the data presented in this work, the experimental uncertainty is mostly unreported as can be observed in the publications by Hino *et al., (*1997), Nayak *et al., (*2014) and Spadina *et al., (*2019). However, when comparing the uncertainty in the results obtained in this work to that published by Williams-Wynn *et al., (*2020) it can be determined that the uncertainty in the results presented herein are consistent with the use of ICP-OES for distribution coefficient measurements.

5.2 Test system 1: Europium

The experiments measuring the europium test system were undertaken at a constant temperature of 298.15 K. The organic extractant mixture used was HDEHP in n-dodecane at a concentration of 0.25 M with nitric acid as the source of the H^+ ions in the aqueous phase. At each acid concentration, three tests were conducted (utilizing aliquots of the same organic and aqueous solution) in three separate stirred cells. The sample from each cell was analyzed twice using ICP-OES. At each acid concentration, three data points for the distribution coefficients are displayed. Table 5.2 presents the data in the form of a table whereas Figure 5.1 presents the data in graphical form.

Table 5.2 The distribution coefficients, D_{Eu}, for Eu^{3+} ions between an organic phase (0.25 M HDEHP in n-dodecane) and aqueous phase concentrations with expanded uncertainties at T= 298.15 K and P = 101.3 kPa.

D_{Eu}	$[H^+]$ /M	$[Eu^{3+}]_{aq}$ /ppm	$U([Eu^{3+}])_{aq}$ /ppm	$[Eu^{3+}]_{org}$ /ppm	$U([Eu^{3+}])_{org}$ /ppm
33.08	0.11	1.33	1.026	43.83	0.849
32.32	0.08	1.36	1.026	43.80	0.829
33.60	0.10	1.31	1.026	43.85	0.862
0.21	0.70	84.25	1.539	17.75	0.009
0.25	0.76	81.60	1.512	20.40	0.011
0.25	0.78	81.90	1.515	20.10	0.010
0.03	1.58	97.60	1.646	3.40	0.002
0.05	1.58	95.75	1.627	5.25	0.003
0.06	1.63	94.85	1.618	6.15	0.003

$U([H^+]) = 0.0003$ for all distribution coefficient values

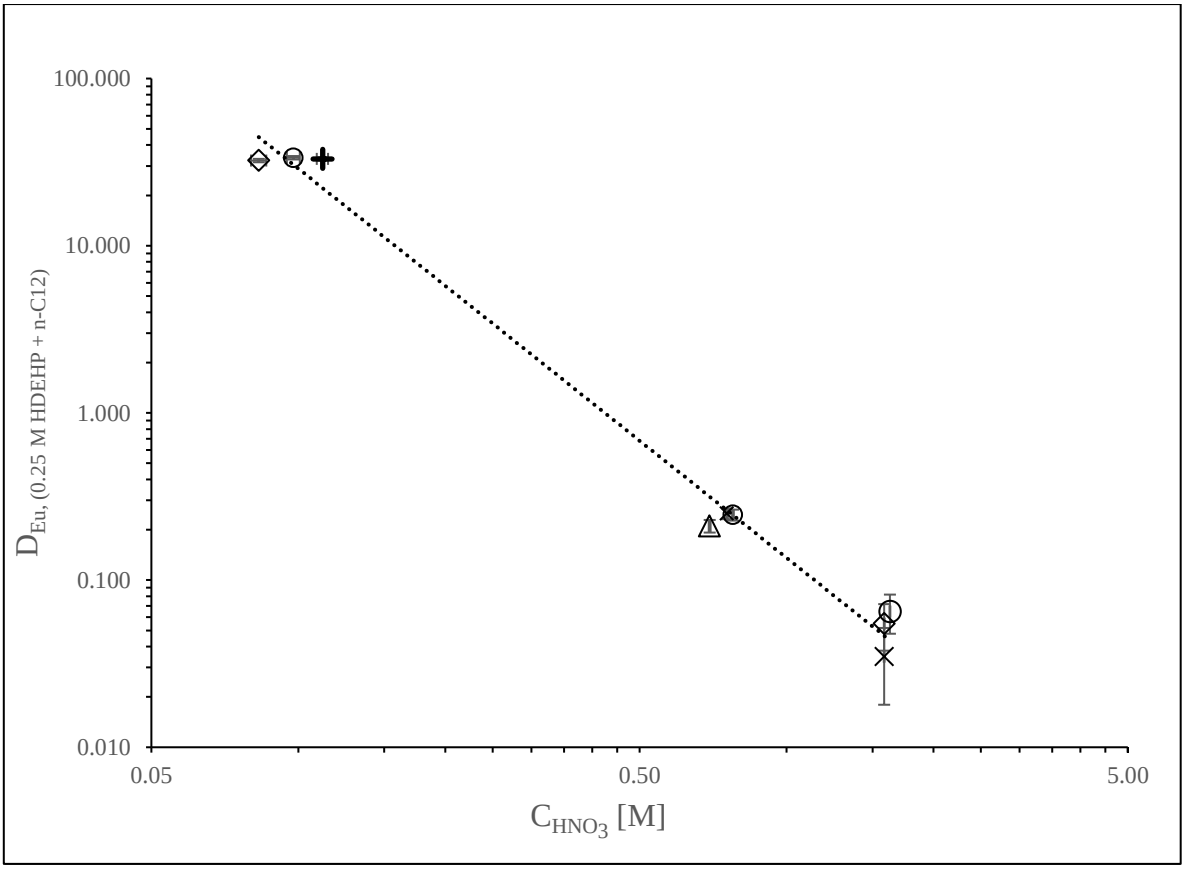

Figure 5.1 The distribution coefficients for Eu^{3+} ions 0.25 M HDEHP in n- dodecane and a nitric acid based aqueous phase.

Figure 5.1 displays the distribution coefficient as calculated from the experimental work and the ICP-OES results as shown in Table 5.2. The data measured in this work is represented by the markers. To track the influence of the cell position in the bath on the distribution coefficient, a varying shape of the data point marker was used to indicate the cell number (Δ-1, ○ – 2, + - 3, ■ – 4, ♦ - 5 and ● - 6). No significant trend of the measured equilibrium distribution coefficient or the measured H^+ concentration was exhibited in relation to cell number, which confirmed that repeatable results were obtained independent of the equilibrium cell's position in the water bath.

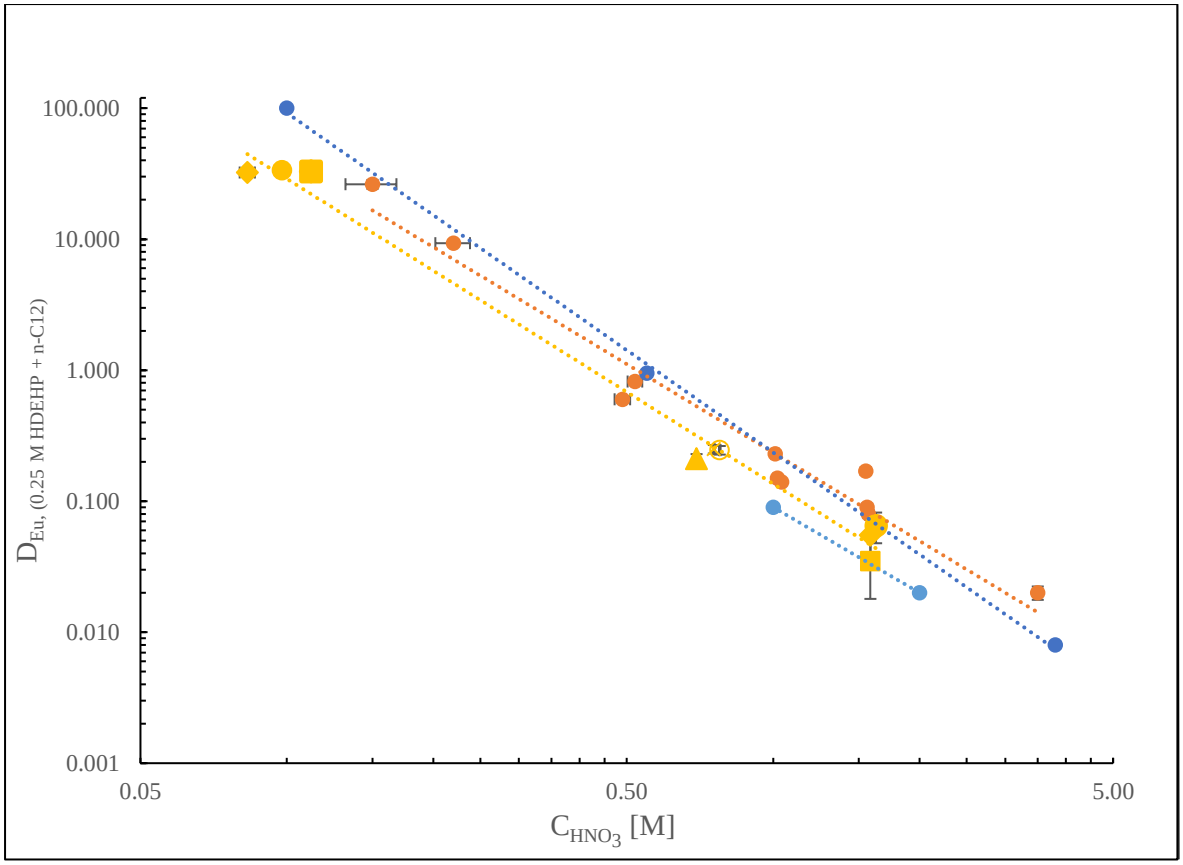

Figure 5. 2 The distribution coefficients for Eu^{3+} ions between the organic phase of 0.25 M HDEHP in n-dodecane and a nitric acid aqueous phase at T = 298.15 K and P = 101.3 kPa. ●, This work; ●, Nayak *et al.*, *(*2014); ●,Williams-Wynn *et al.*, *(*2020).

Measurements of the distribution coefficients at the same conditions as applied in this work were previously investigated by Nayak *et al.*, *(*2014) and Williams-Wynn *et al.*, *(*2020) therefore making their use suitable to determine the validity of the experimental approach employed in this study. The study by Nayak *et al.*, *(*2014) presented the distribution coefficient data graphically, without reporting on experimental uncertainties. The trend shown in

Figure 5. 2 attributed to Nayak *et al.*, *(*2014) is a reproduction from the best reading of the graph. As the readings were taken solely from logarithmic plots, the data presented for Nayak *et al.*, *(*2014) in Figure 5.2 has an inherent measure of subjectivity. In evaluating the concentration of the metal ion, Nayak *et al.*, *(*2014) made use of radioactive isotopes of Eu^{3+} in both the organic and aqueous phases with a well-type NaI(Tl) detector. Whereas the composition analysis in this work, as well as that reported by Williams- Wynn *et al.*, *(*2020), were conducted using ICP-OES analysis of the aqueous phase, with organic phase ion concentrations being determined using mass balance calculations.

Mirroring the work of Nayak *et al., (*2014) an analysis of the linear relationship between ln(D) and ln([H^+]) is undertaken for the Eu system and all those that follow hereunder. The derivative of the linear data, gradient g = $\partial(ln(D))/\partial(ln([H^+]))$, and its value at [$H^+$] = 1 for each data set are presented.

Considering all the caveats made in the presentation of the result obtained by Nayak *et al., (*2014), the degree of agreement between the data presented by Williams-Wynn *et al., (*2020) is acceptable and falls within the uncertainty ranges presented by the latter. This assertion is supported by comparing the gradients, g, at [H^+] = 1 (-2.244 for Williams-Wynn *et al., (*2020); -2.591 for Nayak *et al., (*2014); -2.328 for this study). In the original work by Nayak *et al., (*2014) the data is presented by fitting it to a single line trendline (R^2 = 0.9857), however, in Figure 5.2 this has been presented in two regions to improve the fit of the trend (these being confirmed by the R^2 = 0.9992 displayed by the adoption of this approach). When the data from this work is compared to that of Nayak *et al., (*2014) the degree to which they agree is within experimental uncertainty, as the newly fitted data by Nayak *et al., (*2014) flanks that presented in this work on either side ($D_{Eu}|_{[H^+]=1}$ for Williams-Wynn *et al., (*2020), is equal to 0.24, $D_{Eu}|_{[H^+]}$ for Nayak *et al., (*2014) is 0.24 and $D_{Eu}|_{[H^+]=1}$ for this work is 0.14).

Figure 5. 2 shows that the distribution coefficient of the Eu^{3+} ion in the 0.25 M HDEHP extractant at equilibrium decreases as the H^+ concentration increases. This variation extends from D_{Eu} = 33.60 at low [H^+], to D_{Eu} = 0.03 at the higher end of the [H^+]. This inverse relationship between the distribution coefficient and the H^+ concentration in the aqueous phase conforms to the expectation that an acidic extractant, in this case HDEHP, due to its high H^+ ion concentration, results in an increase in the substitution of the Eu^{3+} from the H^+ ion complexes. In extraction operations these results indicate that operating at lower concentrations of the aqueous H^+ ion would yield a higher level of performance whereas the selection of higher concentrations of the aqueous H^+ ion would be better suited to stripping operations.

5.3 Test System 2: Yttrium

The yttrium test system was measured at a constant temperature of 298.15 K. This system was tested to further validate the method utilized for the experiments in this work. The organic extractant mixture used was HDEHP in n-dodecane at a concentration of 1 M with nitric acid as the source of the H^+ ions in the aqueous phase. At each prepared acid concentration, three tests were conducted (aliquots from a single organic and a single aqueous solution) in three separate stirred cells. The hydronium ion concentration of the sample taken from each cell was tested twice by way of titration, followed by analyses using ICP-OES as described in Chapter 4.3. Table 5.3 presents the data obtained from the test in the form of a table whereas

Figure 5.3 presents the data in graphical form.

Figure 5.3 shows that the distribution coefficient of the Y^{3+} ion in the 1 M HDEHP in n-dodecane extractant decreases with an increase in the equilibrium aqueous H^+ concentration. From each synthesized aqueous solution of a particular acid concentration, a minimum of three data points is displayed. Given the unusual trend displayed by the distribution coefficient of yttrium at H^+ concentrations less 1 M it was then decided that these points be retested at aqueous H^+ concentrations of $\approx 0.2 - 1.8$ M to confirm the results obtained. The results obtained from the confirmatory testing are indicated by an asterisk in Table 5.3 and a ♦ symbol in Figure 5.5.

Table 5.3 The distribution coefficients, D_Y, for Y^{3+} ions between an organic phase (1 M HDEHP in n-dodecane) and aqueous phase concentrations with expanded uncertainties at T = 298.15 K and P = 101.3 kPa

D_Y	$[H^+]$ /M	$[Y^{3+}]_{aq}$ /ppm	$U([Y^{3+}])_{aq}$ /ppm	$[Y^{3+}]_{org}$ /ppm	$U([Y^{3+}])_{org}$ /ppm
13.38	2.1404	1.85	0.209	24.81	0.070
13.04	2.2183	1.90	0.209	24.76	0.068
18.16	2.1127	1.39	0.208	25.27	0.095
65.11	1.8849	0.41	0.208	26.63	0.361
20.46	1.9257	1.26	0.208	25.78	0.107
21.31	1.9085	1.21	0.208	25.83	0.112
33.45	1.5537	0.81	0.208	26.94	0.177
33.86	1.6436	0.80	0.208	26.95	0.179
34.26	1.5312	0.79	0.208	26.96	0.181
44.05	1.3138	0.60	0.208	26.35	0.236
45.05	1.3523	0.59	0.208	26.36	0.242
43.32	1.3211	0.61	0.208	26.34	0.232
54.40	1.0934	0.49	0.208	26.69	0.297
53.59	1.1363	0.50	0.208	26.68	0.292
56.10	1.0993	0.48	0.208	26.71	0.307
67.68	0.7539	0.40	0.208	27.21	0.379
67.64	0.8003	0.40	0.208	27.20	0.379
67.72	0.6880	0.40	0.208	27.21	0.380
*71.46	0.3142	0.37	0.208	26.48	0.406
*71.68	0.2776	0.37	0.208	26.48	0.408
*71.51	0.2698	0.37	0.208	26.48	0.407
*70.71	0.5633	0.37	0.208	26.34	0.402
*70.71	0.5499	0.37	0.208	26.34	0.402
*70.83	0.5361	0.37	0.208	26.34	0.403
*67.49	0.8880	0.40	0.208	27.16	0.378
*67.81	0.8751	0.40	0.208	27.16	0.380
*68.04	0.9235	0.40	0.208	27.16	0.382
*55.37	1.2236	0.49	0.208	27.16	0.302
*55.58	1.2603	0.49	0.208	27.17	0.303
*69.43	1.1749	0.39	0.208	27.26	0.390
*41.69	1.4837	0.61	0.208	25.44	0.223
*42.78	1.5767	0.59	0.208	25.45	0.230
*42.41	1.4596	0.60	0.208	25.45	0.227
*27.51	1.7611	0.93	0.208	25.64	0.145
*27.54	1.8003	0.93	0.208	25.64	0.145
*29.59	1.7122	0.87	0.208	25.70	0.156

*Represents retested data.

$U([H^+])$ = 0.0003 for all distribution coefficient values

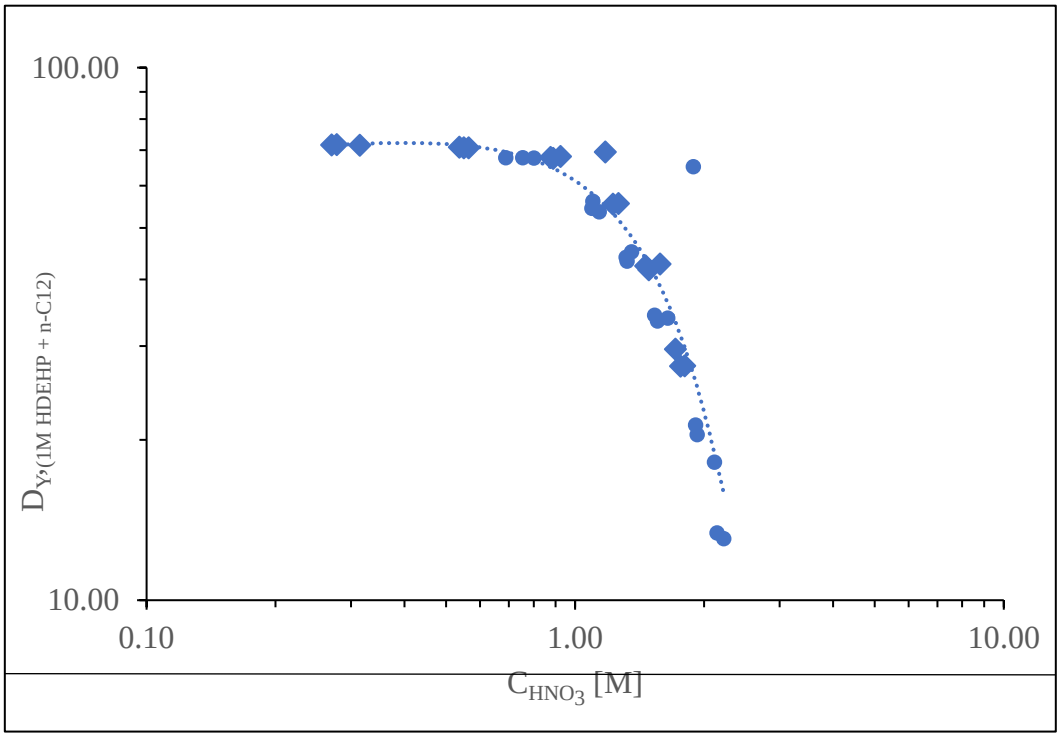

Figure 5.3 The distribution coefficients for Y^{3+} ions between the organic phase of 1 M HDEHP in n-dodecane and a nitric acid aqueous phase at T = 298.15 K and P = 101.3 kPa. ●- initial test; ♦ - confirmatory test.

The variation of the distribution coefficient extends from D_Y = 71.68 at low aqueous equilibrium [H^+] to D_Y = 13.04 at the higher end of [H^+]. The inverse relationship that is observed between the distribution coefficient and the equilibrium H^+ concentration in aqueous phase is typical of what one can expect to see in cases where an acidic extractant is employed, in this case HDEHP. Due to the concentration of H^+ ions present, an increase in the effect of substitution of the Y^{3+} from the H^+ ion complexes can be clearly observed. In the case of extraction, the results imply that operation at lower concentrations of the aqueous H^+ ion would yield a higher level of performance resulting in a higher distribution coefficient. Conversely, the decision can be made to select a higher concentration of the aqueous H^+ ion for the increased benefit this will have on stripping operations.

However, as the concentration of H^+ in the aqueous phase decreases (less than ≈ 1 M) an approach towards a horizontal slope in the trend of the distribution coefficient is observed. This indicates the onset of distribution coefficient saturation effects at $D_Y \approx 70.00$. Upon the realisation of this phenomena the samples analysed were sent for retesting, new solutions were synthesised, and the experiments repeated. This retesting confirmed this saturation (linear fashion) of the organic phase with Y^{3+} at acid concentrations below ≈ 1 M. The competitive

complexation theory presented by Sato (1989) could provide an explanation for the saturation region of the distribution coefficient occurring in LLE extraction systems. This relates to the complexation density of the extractant when contacted with an aqueous mixture of a specified metal ion concentration. To overcome the saturation effects the reader is referred to Sato (1989) whose work suggests an increase in the concentration of the metal ion concentration in the aqueous phase. At lower acid concentrations, it is postulated that the extraction is dominated by the formation of polymeric Y-HDEHP complexes and not simply by a solvating reaction. The nature of the Y-HDEHP complex formed and its Y composition (e.g. 1Y:3HDEHP, 2Y:5HDEHP) is affected by the composition of Y in the aqueous phase. It was then decided to fit (initially) a third-order polynomial to this data yielding an R^2 of 0.7164 and subsequently a $D_Y|_{[H^+]=1}$ value of 61.30.

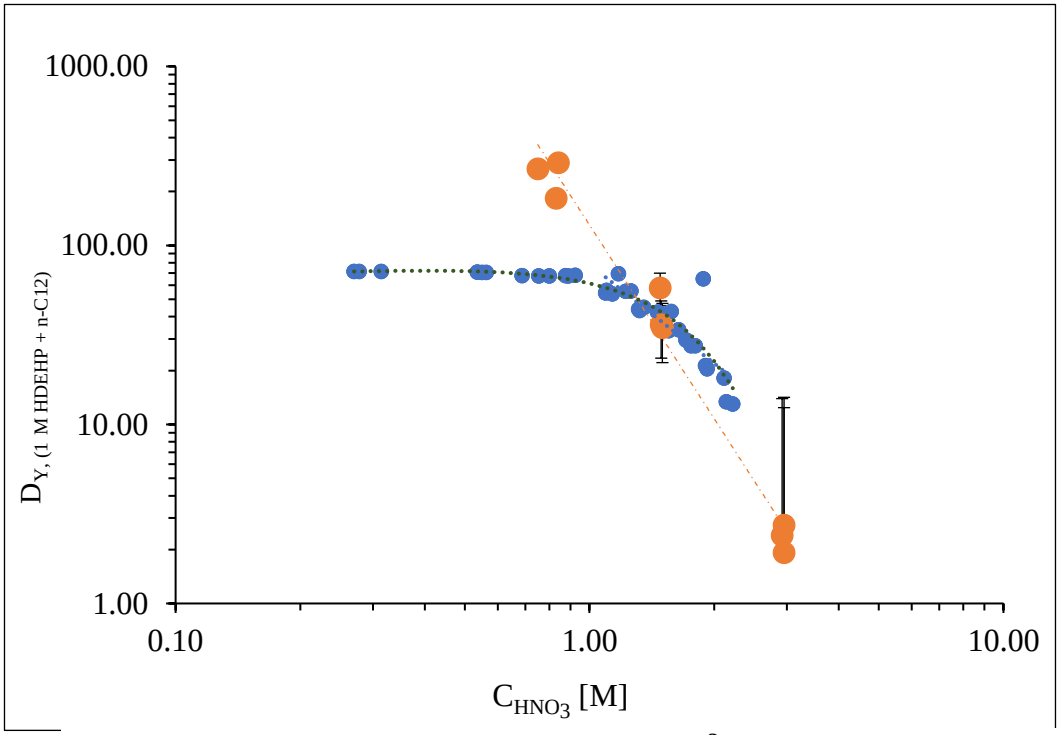

Figure 5.4 The distribution coefficients for Y^{3+} ions between the organic phase of 1 M HDEHP in n-dodecane and a nitric acid aqueous phase at T = 298.15 K and P = 101.3 kPa. ●, This work; ●,Williams-Wynn *et al.* (2020).

Figure 5.3 shows that the distribution coefficient of the Y^{3+} ion in the 1 M HDEHP extractant decreases with an increase in the aqueous H^+ concentration above ≈ 1 M and the onset of organic phase saturation effects for concentrations of the aqueous H^+ less than ≈ 1 M. When the results obtained in this work (see Figure 5.3) are compared with those obtained by Williams-Wynn *et al., (*2020) (Figure 5.4), the saturation behaviour occurring in the acid concentration region below ≈ 1 M becomes more apparent. This is in contrast to the data obtained Williams-Wynn *et al., (*2020) which shows no onset of organic phase saturation effects at aqueous acid concentrations lower than ≈ 1 M (Figure 5.4). As yttrium is not the metal ion of focus in this work, the scenario of increasing the metal ion concentration in the aqueous phase for the purpose of overcoming the saturation effect was not experimentally explored. The uncertainties calculated in this work have been found to be of an order of magnitude that is indiscernible when displayed on the graph. However, those obtained by Williams-Wynn *et al., (*2020) show that the data measured in this work is within an acceptable range for the region in which the organic phase is not saturated.

To aid in comparing the data obtained in this work to that of Williams-Wynn *et al., (*2020), an exponential trendline is fitted to the data; from which an inverse relationship between the distribution coefficient and the acid concentration is observed. The R^2 value obtained for the inversely proportional section of the D_Y from the system of this work is 0.9567 whereas that obtained by Williams-Wynn *et al., (*2020) is 0.9772. The assertion of inverse proportionality between the distribution coefficient D_Y and the aqueous acid concentration H^+ is supported by objectively observing the negative gradients of the trendlines (-3.591 for Williams-Wynn *et al., (*2020); and -2.281 for this work). The $D_Y|_{[H^+] = 1.3}$ value obtained in this work is 50.67 and the value obtained by Williams-Wynn *et al., (*2020) is $D_Y|_{[H^+] = 1.3}$ is 48.80.

5.4 New data: Extraction of Neodymium using HDEHP in n-Dodecane

Neodymium is the REE of focus in this work. All data measured and presented was obtained using the experimental procedure as outlined in Chapter 4 at a constant temperature of 298.15 K and a constant pressure of 101.3 kPa. At each aqueous acid concentration, three tests were conducted (aliquoted from the same organic and aqueous solution) in three separate stirred cells. The sample withdrawn from each cell was tested thrice by ICP-OES analysis. From each synthesized aqueous solution of a particular acid concentration, a minimum of three data points is displayed. The distribution coefficient data obtained is presented first in a table format then in graphical form.

5.4.1 1 M HDEHP in n-Dodecane

The organic extractant mixture used in the results presented hereunder is HDEHP in n-dodecane at a concentration of 1 M, with nitric acid as the source of the H^+ ions in the aqueous phase. Table 5.4 and Figure 5.5 presented below represent the data measured and plotted for the 1 M HDEHP in n-dodecane system. The data is presented graphically as two independent series, the ‘minor’ of which is represented using an asterisk in Table 5.4 and ▲ in Figure 5.5

Table 5.4 The distribution coefficients, D_{Nd}, for Nd^{3+} ions between an organic phase (1 M HDEHP in n-dodecane) and aqueous phase concentrations with expanded uncertainties at T= 298.15 K and P = 101.3 kPa.

D_{Nd}	$[H^+]$ /M	$[Nd^{3+}]_{aq}$ /ppm	$U([Nd^{3+}])_{aq}$ /ppm	$[Nd^{3+}]_{org}$ /ppm	$U([Nd^{3+}])_{org}$ /ppm
0.01	2.1108	20.73	0.217	0.30	0.000
*0.23	2.0903	16.53	0.215	3.90	0.005
0.05	1.7494	19.73	0.216	1.03	0.001
0.03	1.8364	20.13	0.216	0.63	0.001
0.02	1.8739	20.30	0.216	0.47	0.000
0.09	1.4528	19.20	0.216	1.63	0.002
0.05	1.5018	19.80	0.216	1.03	0.001
0.06	1.4851	19.73	0.216	1.10	0.001
0.09	1.2511	18.80	0.217	1.63	0.002
0.14	1.2258	17.90	0.216	2.53	0.003
0.08	1.2624	18.90	0.216	1.53	0.002
0.16	0.9445	16.90	0.217	2.73	0.003
0.18	0.9851	16.60	0.217	3.03	0.003
0.13	1.0084	17.30	0.217	2.33	0.003
0.43	0.7120	14.00	0.218	6.00	0.007
0.56	0.6597	12.80	0.217	7.20	0.009
0.56	0.6734	12.83	0.217	7.17	0.009
3.45	0.4775	4.52	0.218	15.51	0.026
2.66	0.5052	5.48	0.220	14.55	0.023
2.60	0.4491	5.58	0.220	14.46	0.022
*274.26	0.2701	0.06	12.347	19.51	70.706
182.63	0.1728	0.09	12.878	19.48	69.877
*394623.49	0.2386	0.01	12.028	19.58	76.519
6.34	0.2156	2.89	0.231	18.30	0.043
9.93	0.2886	1.94	0.227	19.25	0.053
7.37	0.2782	2.53	0.229	18.66	0.046

*Represents the distribution coefficient values D_{Nd} that form part of the 'minor' independent series.

$U([H^+]) = 0.0003$ for all distribution coefficient values

It becomes apparent from cursory analysis of the data presented in Table 5.4 above that two of the measured distribution coefficient data points lie outside the general trend of the line describing the distribution coefficient (D_{Nd} =274.26, D_{Nd} =394623.49). To confirm the anomalous nature of the two aforementioned data points further measurements were conducted. These further measurements yielded results that were consistent with the initially measured data set. No differentiation has been made between the remeasured data and the initially measured data as no significant technical value would be gained from denoting them differently

or as part of a new independent series. By assigning the anomalous distribution coefficient data to a 'minor' independent series the precision and predictive accuracy of the distribution coefficient data at a 1 M HDEHP concentration was enhanced.

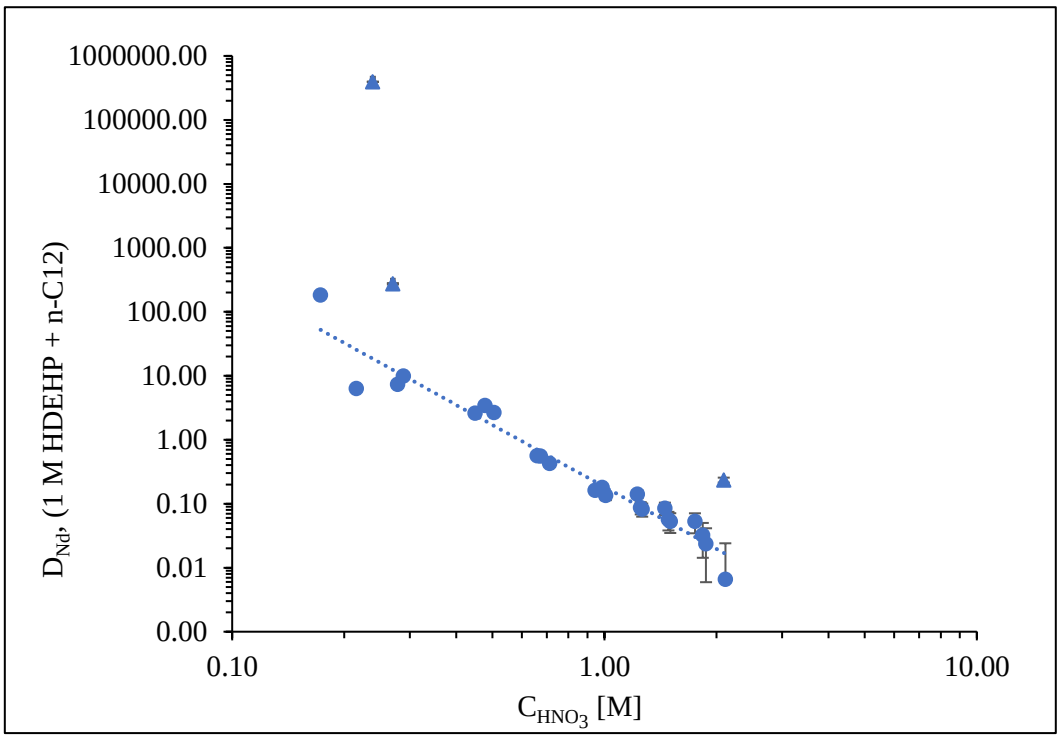

Figure 5.5 distribution coefficients for Nd^{3+} ions between the organic phase of 1 M HDEHP in n-dodecane and a nitric acid aqueous phase at T = 298.15 K and P = 101.3 kPa. ●, This work (major trendline); ▲, This work (independent series).

Figure 5.5, shown above, is a graphical representation of the distribution coefficient of neodymium extracted with 1 M HDEHP in n-dodecane plotted at various acid concentrations. The trendline fitted to the plotted data (with an R^2 value of 0.9528) shows that the distribution coefficient of the Nd^{3+} ion in the 1 M HDEHP extractant decreases with an increase in the aqueous H^+ concentration. This can be said to be an inversely proportional relationship between the distribution coefficient (D_{Nd}) and the aqueous acid concentration ($[H^+]$).

The assertion of inverse proportionality between the distribution coefficient D_{Nd} and the aqueous acid concentration is supported by objectively observing the less than zero gradient, g, of the trendline described by $(\partial(ln(D))/\partial(ln([H^+]))$ = -3.22. The value of the distribution coefficient at the aqueous acid concentration of 1 M ($D_{Nd|[H^+]=1}$) is equal to a value of 0.18.

5.4.2 0.5 M HDEHP in n-Dodecane

In Table 5.5 and the subsequently presented Figure 5.6 the distribution coefficients, aqueous acidic H^+ concentrations at equilibrium and associated uncertainties are shown. The organic extractant mixture used in the results presented below is HDEHP in n-dodecane at a concentration of 0.5 M HDEHP. The hydronium ion in the prepared aqueous solutions was a result of nitric acid being employed.

Table 5.5 The distribution coefficients, D_{Nd}, for Nd^{3+} ions between an organic phase (0.5 M HDEHP in n-dodecane) and aqueous phase concentrations with expanded uncertainties at T= 298.15 K and P = 101.3 kPa.

D_{Nd}	$[H^+]$ /M	$[Nd^{3+}]_{aq}$ /ppm	$U([Nd^{3+}])_{aq}$ /ppm	$[Nd^{3+}]_{org}$ /ppm	$U([Nd^{3+}])_{org}$ /ppm
0.03	1.6790	20.17	0.22	0.60	0.001
0.03	1.8616	20.27	0.22	0.50	0.001
0.06	1.8380	19.53	0.22	1.23	0.001
0.03	1.4924	20.20	0.22	0.63	0.001
0.03	1.5522	20.17	0.22	0.67	0.001
0.05	1.5400	19.93	0.22	0.90	0.001
0.03	1.3154	19.93	0.22	0.50	0.001
0.02	1.3127	20.03	0.22	0.40	0.001
*0.01	1.0192	19.43	0.22	0.20	0.000
*0.005	0.9987	19.53	0.22	0.10	0.000
0.15	0.7576	17.30	0.22	2.70	0.003
0.12	0.7451	17.90	0.22	2.10	0.003
0.10	0.7712	18.23	0.22	1.77	0.002
0.75	0.4715	11.43	0.22	8.60	0.011
0.64	0.4573	12.20	0.22	7.83	0.010
0.64	0.4670	12.23	0.22	7.80	0.007
*61.59	0.1698	0.31	0.71	19.26	0.690
*29.19	0.1843	0.63	0.82	18.94	0.574
*141.49	0.1808	0.13	0.70	19.44	0.817
7.16	0.1357	2.60	0.23	18.59	0.048
7.13	0.1336	2.61	0.23	18.58	0.048
20.12	0.1201	1.00	0.23	20.18	0.086
0.17	0.7640	16.76	0.22	2.86	0.004
0.06	0.8286	18.45	0.22	1.17	0.002
0.09	0.8109	17.97	0.22	1.66	0.002
0.02	2.1215	19.43	0.22	0.39	0.000

*Represents values assigned to an independent series

$U([H^+]) = 0.0003$ for all distribution coefficient values

The data points first measured displayed an appreciable degree of scatter at the hydronium ion concentration regions of ≈ 0.1 M, ≈ 0.9 M and ≈ 2.9 M [H^+]. It was deemed necessary to retest these points to further investigate the behavior of the distribution in these regions. In the table above (Table 5.5) the distribution coefficients are presented including retested data points. This additional data was then used to observe the clustering of data and determine the accurate values of the distribution coefficient in the mentioned regions and assigning the anomalous values of the distribution coefficient as part of an independent series, as shown in Figure 5.6.

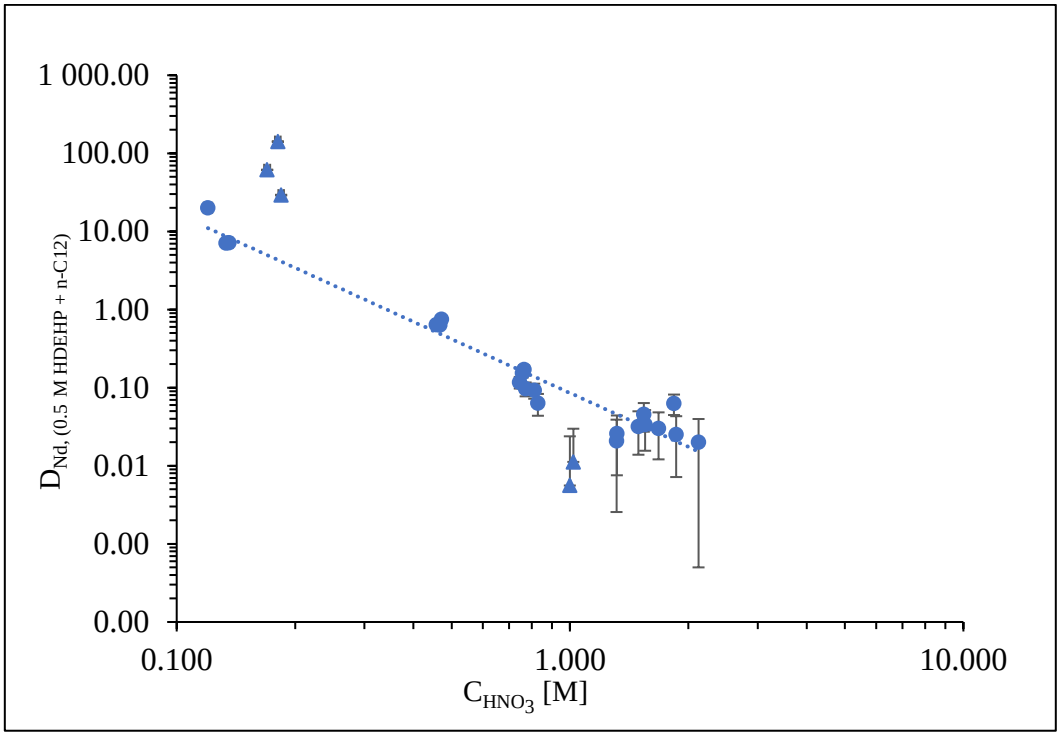

Figure 5.6 The distribution coefficients for Nd^{3+} ions between the organic phase of 0.5 M HDEHP in n-dodecane and a nitric acid aqueous phase at T = 298.15 K and P = 101.3 kPa. ●, This work (major trendline); ▲, This work (independent series).

The distribution coefficient of neodymium was plotted at various acid concentrations (see Figure 5.6). When the distribution coefficient of neodymium when extracted with 0.5 M HDEHP in n-dodecane a trendline (with an R^2 value of 0.9507) was fitted. The negative gradient of the trendline indicates that the distribution coefficient of the Nd^{3+} ion in the 0.5 M HDEHP extractant decreases with an increase in the aqueous H^+ concentration. This is an inversely proportional relationship between the distribution coefficient (D_{Nd}) and the aqueous acid concentration ([H^+]). The negative gradient of the trendline described by

$(\partial(ln(D))/\partial(ln([H^+]))$ = -2.29 quantifies the value of the gradient and supports the assertion of inverse proportionality between the distribution coefficient D_{Nd} and the acid concentration $[H^+]$. The value of the distribution coefficient at the acid concentration of 1 M ($D_{Nd|[H^+]=1}$) can be found using the trendline and was found to be 0.09.

5.4.3 0.5 M and 1 M HDEHP in n-dodecane

The data presented graphically and summarized below is the distribution coefficient measured using the 0.5 M HDEHP and 1 M HDEHP extractants in n-dodecane. This is the same data as presented in Figure 5.5 and Figure 5.6, above, but is presented on the same set of axes for the purpose of comparison and discussion

Table 5.6 Parameters for the linear relationship between $ln(D)$ and ($ln([H^+])$ for the experimentally measured distribution coefficients of HDEHP extractant systems.

[HDEHP]	$(\partial(ln(D))/\partial(ln([H^+]))$	$D_{Nd\|[H^+]=1}$	R^2
1	-3.22	0.18	0.9528
0.5	-2.29	0.09	0.9507

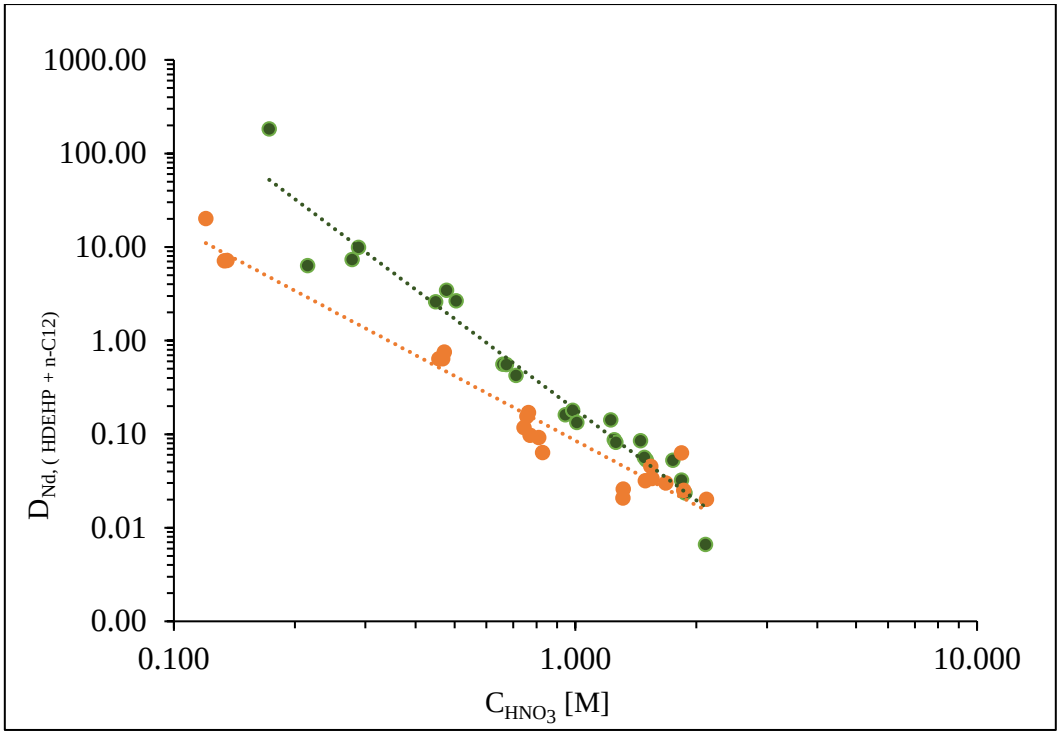

Figure 5.7 The distribution coefficients for Nd^{3+} ions between the organic phase of HDEHP in n-dodecane and a nitric acid aqueous phase at T = 298.15 K and P = 101.3 kPa. ●, 1 M HDEHP extractant and ●, 0.5 M HDEHP extractant.

It can be seen from Figure 5.7 that the distribution coefficient of neodymium, when extracted with HDEHP in n-dodecane, shows an inversely proportional relationship with the concentration of the acid in the aqueous phase. The gradient $(\partial(ln(D))/\partial(ln([H^+]))$ of both LLE systems displays this in their negative non-zero values (see Table 5.6). It is evident from the graphical representation of this data that the distribution coefficient of neodymium with 1 M HDEHP extractant in n-dodecane is greater than that displayed by extraction using 0.5 M HDEHP in n-dodecane at the acid concentrations tested in this work. This is directly related to the proportion of extracting ions in the phosphorous acid able to form aqueous soluble complexes. Furthermore, observing the value of $D_{Nd|[H^+]=1}$ (see Table 5.6) for both the 0.5 M and 1 M HDEHP extractant concentrations (0.09 and 0.18 respectively; it can be stated that for aqueous solutions with a nitric acid concentration less than ≈ 2.27 M, the distribution coefficient has a directly proportional relationship with the concentration of the HDEHP in the organic extractant solution. The existence of this direct proportionality is indicative of the extraction process being governed by ion exchange reaction principles. The value of $(\partial(ln(D))/\partial(ln([H^+]))$ (≈ 3) further supports this assertion as this is consistent with the ratio of H^+ ions provided by the dissociation of nitric acid (HNO_3). This also indicates the dissociation

and participation of a single acid group in a HDEHP dimer in the organic phase of the extraction reaction.

It is also evident, however, from Figure 5.7 that the proportional relationship between the HDEHP concentration and the distribution coefficient does not hold for all nitric acid concentrations. Using the data presented in Table 5.6 and Figure 5.7 it can be determined by calculation that at an acid concentration of 2.27 M, the distribution coefficient obtainable with extractant with a 1 M and 0.5 M HDEHP concentration is equal (D_{Nd} = 0.01). Thereafter (i.e., at acid concentrations greater than 2.27 M), using the fitted trendlines, it is predicted that the relationship between the distribution coefficient and the concentration of the acid in the organic phase becomes inversely proportional.

5.4.4 0.1 M HDEHP in n-dodecane

Presented below in Table 5.7 are the results for the distribution coefficient as obtained for neodymium-nitric acid solutions, when contacted with an organic phase of 0.1 M HDEHP in n-dodecane. Given the relatively high degree of scatter and an unclear trend observed in the entire data set, the entire system was retested to provide a clearer understanding of the behavior of the distribution coefficient behavior at these conditions. This additional data was plotted on the same set of axes, without any improvement in the observability of a general trend. Table 5.7 below displays the measured data, showing the first set of measurements and the retested measurements.

Table 5.7 The distribution coefficients, D_{Nd}, for Nd^{3+} ions between an organic phase (0.1 M HDEHP in n-dodecane) and aqueous phase concentrations with expanded uncertainties at T= 298.15 K and P = 101.3 kPa.

D_{Nd}	$[H^+]$ /M	$[Nd^{3+}]_{aq}$ /ppm	$U([Nd^{3+}])_{aq}$ /ppm	$[Nd^{3+}]_{org}$ /ppm	$U([Nd^{3+}])_{org}$ /ppm
0.08	1.9067	18.87	0.22	1.57	0.0020
0.02	1.8912	20.43	0.22	0.33	0.0005
0.00	1.8722	20.77	0.22	0.00	0.0001
0.12	1.7254	18.47	0.22	2.30	0.0027
0.03	1.6489	20.13	0.22	0.70	0.0009
0.03	1.6315	20.30	0.22	0.53	0.0006
0.03	1.5699	20.23	0.22	0.60	0.0007
0.02	1.3478	20.13	0.22	0.30	0.0003
0.01	0.7724	19.73	0.22	0.27	0.0004
1.30	0.2213	8.51	0.21	11.06	0.0153
1.21	0.1809	8.84	0.22	10.73	0.0144
1.34	0.2128	8.38	0.22	11.19	0.0156
Retested Data					
1.33	0.1099	9.08	0.22	12.11	0.0180
1.23	0.1340	9.52	0.22	11.67	0.0173
1.28	0.1128	9.28	0.22	11.91	0.0177
0.01	0.4477	20.35	0.21	0.29	0.0005
0.01	0.4546	20.31	0.22	0.23	0.0004
0.08	0.8296	18.19	0.22	1.43	0.0022
0.02	1.3891	18.84	0.22	0.39	0.0013
0.04	1.3518	18.84	0.22	0.85	0.0014

$U([H^+]) = 0.0003$ for all distribution coefficient values

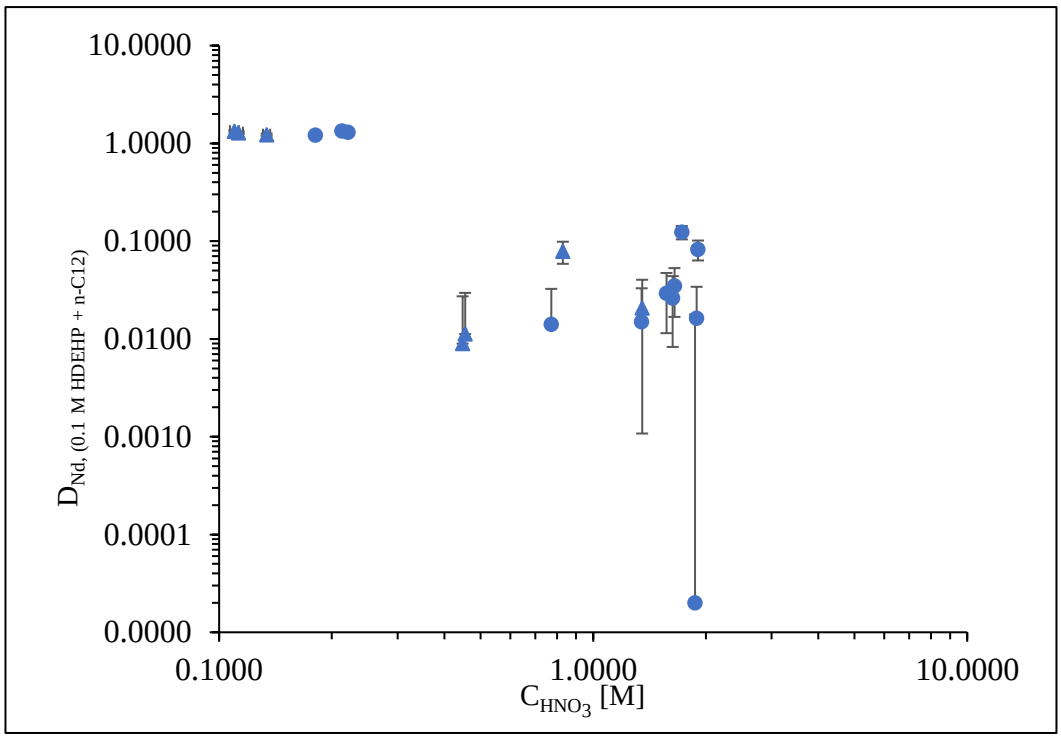

Figure 5.8 The distribution coefficients for Nd^{3+} ions between the organic phase of 0.1 M HDEHP in n-dodecane and a nitric acid aqueous phase at T = 298.15 K and P = 101.3 kPa. ●, This work (first test); ▲, This work (retest).

HDEHP of 0.1 M in n-dodecane is the extractant that was employed to yield the distribution coefficients plotted at various acid concentrations (see Figure 5.8). Observing that no consistent clusters appeared in the plotted data, no trendline was fitted with a satisfactory coefficient of correlation. However, it can be observed from the data (despite the large uncertainties and wide range of scatter) that the inversely proportional relationship between the distribution coefficient of the Nd^{3+} ion and the H^{+} concentration as observed in the 1 M and 0.5 M HDEHP (see Section 5.4.1 and 5.4.2) extractant systems is apparent.

5.5 Neodymium extracted with HDEHP and $BMImNTf_2$ in n-dodecane

5.5.1 0.5 M HDEHP, 0.19 M $BMImNTf_2$ in n-dodecane

The organic extractant mixture of 0.5 M HDEHP and 0.19 M $BMImNTf_2$ in n-dodecane together with nitric acid as the source of the H^+ ions in the aqueous phase were measured at 298.15 K. At each acid concentration, triplicate measurements were conducted (equivalent aliquots of the same organic and aqueous solution) in three separate stirred glass cells. The sample from each cell was tested thrice using ICP-OES testing. For each acid concentration (i.e., same synthesized solution) three data points are displayed. The data obtained is presented in the form of a table in Table 5.8 and presented graphically in Figure 5.9.

Table 5.8 The distribution coefficients, D_{Nd}, for Nd^{3+} ions between an organic phase (0.5 M HDEHP and 0.19 M $BMImNTf_2$ in n-dodecane) and aqueous phase concentrations with expanded uncertainties at T= 298.15 K and P = 101.3 kPa.

D_{Nd}	$[H^+]$ /M	$[Nd^{3+}]_{aq}$ /ppm	$U([Nd^{3+}])_{aq}$ /ppm	$[Nd^{3+}]_{org}$ /ppm	$U([Nd^{3+}])_{org}$ /ppm
64.50	0.0878	0.30	0.61	19.54	0.61
63.57	0.1053	0.31	0.61	19.53	0.58
158.70	0.1161	0.12	0.60	19.71	0.96
0.70	0.5089	11.80	0.21	8.27	0.01
0.73	0.5041	11.60	0.21	8.47	0.01
0.69	0.5171	11.87	0.21	8.20	0.01
0.13	0.8002	17.85	0.21	2.28	0.00
0.12	0.8289	17.98	0.21	2.15	0.00
0.13	0.7847	17.75	0.21	2.38	0.00
0.05	1.1582	18.98	0.21	0.96	0.00
0.04	1.1848	19.14	0.21	0.80	0.00
0.03	1.1493	19.34	0.21	0.60	0.00
0.04	1.4578	20.07	0.21	0.90	0.00
0.03	1.4329	19.84	0.21	0.53	0.00
0.01	1.4809	20.20	0.21	0.25	0.00
0.07	1.6689	19.08	0.21	1.26	0.00
0.04	1.6508	19.47	0.21	0.86	0.00
0.28	1.5919	15.71	0.21	4.36	0.01
0.00	2.2483	21.10	0.21	0.00	0.00

$U([H^+]) = 0.0003$ for all distribution coefficient values

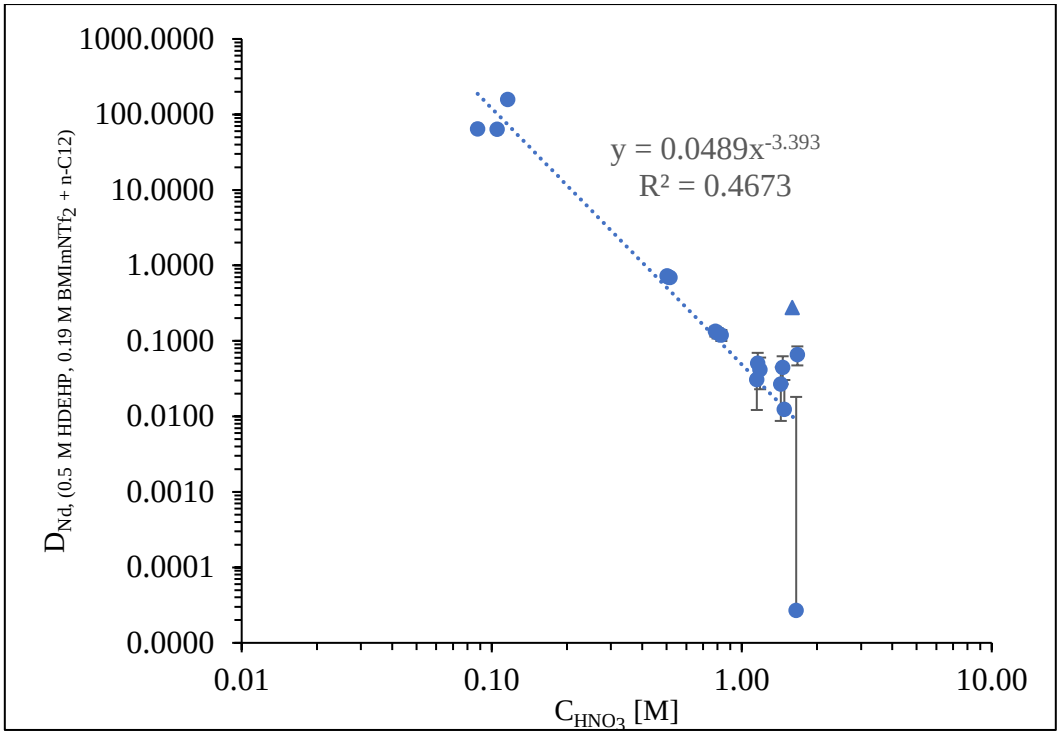

Figure 5.9 The distribution coefficients for Nd^{3+} ions between the organic phase of 0.5 M HDEHP, 0.19 $BMImNTf_2$ in n-dodecane and a nitric acid aqueous phase at T = 298.15 K and P = 101.3 kPa.

From Figure 5.9 presented above the distribution coefficient of neodymium extracted from solutions of varying aqueous nitric acid concentrations can be seen.

With the line of "best fit" plotted against the distribution coefficient data, a correlation coefficient value of R^2 = 0.8055 was determined. This value of 0.8055 is indicative of a distribution coefficient trend in which the Nd^{3+} ion in the 0.5 M HDEHP and 0.19 M $BMImNTf_2$ extractant decreases with an increase in the aqueous H^+ concentration. This type of exhibited behaviour can be described as inversely proportional. The gradient, g, of the trendline fitted to the data in Figure 5.9, can be described in the following expression $(\partial(ln(D))/\partial(ln([H^+]))$ = -3.39. This less than zero gradient of the trendline supports the assertion of inverse proportionality between the distribution coefficient D_{Nd} and the aqueous $[H^+]$. When the solution of 0.5 M HDEHP and 0.19 M $BMImNTf_2$ in n-dodecane was contacted with an aqueous solution containing neodymium ions in a 1 M $[H^+]$ the distribution coefficient observed (ie. $D_{Nd|[H^+]=1}$) was 0.04.

5.5.2 0.5 M HDEHP, 0.019 M $BMImNTf_2$ in n-dodecane

The distribution coefficient of neodymium was determined between an organic solution of 0.5 M HDEHP with 0.019 M $BMImNTf_2$ in n-dodecane and a solution containing nitric acid as the source of the H^+ ions in the aqueous phase at a constant temperature of 298.15 K. Measurements were conducted in triplicate and analyzed in triplicate by ICP-OES testing. At each acid concentration three data points are displayed. Table 5.9 presents the data in the form of a table whereas Figure 5.10 presents the data in graphical form.

Table 5.9 The distribution coefficients, D_{Nd}, for Nd^{3+} ions between an organic phase (0.5 M HDEHP and 0.019 M $BMImNTf_2$ in n-dodecane) and aqueous phase concentrations with expanded uncertainties at T= 298.15 K and P = 101.3 kPa.

D_{Nd}	$[H^+]$ /M	$[Nd^{3+}]_{aq}$ /ppm	$U([Nd^{3+}])_{aq}$ /ppm	$[Nd^{3+}]_{org}$ /ppm	$U([Nd^{3+}])_{org}$ /ppm
83.11	0.1002	0.24	0.54	19.60	0.74
59.52	0.1016	0.33	0.55	19.51	0.65
72.77	0.1189	0.27	0.54	19.57	0.70
0.73	0.4753	11.60	0.21	8.47	0.01
0.75	0.5114	11.44	0.21	8.63	0.01
0.74	0.4950	11.54	0.21	8.53	0.01
0.23	0.9049	16.43	0.21	3.70	0.00
0.19	0.8533	16.93	0.21	3.21	0.00
0.16	0.9414	17.36	0.21	2.78	0.00
0.09	1.1873	18.32	0.21	1.62	0.00
0.09	1.1093	18.28	0.21	1.65	0.00
0.12	1.0881	17.75	0.21	2.18	0.00
0.05	1.4114	19.44	0.21	0.93	0.00
0.04	1.3958	19.67	0.21	0.70	0.00
0.05	1.4029	19.34	0.21	1.03	0.00
0.04	1.6639	19.54	0.21	0.80	0.00
0.01	1.6621	20.04	0.21	0.30	0.00
0.05	1.6921	19.27	0.21	1.06	0.00

$U([H^+])$ = 0.0003 for all distribution coefficient values

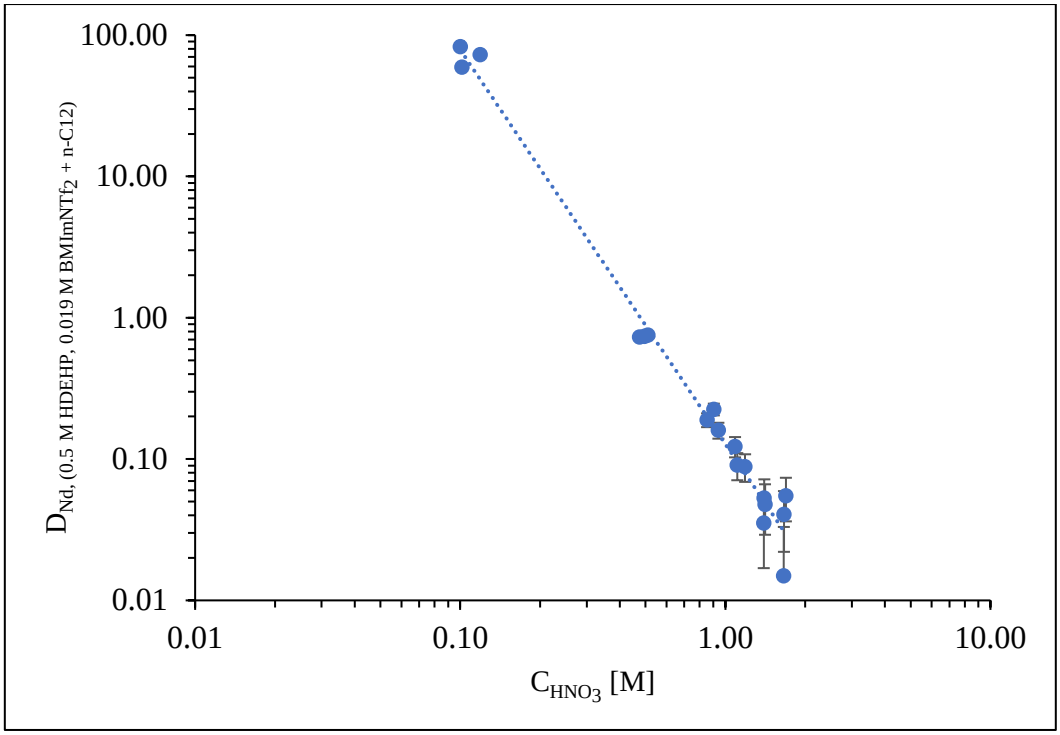

Figure 5.10 The distribution coefficients for Nd^{3+} ions between the organic phase of 0.5 M HDEHP, 0.019 M $BMImNTf_2$ in n-dodecane and a nitric acid aqueous phase at T = 298.15 K and P = 101.3 kPa.

The distribution coefficient that quantifies the behaviour of neodymium when extracted with a solution of 0.5 M HDEHP with 0.019 M $BMImNTf_2$ in n-dodecane was plotted at various acid concentrations (see Figure 5.10). To gain understanding into the overall behaviour of the distribution coefficient at these conditions a trendline was fitted to the plotted data (with an R^2 value of 0.9865). This plotted trendline shows that the distribution coefficient of the Nd^{3+} ion in the 0.5 M HDEHP and 0.019 M $BMImNTf_2$ extractant decreases with an increase in the aqueous H^+ concentration. This behaviour between the distribution coefficient (D_{Nd}) and the aqueous acid concentration is what can be described as typical inverse proportionality. Using the trendline plotted in Figure 5.10 two additional parameters can be calculated: the gradient and the value of the distribution coefficient at an aqueous acid concentration of 1M. The assertion of inverse proportionality between the distribution coefficient D_{Nd} and the aqueous $[H^+]$ is supported by objectively observing the calculated less than zero gradient (-2.79). At the aqueous acid concentration of 1 M the value of the distribution coefficient (ie. $D_{Nd}|_{[H^+]=1}$) was found to be 0.13.

5.5.3 0.5 M HDEHP and $BMImNTf_2$ concentration comparison in n-dodecane

The data presented graphically hereunder is the distribution coefficient measured with an extractant of 0.5 M HDEHP combined synergistically with 0.19 M $BMImNTf_2$ and 0.5 M HDEHP with 0.0191 M $BMImNTf_2$ in n-dodecane. This is the same data as presented in Table 5.10 and Figure 5.9 above, but below it is presented on the same set of axes for the purpose of comparison. To observe the effect of the addition of the $BMImNTf_2$, the data of 0.5 M HDEHP in n-dodecane (Figure 5.6) is also presented in Figure 5.11 below.

Table 5.10 Parameters for the linear relationship between $ln(D)$ and ($ln([H^+])$ for the experimentally measured distribution coefficients of HDEHP an $BMImNTf_2$ (IL) extractant systems

[HDEHP]/ M	IL/ M	$(\partial(ln(D))/\partial(ln([H^+]))$	$D_{Nd\|[H^+]=1}$	R^2
0.5	0.19	-3.39	0.04	0.8055
0.5	0.019	-2.79	0.13	0.9865
0.5	0	-2.29	0.09	0.9507

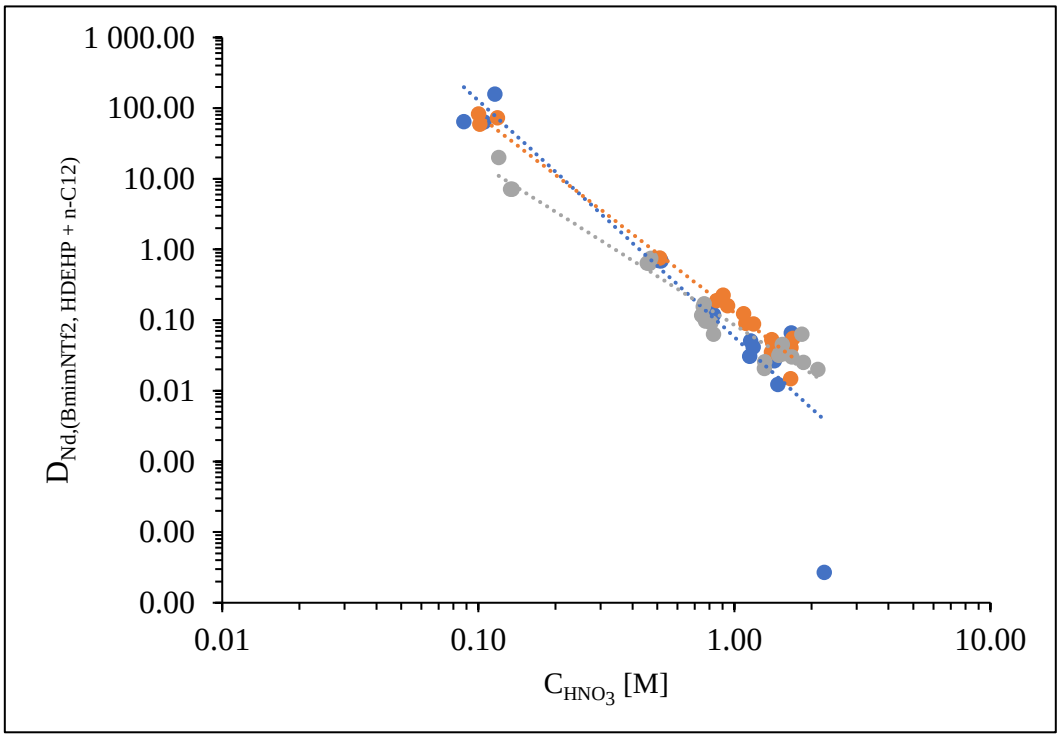

Figure 5.11 The distribution coefficients for Nd3+ ions between the organic phase of 0.5 M HDEHP in n-dodecane and a nitric acid aqueous phase at T = 298.15 K and P = 101.3 kPa. ●, indicating 0.019 M $BMImNTf_2$ extractant; ●, indicating 0.19 M $BMImNTf_2$ and ●, indicating 0 M $BMImNTf_2$.

It can be seen from Figure 5.11 above that the distribution coefficient of neodymium when extracted with HDEHP and $BMImNTf_2$ in n-dodecane shows an inversely proportional relationship with the concentration of the acid in the aqueous phase. The gradient $(\partial(ln(D))/\partial(ln([H^+]))$ of the ionic liquid containing LLE systems further supports the observation (negative non-zero values (see Table 5.10). It can also be stated that the distribution coefficient has an inversely proportional relationship to the concentration of the H^+ ion in the aqueous solution across the range of investigated nitric acid concentrations. The existence of this inverse proportionality is indicative of the extraction process being governed by ion exchange reaction principles. The values of $(\partial(ln(D))/\partial(ln([H^+]))$ (≈ 3) further support this assertion as this is consistent with the ratio of H^+ ions provided by the dissociation of nitric acid (HNO_3). This also indicates the dissociation and participation of a single acid group in a HDEHP dimer in the organic phase of the extraction reaction.

It is evident from the graphical representation of this data that the distribution coefficient of neodymium with 0.19 $BMImNTf_2$ containing extractant in n-dodecane is greater than that displayed by extraction using 0.019 $BMImNTf_2$ in n-dodecane at the acid concentrations tested in this study. It can be seen from Figure 5.11 that the presence of the ionic liquid in the organic extractant mixture increases the distribution coefficient compared to only HDEHP in n-dodecane. This assertion is only valid when comparing the HDEHP in n-dodecane extractant at aqueous H^+ concentrations less than 0.6024 M where the 0.019 $BMImNTf_2$ containing extractant is concerned and 2.2504 M where the 0.19 $BMImNTf_2$ containing extractant is concerned.

0.19 M $BMImNTf_2$ and 0 M $BMImNTf_2$ doped extractant

When observing the trendlines fitted to the distribution coefficients obtained by the use of 0.19 M $BMImNTf_2$ and 0 M $BMImNTf_2$ doped extractants, the general assertion of the distribution coefficient of increasing proportionally with an increase in the $BMImNTf_2$ concentration is only valid for aqueous H^+ concentrations less than 0.6024 M.

Using the data presented in Table 5.10 and Figure 5.11 it can be surmised by calculation that at the acid concentration of 0.6024 M the distribution coefficient displayed by the extractant doped with a 0.19 M $BMImNTf_2$ and 0 M $BMImNTf_2$ concentration of IL is equal ($D_{Nd} = 0.27$). Thereafter (i.e., at acid concentrations greater than 0.6024 M), using the fitted trendlines, it can

be said that the relationship between the distribution coefficient and the concentration of $BMImNTf_2$ in the organic phase becomes inversely proportional. Furthermore, observing the value of $D_{Nd}|_{[H^+]=1}$ (see Figure 5.11) for both the 0.19 M $BMImNTf_2$ and 0 M $BMImNTf_2$ extractant concentrations (0.04 and 0. 09 respectively), demonstrates the inversely proportional relationship of the concentration of $BMImNTf_2$ in the extractant to the distribution coefficient at aqueous acid concentrations greater than 0.6024 M.

0.019 M $BMImNTf_2$ and 0 M $BMImNTf_2$ doped extractant

When distribution coefficients are used as the basis to fit trendlines to the data that pertains to the 0.019 M $BMImNTf_2$ and 0 M $BMImNTf_2$ doped extractants, it can be stated that the distribution coefficient increases in an apparent linear manner on a log-log plot. This statement is only applicable for aqueous H^+ concentrations less than 2.2504 M.

Taking into account the data as presented in Table 5.10 and Figure 5.11, calculations can be used to find that at the aqueous acid concentration of 2.2504 M, the distribution coefficient displayed by the extractants containing concentrations of 0.019 M $BMImNTf_2$ and 0 M $BMImNTf_2$ is equal ($D_{Nd} = 0.01$). Inverse proportionality then defines the relationship between the distribution coefficient and the concentration of $BMImNTf_2$ in the organic phase for aqueous acid concentrations greater than 2.2504 M. The values of $D_{Nd}|_{[H^+]=1}$ are equal to 0.13 and 0. 09) for both the 0.019 M $BMImNTf_2$ and 0 M $BMImNTf_2$ extractant concentrations respectively (see Table 5.10). This is a demonstration of the proportional relationship between the concentration of $BMImNTf_2$ in the extractant to the distribution coefficient at aqueous acid concentrations below 2.2504 M.

0.19 M $BMImNTf_2$ and 0.019 M $BMImNTf_2$ doped extractant

The general assertion of the distribution coefficient increasing proportionally with an increase in the $BMImNTf_2$ concentration is only valid for aqueous H^+ concentrations greater than 0.2032 M, according to the trendlines fitted to the distribution coefficients achieved by using 0.19 M $BMImNTf_2$ and 0.019 M $BMImNTf_2$ extractants. Calculation (by using the data in Table 5.10 and Figure 5.11) showed that the distribution coefficient determined by the use of extractants with a 0.19 M $BMImNTf_2$ and a 0.019 M $BMImNTf_2$ concentration is equal (D_{Nd} = 10.88) at an aqueous acid concentration of 0.2032 M. The link between the distribution coefficient and the fitted trendlines may then be asserted (for acid concentrations less than 0.2032 M) to be inversely proportional. Furthermore, for both the 0.019 M $BMImNTf_2$ and 0

M $BMImNTf_2$ extractant concentrations, the value of $D_{Nd|[H+]} = 1$ (see Table 5.10) was observed (0.13 and 0.09 respectively). At aqueous acid concentrations below 2.2504 M, the data presented in Figure 5.11 shows the proportional relationship between the concentration of $BMImNTf_2$ in the extractant and the distribution coefficient.

5.6 Neodymium extracted with HDEHP and tributylmethylphosphonium methyl sulfate in n-Dodecane

Unique observations were made with regards to the homogeneity of the organic phase when experiments with the synergistic extractant of HDEHP and n-dodecane doped with tributylmethylphosphonium methyl sulfate were carried out. Upon the dispensing of the organic extractant into the equilibrium cells as described in Section 4.4.4, the mixture was observed to separate into two layers. This phenomenon was only observed when the concentration of the ionic liquid (tributylmethylphosphonium methyl sulfate) in the 0.5 M HDEHP and n-dodecane solution was 0.25 M and not at the lower concentrations (0.1 and 0.01 M). This could be attributed to a saturated solution with regards to miscibility. The inconsistency in the concentration of the organic phase dispensed to the equilibrium cells that could have resulted from the phase separation was mitigated by vigorous mixing of the organic phase before the dispensing of the organic phase to each equilibrium cell.

5.6.1 0.5 M HDEHP, 0.01 M tributylmethylphosphonium methyl sulfate in n-dodecane

The results obtained for distribution coefficient of neodymium (in nitric acid solution) extracted with the organic mixture of 0.5 M HDEHP and 0.01 M tributylmethylphosphonium methyl sulfate in n-dodecane at 298.15 K is displayed in Table 5.11 and Figure 5.12. For each synthesized aqueous solution (at a specified acid concentration) three tests were conducted (from the same organic and aqueous solutions) in three independent stirred cells. From each cell, a sample was withdrawn as per the procedure mentioned in Chapter 4. Each sample was tested three times using ICP-OES. Figure 5.12 displays three data points for the distribution coefficients obtained from a single nitric acid aqueous solution.

Table 5.11 The distribution coefficients, D_{Nd}, for Nd^{3+} ions between an organic phase 0.5 M HDEHP and 0.01 M tributylmethylphosphonium methyl sulfate in n-dodecane) and and aqueous phase concentrations with expanded uncertainties at T= 298.15 K and P = 101.3 kPa.

D_{Nd}	$[H^+]$ /M	$[Nd^{3+}]_{aq}$ /ppm	$U([Nd^{3+}])_{aq}$ /ppm	$[Nd^{3+}]_{org}$ /ppm	$U([Nd^{3+}])_{org}$ /ppm
19.56	0.1060	1.03	0.29	20.16	0.11
18.74	0.1107	1.07	0.29	20.11	0.11
21.85	0.0961	0.93	0.28	20.26	0.12
0.37	0.4361	14.98	0.21	5.56	0.01
0.59	0.4142	12.92	0.21	7.61	0.01
0.64	0.4140	12.53	0.21	8.00	0.01
0.09	0.6858	17.97	0.21	1.66	0.00
0.06	0.6798	18.58	0.21	1.04	0.00
0.05	0.7239	18.75	0.21	0.88	0.00
0.04	1.3295	18.78	0.21	0.68	0.00
0.00	2.0177	19.79	0.21	0.03	0.00

$U([H^+]) = 0.0003$ for all distribution coefficient values

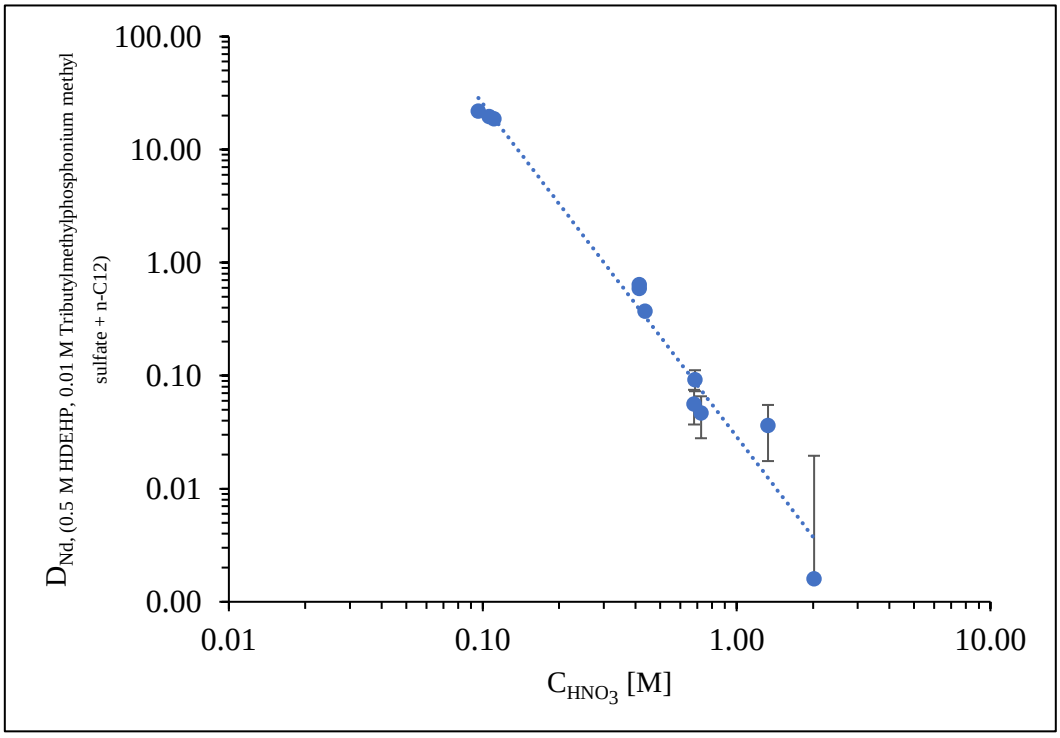

Figure 5.12 The distribution coefficients for Nd3+ ions between the organic phase of 0.5 M HDEHP, 0.01 M tributylmethylphosphonium methyl sulfate in n-dodecane and a nitric acid aqueous phase at T = 298.15 K and P = 101.3 kPa.

Figure 5.12 is a graphical representation of the distribution coefficient measured when undertaking experiments using an extractant of 0.5 M HDEHP and 0.01 M tributylmethylphosphonium methyl sulfate in n-dodecane along with an aqueous phase at various acid concentrations. An R^2 value of 0.9700 was calculated upon fitting a line to the data to represent its overall trend. This trend shows that the distribution coefficient of the Nd^{3+} ion in the 0.5 M HDEHP and 0.01 M tributylmethylphosphonium methyl sulfate extractant decreases with an increase in the aqueous H^+ concentration. Inverse proportionality between the distribution coefficient (D_{Nd}) and the aqueous acid concentration can therefore be asserted. Inverse proportionality between the distribution coefficient D_{Nd} and the acid concentration can be explored further by evaluating the gradient of the trendline, which for Figure 5.12 is described by $(\partial(ln(D))/\partial(ln([H^+]))$ = -2.945. For comparison of the trendlines in the latter part of this chapter it is worthwhile to calculate the value of the distribution coefficient at the aqueous acid concentration of 1 M ($D_{Nd}|_{[H^+]=1}$), which is equal to 0.02.

5.6.2 0.5 M HDEHP, 0.1 M tributylmethylphosphonium methyl sulfate in n-dodecane

The data for the distribution coefficient obtained using an organic extractant mixture of 0.5 M HDEHP and 0.1 M tributylmethylphosphonium methyl sulfate in n-dodecane at 298.15 K is presented in Table 5.12 and Figure 5.13. Triplicate distribution coefficient measurements and ICP-OES analyses were conducted. Each sample withdrawn from the equilibrium cell is represented by a single data point in Figure 5.13.

Table 5.12 The distribution coefficients, D_{Nd}, for Nd^{3+} ions between an organic phase (0.5 M HDEHP and 0.1 M tributylmethylphosphonium methyl sulfate in n-dodecane) and aqueous phase concentrations with expanded uncertainties at T= 298.15 K and P = 101.3 kPa.

D_{Nd}	$[H^+]$ /M	$[Nd^{3+}]_{aq}$ /ppm	$U([Nd^{3+}])_{aq}$ /ppm	$[Nd^{3+}]_{org}$ /ppm	$U([Nd^{3+}])_{org}$ /ppm
16.82	0.1125	1.19	0.27	20.00	0.10
19.48	0.1177	1.03	0.27	20.15	0.11
23.45	0.0974	0.87	0.27	20.32	0.12
0.53	0.5008	13.42	0.21	7.12	0.01
0.57	0.4671	13.09	0.21	7.45	0.01
0.57	0.4542	13.09	0.21	7.45	0.01
0.18	0.6825	16.57	0.21	3.06	0.00
0.21	0.6950	16.24	0.21	3.38	0.00
0.19	0.7040	16.50	0.21	3.12	0.00
0.07	1.0037	17.87	0.21	1.20	0.00
0.07	1.0660	17.80	0.21	1.27	0.00
0.08	1.0202	17.74	0.21	1.33	0.00
0.07	1.3708	17.93	0.21	1.30	0.00
0.02	1.4316	18.78	0.21	0.46	0.00
0.02	1.3639	18.94	0.21	0.29	0.00
0.03	1.5318	19.10	0.21	0.59	0.00
0.05	1.5042	18.78	0.21	0.91	0.00
0.04	1.4953	19.01	0.21	0.68	0.00
0.01	1.8175	19.20	0.21	0.16	0.00
0.02	1.8199	19.04	0.21	0.33	0.00
0.04	1.8055	18.58	0.21	0.78	0.00
0.01	2.0202	19.69	0.21	0.13	0.00
0.02	2.0039	19.36	0.21	0.46	0.00
0.05	2.1375	18.84	0.21	0.98	0.00

$U([H^+])$ = 0.0003 for all distribution coefficient values

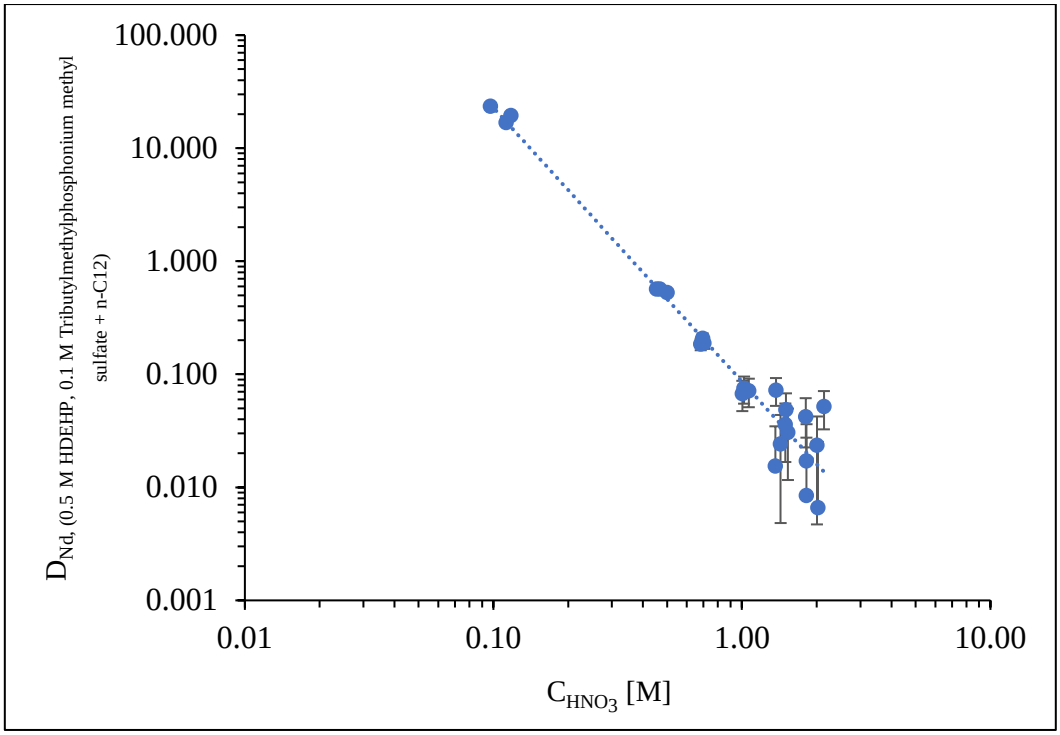

Figure 5.13 The distribution coefficients for Nd^{3+} ions between the organic phase of 0.5 M HDEHP, 0.1 M tributylmethylphosphonium methyl sulfate in n-dodecane and a nitric acid aqueous phase at T = 298.15 K and P = 101.3 kPa.

With the aqueous acid concentration varying, the distribution coefficient was measured with 0.5 M HDEHP and 0.1 M tributylmethylphosphonium methyl sulfate in n-dodecane as the extractant and neodymium as the REE of interest existing in the aqueous phase. The 0.5 M HDEHP and 0.1 M tributylmethylphosphonium methyl sulfate extractant causes the distribution coefficients that can be fitted to a trendline with an R^2 value of 0.9526. Observing the directionality of this trend, an increase in the H^+ concentration correlates with a decrease in the distribution coefficient for the Nd^{3+} ion. This directionality indicates that an inversely proportional relationship exists between the distribution coefficient (D_{Nd}) and the aqueous acid concentration . To further support the assertion of inverse proportionality between the distribution coefficient D_{Nd} and the aqueous acid concentration, an analysis of the gradient of the trendline ($\partial(ln(D))/\partial(ln([H^+]))$ = -2.42) can be utilised. Since a negative gradient is observed, this inverse proportionality is confirmed. The distribution coefficient at the acid concentration of 1 M ($D_{Nd|[H^+]=1}$) was found to be 0.08.

5.6.3 0.5 M HDEHP, 0.25 M tributylmethylphosphonium methyl sulfate in n-dodecane

Measurements of distribution behaviour for neodymium in the aqueous phase contacted with a mixture of 0.5 M HDEHP and 0.25 M tributylmethylphosphonium methyl sulfate in n-dodecane at 298.15 K, are presented in Table 5.13 and Figure 5.14. Three tests were conducted for each acid concentration (same organic and aqueous solution). All samples were tested in triplicate using ICP-OES testing.

Table 5.13 The distribution coefficients, D_{Nd}, for Nd^{3+} ions between an organic phase (0.5 M HDEHP and 0.25 M tributylmethylphosphonium methyl sulfate in n-dodecane) and and aqueous phase concentrations with expanded uncertainties at T= 298.15 K and P = 101.3 kPa

D_{Nd}	$[H^+]$ /M	$U([H^+])$	$[Nd^{3+}]_{aq}$ /ppm	$U([Nd^{3+}])_{aq}$ /ppm	$[Nd^{3+}]_{org}$ /ppm	$U([Nd^{3+}])_{org}$ /ppm
26.16	0.117	0.003	0.78	0.27	20.41	0.15
19.27	0.117	0.003	1.05	0.27	20.14	0.13
18.46	0.117	0.003	1.09	0.27	20.10	0.12
0.52	0.466	0.003	13.54	0.21	7.00	0.01
0.51	0.491	0.003	13.63	0.21	6.91	0.01
0.47	0.521	0.003	13.92	0.21	6.61	0.01
0.24	0.682	0.003	15.88	0.21	3.74	0.00
0.16	0.668	0.003	16.99	0.21	2.64	0.00
0.18	0.670	0.003	16.57	0.21	3.06	0.00
0.10	1.033	0.003	17.31	0.21	1.76	0.00
0.10	1.010	0.003	17.38	0.21	1.69	0.00
0.09	1.025	0.003	17.48	0.21	1.59	0.00
0.09	1.331	0.003	17.67	0.21	1.56	0.00
0.06	1.324	0.003	18.13	0.21	1.11	0.00
0.08	1.378	0.003	17.77	0.21	1.46	0.00
0.15	1.446	0.003	17.18	0.21	2.51	0.00
0.10	1.565	0.003	17.83	0.21	1.85	0.00
0.09	1.574	0.003	18.00	0.21	1.69	0.00
0.14	1.748	0.003	16.99	0.21	2.38	0.00
0.08	1.731	0.003	17.87	0.21	1.50	0.00
0.29	1.565	0.003	14.97	0.21	4.39	0.00
0.08	2.085	0.003	18.32	0.21	1.50	0.00
0.10	2.119	0.003	18.06	0.21	1.76	0.00
0.20	2.076	0.003	16.50	0.21	3.32	0.00

$U([H^+]) = 0.0003$ for all distribution coefficient values

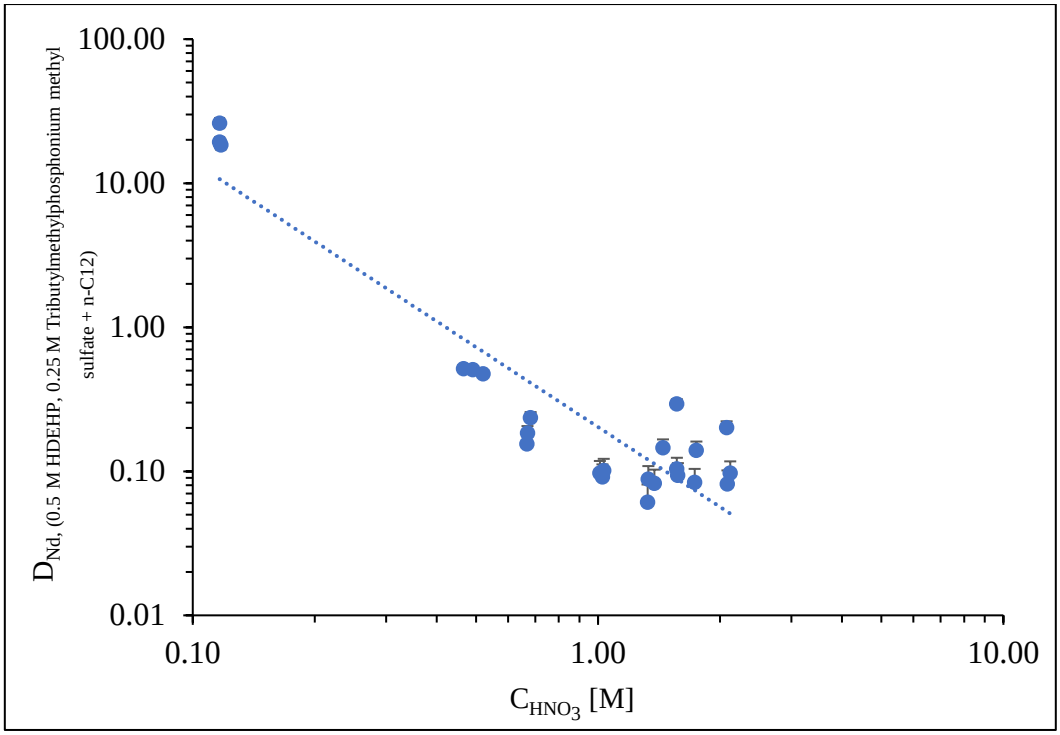

Figure 5.14 The distribution coefficients for Nd^{3+} ions between the organic phase of 0.5 M HDEHP, 0.25 M tributylmethylphosphonium methyl sulfate in n-dodecane and a nitric acid aqueous phase at T = 298.15 K and P = 101.3 kPa.

With 0.5 M HDEHP and 0.25 M tributylmethylphosphonium methyl sulfate in n-dodecane as the organic extractant solution the distribution coefficient of neodymium was plotted at varying aqueous acid concentrations (see Figure 5.14). The distribution coefficient of the Nd^{3+} ion in the 0.5 M HDEHP and 0.25 M tributylmethylphosphonium methyl sulfate extractant decreases with an increase in the H^+ concentration. When a trendline was fitted to the plotted data an R^2 value of 0.8559 was calculated. When the gradient of the trendline fitted to the above data the value of the gradient was found to be $(\partial(ln(D))/\partial(ln([H^+]))$ = -1.843. The negative value of the gradient supports the assertion of inverse proportionality between the distribution coefficient D_{Nd} and the aqueous acid concentration. Using this fitted trendline the value of the distribution coefficient at the acid concentration of 1 M ($D_{Nd}|_{[H^+]=1}$) was found to be equal to 0.20.

5.6.4 0.5 M HDEHP and tributylmethylphosphonium methyl sulfate concentration comparison in n-dodecane

The data presented graphically below in Figure 5.15 shows the distribution coefficient measured with an extractant of 0.50 M HDEHP and doped with 0.01, 0.10 and 0.25 M tributylmethylphosphonium methyl sulfate in n-dodecane. This is the same data as presented in Figure 5.12 to Figure 5.14 above, but is presented below on the same set of axes for the purpose of comparison. To observe the effect of the addition of the tributylmethylphosphonium methyl sulfate, the data of 0.50 M HDEHP in n-dodecane (Figure 5.6) is also presented in Table 5.14 and Figure 5.15 below.

Table 5.14 Parameters for the linear relationship between $ln(D)$ and ($ln([H^+])$ for the experimentally measured distribution coefficients of HDEHP and $BMImNTf_2$ extractant systems.

[HDEHP]/ M	IL/ M	$(\partial(ln(D))/\partial(ln([H^+]))$	$D_{Nd\|[H^+]=1}$	R^2
0.50	0.01	-2.95	0.02	0.9700
0.50	0.10	-2.42	0.08	0.9526
0.50	0.25	-1.84	0.20	0.8559
0.50	0.00	-2.29	0.09	0.9507

It can be seen from Figure 5.15 that the distribution coefficient of neodymium when extracted with various combinations of HDEHP and tributylmethylphosphonium methyl sulfate in n-dodecane shows an inversely proportional relationship with the concentration of the acid in the aqueous phase. The gradient $(\partial(ln(D))/\partial(ln([H^+]))$ of the ionic liquid containing LLE systems displays this in its negative non-zero values (see Figure 5.15). It can also be stated that the distribution coefficient has an inversely proportional relationship to the concentration of the H^+ ion in the aqueous solution across the range of investigated nitric acid concentrations. The existence of this inverse proportionality is indicative of the extraction process being governed by ion-exchange reaction principles. The values of $(\partial(ln(D))/\partial(ln([H^+]))$ (≈ 3) further support this assertion as this is consistent with the ratio of H^+ ions provided by the dissociation of nitric acid (HNO_3). This also indicates the dissociation and participation of a single acid group in a HDEHP dimer in the organic phase of the extraction reaction.

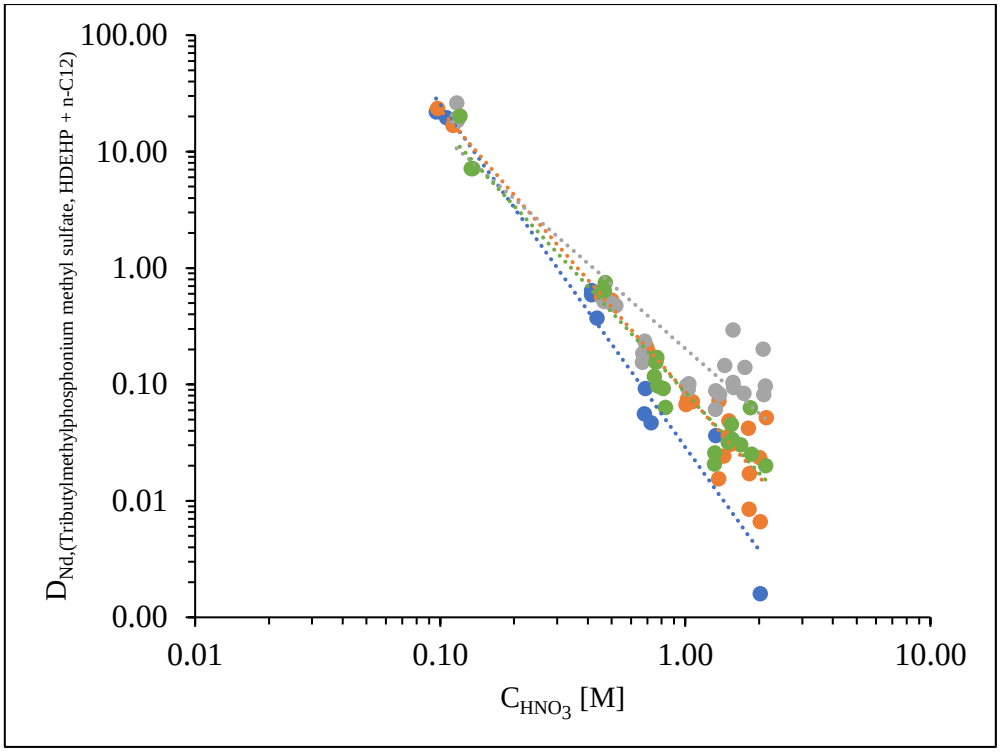

Figure 5.15 The distribution coefficients for Nd^{3+} ions between the organic phase of 0.5 M HDEHP in n-dodecane and a nitric acid aqueous phase at T = 298.15 K and P = 101.3 kPa. ●, 0.01 M tributylmethylphosphonium methyl sulfate; ●, 0.1 M tributylmethylphosphonium methyl sulfate; ●, 0.25 M tributylmethylphosphonium methyl sulfate; ●, 0 M tributylmethylphosphonium methyl sulfate.

It is evident from the graphical representation of this data that the distribution coefficient of neodymium in aqueous solution contacted with tributylmethylphosphonium methyl sulfate-containing extractant in n-dodecane increases in the following order of ionic liquid concentration 0.01, 0, 0.1 and 0.25 M at the acid concentrations tested in this work. It can be seen from Figure 5.15 that the presence of the ionic liquid in the organic extractant mixture generally enables a greater distribution coefficient than pure HDEHP in n-dodecane extractant in all cases except for the case of 0.01 M of tributylmethylphosphonium methyl sulfate doped extractant. This assertion is only valid subject to the exclusions and conditions discussed in the sections below.

0.01 M tributylmethylphosphonium methyl sulfate and 0 M tributylmethylphosphonium methyl sulfate doped extractant

The assertion of the distribution coefficient increasing proportionally with an increase in the tributylmethylphosphonium methyl sulfate concentration can be made by simple observation

of the trendlines fitted to the distribution coefficients obtained during the testing of LLE extraction systems using of 0.01 M and 0 M tributylmethylphosphonium methyl sulfate extractants. This assertion, however, is only valid for aqueous H^+ concentrations less than 0.1989 M. The point of deviation from the above statement was calculated using the data presented in Table 5.14 and Figure 5.15. The distribution coefficient at this equivalence point was found by calculation to be 3.46 for both the 0.01 M and 0 M tributylmethylphosphonium methyl sulfate concentration doped extractants. Beyond this equivalence point (ie. at acid concentrations greater than 0.1989 M), the relationship between the distribution coefficient and the concentration of tributylmethylphosphonium methyl sulfate in the organic phase becomes inversely proportional (this is confirmed by a visual analysis of Figure 5.15). For aqueous acid concentrations greater than 0.19889 M it can be stated that by observing the value of $D_{Nd}|_{[H^+]=1}$ (see Figure 5.15) for both the 0.01 M and 0 M tributylmethylphosphonium methyl sulfate doped extractant concentrations (0.03 and 0.09 M respectively), the inverse proportionality between the concentration of tributylmethylphosphonium methyl sulfate in the extractant to the distribution coefficient is further justified.

0.1 M tributylmethylphosphonium methyl sulfate and 0 M tributylmethylphosphonium methyl sulfate doped extractant

To further expound upon the significance of the trendlines fitted to the distribution coefficients achieved using 0.1 M and 0 M tributylmethylphosphonium methyl sulfate doped extractants, the general assertion of the distribution coefficient increasing proportionally with the tributylmethylphosphonium methyl sulfate concentration must be noted. This increasing proportionality is only valid for aqueous H^+ concentrations less than 1.0846 M.

The caveat presented in the previous statement can be explored briefly using the information presented in Figure 5.15 and Table 5.14. However, to quantify the conditions at which the caveat applies simultaneous equations were utilised to find that at the aqueous acid concentration of 1.0846 M the distribution coefficient displayed by the extractants with a 0.1 M and 0 M tributylmethylphosphonium methyl sulfate concentration is equal ($D_{Nd} = 0.07$). Thereafter again by observing the trendlines presented in Figure 5.15 the relationship between the distribution coefficient and the concentration of tributylmethylphosphonium methyl sulfate doping in the organic phase becomes inversely proportional at aqueous acid concentrations greater than 1.0846 M. Consideration of $D_{Nd}|_{[H^+]=1}$ for both the 0.1 M and 0 M tributylmethylphosphonium methyl sulfate extractant concentrations (0.09 and 0.09 respectively), supports the statement of the proportional relationship between the concentration

of tributylmethylphosphonium methyl sulfate in the extractant and the distribution coefficient at aqueous acid concentrations below 1.0846 M.

Although the information discussed in the above paragraphs is valid, further inspection of the trends produced by the data shows that the addition of tributylmethylphosphonium methyl sulfate at a concentration of 0.1 M does not have an appreciable effect on the behaviour of the distribution coefficient. This can be seen in the respective values of $(\partial(ln(D))/\partial(ln([H^+]))$ for the 0.1 M tributylmethylphosphonium methyl sulfate and 0 M tributylmethylphosphonium methyl sulfate doped extractant concentrations (-2.42 and -2.29 respectively). This phenomenon could, in some cases, be due to the trendline fit to the data or the bias introduced by three anomalous data points. The coefficients of correlation for the 0.1 M tributylmethylphosphonium methyl sulfate and 0 M tributylmethylphosphonium methyl sulfate containing extractant species are however high at 0.95 and 0.95 respectively.

0.25 M tributylmethylphosphonium methyl sulfate and 0 M tributylmethylphosphonium methyl sulfate doped extractant

When the trendlines fitted to the distribution coefficients were evaluated by the use of extractants containing 0.25 M and 0 M tributylmethylphosphonium methyl sulfate are plotted on a set of axes, a general trend of increasing proportionally in the distribution coefficient can be seen for for aqueous H^+ concentrations greater than 0.0001 M. For the region in which the aqueous acid concentrations are less than 0.0001 M, the fitted trendlines show that the relationship between the distribution coefficient and the concentration of tributylmethylphosphonium methyl sulfate in the organic phase becomes inversely proportional.

By using the data presented in Table 5.14 and Figure 5.15 and the concept of solving the trendline equations simultaneously it was found that at the aqueous acid concentration of 0.0001 M the distribution coefficient displayed by use of the 0.25 M and 0 M tributylmethylphosphonium methyl sulfate containing extractants is equal (D_{Nd} = 24.38). To provide further quantitative evidence to support the idea of a proportional relationship between the concentration of tributylmethylphosphonium methyl sulfate in the extractant to the distribution coefficient at aqueous acid concentrations greater than 0.0001; Table 5.14 lists the value of $D_{Nd}|_{[H^+]\,=\,1}$ for both the 0.25 M and 0 tributylmethylphosphonium methyl sulfate containing extractants to be 0.20 and 0.09 M respectively.

0.25 & 0.01 M tributylmethylphosphonium methyl sulfate and 0.01 M tributylmethylphosphonium methyl sulfate doped extractant

Upon observation it was noted that the trendlines fitted to the distribution coefficient data of obtained using the 0.25 M tributylmethylphosphonium methyl sulfate and 0.01 M tributylmethylphosphonium methyl sulfate extractants, the overall statement of the distribution coefficient increasing together with an increment in the tributylmethylphosphonium methyl sulfate concentration is legitimate for aqueous H^+ ions concentrations more than 1.3785 M. Utilising the information presented in Table 5.14 and Figure 5.15 it may be deduced by computation that at the aqueous acid concentration of 1.3785 M the distribution coefficient effected by the extractants with a 0.25 M tributylmethylphosphonium methyl sulfate and 0.01 M tributylmethylphosphonium methyl sulfate concentrations is equivalent (D_{Nd} = 0.01). At acid concentrations less than 1.3785 M, the relationship between the distribution coefficient and the concentration of tributylmethylphosphonium methyl sulfate in the organic phase becomes inversely proportional. In furtherance of the concept of the proportionality of the distribution coefficient within the aqueous acid concentration range previously mentioned (greater than 1.3785 M), analysis of the $D_{Nd}|_{[H^+]=1}$ value (see Table 5.14) for both the 0.25 M tributylmethylphosphonium methyl sulfate and 0.01 M tributylmethylphosphonium methyl sulfate extractant concentrations (each one being equal to 0.20 and 0.03 respectively) is applied.

0.25 & 0.1 M tributylmethylphosphonium methyl sulfate doped extractant

The trendlines as fitted to the distribution coefficients which result from extraction of neodymium in acidic aqueous media with 0.25 M tributylmethylphosphonium methyl sulfate and 0.1 M tributylmethylphosphonium methyl sulfate extractants show an increasing proportionality trend between the distribution coefficient and aqueous acid concentration. This increasing proportionality is only valid for the region in which aqueous H^+ concentrations are greater than 0.0200 M. Calculations using simultaneous equations were performed to find the value of the aqueous acid concentration at which the distribution coefficient for extraction performed with 0.25 M tributylmethylphosphonium methyl sulfate and 0.1 M tributylmethylphosphonium methyl sulfate concentration is equal. This point was found to be 0.0200 M and D_{Nd} = 12.17 (see Table 5.14 and Figure 5.15). The use of the trendlines at acid concentrations less than 0.0200 M show that the relationship between the distribution coefficient and the concentration of tributylmethylphosphonium methyl sulfate in the organic phase becomes inversely proportional. Additional observations made for $D_{Nd}|_{[H^+]=1}$ (see Table 5.14) for both the 0.25 M tributylmethylphosphonium methyl sulfate and 0.1 M

tributylmethylphosphonium methyl sulfate doped extractant concentrations (0.20 and 0.09 M respectively), demonstrated more solidly the proportional relationship of the concentration of tributylmethylphosphonium methyl sulfate in the extractant to the distribution coefficient at aqueous acid concentrations greater than 0.0200 M.

0.1 M tributylmethylphosphonium methyl sulfate and 0.01 M tributylmethylphosphonium methyl sulfate doped extractant

0.1 M tributylmethylphosphonium methyl sulfate and 0.01 M tributylmethylphosphonium methyl sulfate doped extractants exhibit distribution coefficients whose trendlines are proportional to an increase in the tributylmethylphosphonium methyl sulfate doping conncentration. However, this statement of proportionality is only valid for aqueous H^+ concentrations greater than 0.1235 M. Taking into account the data presented Table 5.14 and Figure 5.15 simultaneous equations were used to locate the point (0.1235 M, $D_{Nd} = 13.69$); this is the point where the distribution coefficients achieved by the extractant doped with 0.1 M tributylmethylphosphonium methyl sulfate and 0.01 M tributylmethylphosphonium methyl sulfate concentrations are equal. Thereafter (ie. at acid concentrations less than 0.1235 M), using the fitted trendlines, the relationship between the distribution coefficient and the concentration of tributylmethylphosphonium methyl sulfate in the organic phase becomes inversely proportional. Observation of the $D_{Nd|[H^+] = 1}$ value (see Table 5.14) for both the 0.1 M tributylmethylphosphonium methyl sulfate and 0.01 M tributylmethylphosphonium methyl sulfate doped extractant concentrations 0.1 and 0.01 M respectively, demonstrate the proportional relationship of the concentration of tributylmethylphosphonium methyl sulfate in the extractant to the distribution coefficient at aqueous acid concentrations greater than 0.1235 M.

In summary, it can be said that the addition of ionic liquids to organic extractants result in an alteration of the extraction ability. This change has not been found to be either directly or inversely proportional to the concentration of the extractant. The data presented shows that the use of ionic liquid LLE systems must be carefully considered with particular attention to the concentration to achieve the intended effect. Due to the non-homogeneity displayed by the synergistic extractant containing tributylmethylphosphonium methyl sulfate at a concentration of 0.25 M, its use is not recommended for applications in which it is intended to recover metal ions from the organic phase. Where $BMImNTf_2$ is added to the 0.5 M HDEHP extractant both the 0.019 M and 0.19 M concentrations of ionic liquid could be used to enhance the extraction of Nd into the organic phase at aqueous acid concentrations lower than 0.2032 M. In the region between 0.2032 M and 0.6024 M the extractive efficiency of the $BMImNTf_2$ concentration was found to decrease in the following sequence 0.19 M > 0.019 M > 0 M. The observed behaviour could enable one to make use the ILs to suppress or enhance the extractive capabilities of the organic phase as required by the application at hand.

5.7 LLE Separation Column

The measurements of the distribution coefficients of neodymium were used in a preliminary design and sizing of an LLE separation. As described in the introduction of this work, the initial project scope was to study the degree to which neodymium can be extracted from solutions in which NdFeB magnets are dissolved in nitric acid solutions. As this study's original objectives were modified due to the COVID-19 pandemic, the separation of neodymium from iron in nitric acid aqueous media was modelled using a theoretical neodymium and iron solution in Microsoft Excel™. Iron and neodymium were chosen for this simulation as they are the most abundant species in solutions formulated by the dissolution of NdFeB magnets. The calculations carried out were based on the theoretical methods of Hino *et al., (*1997) (see Section 2.3.4) incorporating the LLE extraction column investigation presented by Gruber and Carsky (2020) for the initial assumptions of the simulation. The extractant solution used for the simulation presented below was 0.5 M HDEHP. It was envisaged at the outset of this work that the calculations below would be carried out using a synergistic extractant species containing an ionic liquid. Only the extraction behaviour of Fe with an extractant species of 0.5 M HDEHP extractant was available as the supply chain constraints (due to the COVID-19 pandemic) to obtain additional ionic liquid would prolong the testing phase of this work and the complementary unpublished study by Bridgemohan *et al., (*2021) beyond a reasonable timeline. The neodymium distribution coefficients applied in the calculations were those measured in this work (see Section 5.4.2), while the iron distribution coefficients utilised were taken from a parallel study by Bridgemohan *et al., (*2021).

5.7.1 Distribution Coefficient Data

In the formulation of the theoretical Nd-Fe solution in an LLE extraction column, the behaviour of the distribution coefficient of iron first had to be quantified. Figure 5.16 presented below provided the necessary information. Bridgemohan *et al., (*2021) investigated the distribution coefficient of iron in aqueous solutions of 0.1 -1.0 M nitric acid solutions when extracted with 0.5 M HDEHP in n-dodecane.

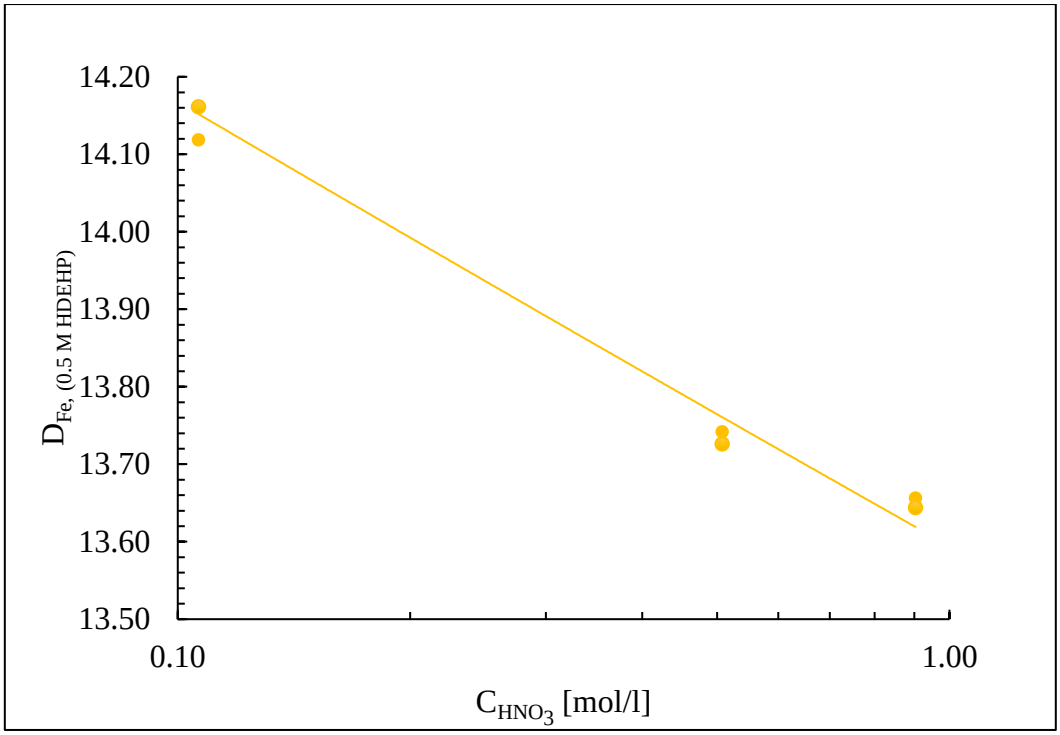

Figure 5.16 The distribution coefficients for Fe^{3+} ions between the organic phase of 0.5 M HDEHP in n-dodecane and a nitric acid aqueous phase at T = 298.15 K and P = 101.3 kPa.

Comparing the results obtained by Bridgemohan *et al., (*2021) to published work by Suarez *et al., (*2002) wherein the distribution coefficient of iron between an organic phase of ≈ 0.9 M HDEHP and an aqueous phase of varying sulphuric acid concentrations (1 – 6 M).The trend inversely proportional relationship displayed by the data obtained by Bridgemohan *et al., (*2021) concurs with the results of the work by Suarez *et al., (*2002) to which the reader is referred to for more detail on the liquid-liquid extraction of iron.

5.7.2 Calculation Strategy

Between the two most abundant elements in NdFeB solutions produced by dissolution in acid (Fe and Nd, see Table 1.1), it was decided to execute the calculation for the optimisation of the concentration of neodymium as this has been identified as a scarce resource, the demand for which is set to increase (see Figure 1.1). From the equations presented in the work of Hino *et al., (*1997) the parameters that are considered to achieve optimisation of the neodymium purity are: the concentration of the aqueous phases used for the feed and stripping solutions, the concentration of the extractant species in the organic solution, the ratio of aqueous to organic solution flowrates, the number of extraction stages as well as the number of stripping

stages. The distribution coefficient data measured using available chemical stocks at the time of carrying out the study were with a 0.5 M HDEHP extractant. This limitation of available data sets one of the parameters that were considered for the optimisation of neodymium purity. The remaining optimisation parameters are discussed in the section below.

Aqueous Feed Concentration Selection

As determined in Sections 5.4 – 5.6 the distribution coefficient of neodymium between the aqueous and organic phases, exhibits an inverse relationship with the concentration of the $[H^+]$ in the aqueous phase. Hence, it can be surmised that the lowest acid concentration must be selected to achieve the greatest degree of recovery of the targeted metal ion. However, when considering a system with multiple metal ion species dissolved in the aqueous phase, the selectivity (β) of the organic phase must be taken into account (see Section 2.3.4). To enable separation, the selectivity of the target ion must exceed 1 at the selected aqueous feed concentration. To aid in the identification of the region in which the value of the selectivity exceeds 1, the distribution trendlines as determined in Figure 5.6 and Figure 5.16 were used in equation 2.10 (see Section 2.3.4) to produce the plot of the selectivity as shown in Figure 5.17 below.

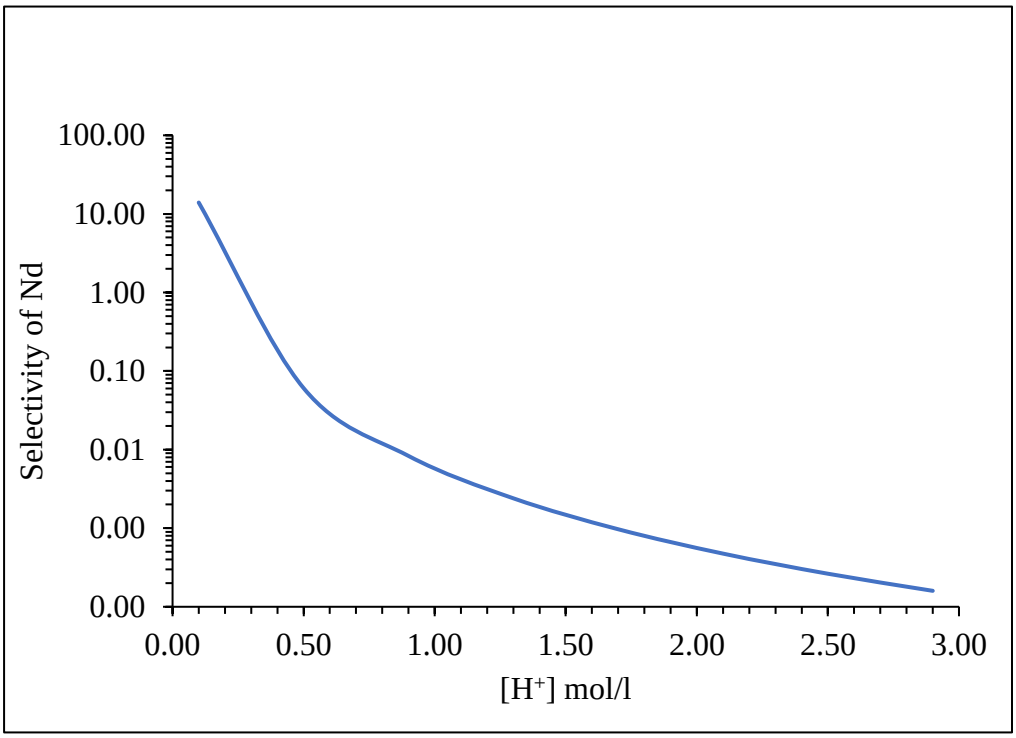

Figure 5.17 Selectivity of neodymium from neodymium iron nitric acid solution using 0.5 M HDEHP in n-dodecane extractant.

From Figure 5.17 above at an aqueous [H^+] of 0.22 M the value of β is equal to a value of 1. This infers that the separation of neodymium from iron is possible using an extractant of 0.5 M HDEHP. For the simulation undertaken in this work, the aqueous [H^+] yielding the greatest value for the selectivity in the tested region was chosen, this was a value of 0.11 M.

5.7.2 Assumptions

For the designing of a LLE extraction column using distribution coefficient data, it is necessary to make assumptions regarding the relative concentrations of neodymium and iron that would exist in a solution created from the dissolution of NdFeB magnets. For the calculations carried out the concentrations of 15.78 g/l for neodymium and 8.30 g/l for iron as presented in the work of Gruber and Carsky (2020) were used. Using rates from the calculation investigation undertaken by Hino *et al.*, *(*1997), the flow rate of the aqueous solution and the organic extractant was set to 1.1 l/min and 1.0 l/min as an initial value in the calculation. Figure 5.18 below is a schematic of the LLE extraction column with flowrates, with the metal ion concentrations and the initially modelled flowrates indicated.

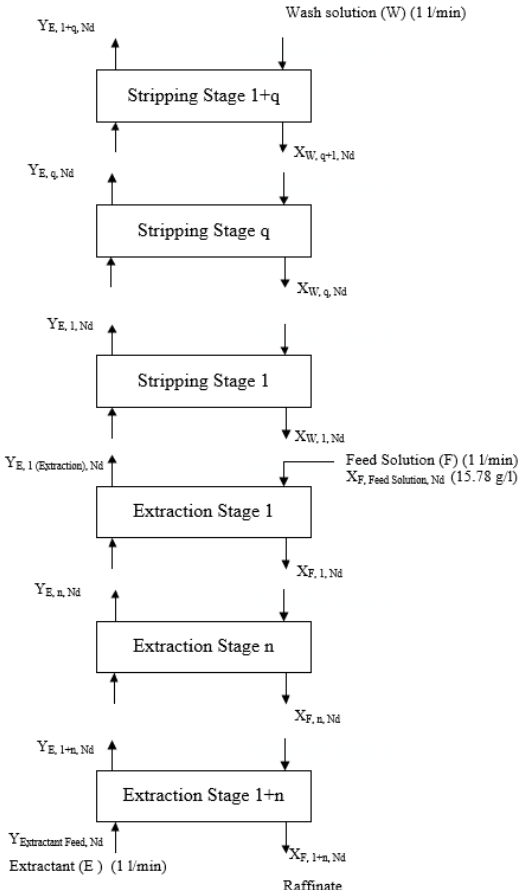

Figure 5.18 Schematic of the equilibrium stages in the simulation of the LLE column.

5.7.3 LLE Column Flow Profiles and Sensitivity Analyses

Extraction Stages

In the recovery of neodymium, the aqueous phase must be contacted with the organic extractant solution; this occurs in the extraction stages. A cursory glance at Figure 5.17 indicates that the separation of neodymium from iron is possible. However, this possibility does not necessarily mean that the complete separation of neodymium from iron is possible. For complete separation to occur, there would have to exist a value of C_{HNO3} in the tested region where the selectivity (β) is far greater than a value of 1. The lack of a tested region meeting such criteria indicates that multiple equilibrium stages will be required if complete separation is to be realised. Figure 5.19 shown below presents the amount of metal ion recovered in each extraction stage and the solvent free purity (purity considering only metal constituents) of neodymium and iron in the organic extractant phase as the extractant moves through the column.

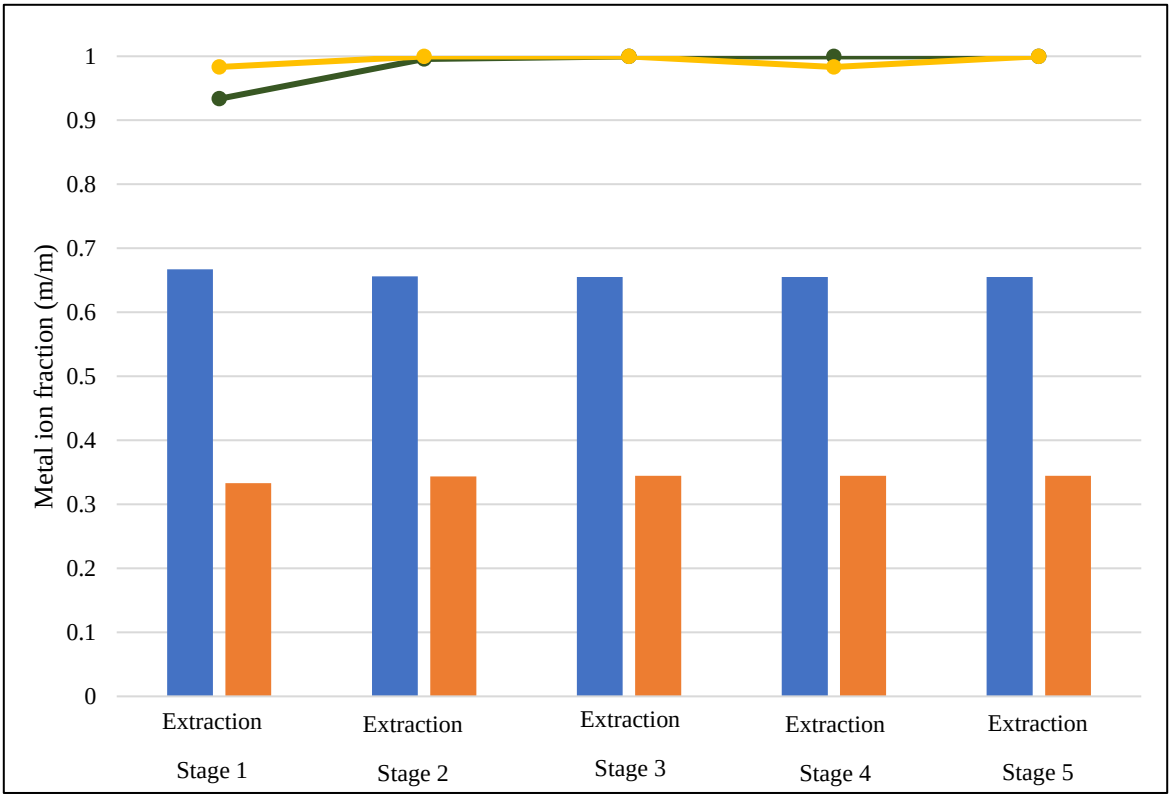

Figure 5.19 The amount of metal ion recovered in each extraction stage and the purity of the metal ion in the organic extractant leaving each extraction stage. , Neodymium extracted; , Iron extracted; , Iron purity in the extractant solution and , Neodymium purity in the extractant solution (All data shown on a solvent free basis).

It can be seen from Figure 5.19 above that only a marginal degree of beneficiation of neodymium can be achieved with a solvent free purity of 0.6669 in the first extraction stage. The addition of further stages results in an increase in the amount of neodymium extracted, however this effect is more pronounced for iron resulting in a decrease of the solvent free neodymium purity; 0.6562 in the second extraction stage, 0.6553 in the third, 0.6553 in the fourth and 0.6553 in the fifth extraction stage. It was noted that the solvent free purity of iron in the extractant solution increases with an increase in the number of extraction stages employed. Considering the other parameters under consideration, it could be surmised that a modification in the ratio of the extractant to the aqueous feed extractant flow rates could yield a greater recovery or a purity of the target metal ion. Table 5.15 below indicates the variation in the solvent free purity of neodymium obtained from the 5 extraction stages shown above, as the extractant to aqueous feed rate ratio is varied from 0.05 to 2.

Table 5.15 Sensitivity analysis for the effect of the extractant to aqueous feed flow rate ratios for a 5-stage extraction section in an LLE column.

Organic Extractant to Aqueous Feed Ratio	0.05	0.10	0.20	0.33	1.00	2.00
Neodymium Purity	0.6664	0.6658	0.6647	0.6633	0.6553	0.6374

The results shown in Table 5.15 above indicate a marginal increase in the purity of neodymium obtainable through an increase in the amount of extractant (relative to the aqueous feed) or a decrease in the flow rate of the aqueous feed flow rate (relative to the extractant flow rate). At an extractant to aqueous feed flow rate ratio of 0.1, the neodymium purity obtained is 0.6658 whereas at a ratio of 0.05 (indicating either a halving of the extractant flow rate or a doubling of the aqueous feed flow rate) the purity of neodymium obtained is 0.6664. An increase of 0.06 %, is indicative that further decreasing of the extractant to aqueous feed ratio in the extraction section of the LLE column is unfeasible, as it is outweighed by the costs of increasing the feed flowrate.

Stripping Stages

Reviewing Table 5.15 and Figure 5.19 it was noted that the maximum obtainable purity of neodymium in the extraction stage is less than 0.70 g/g. As the rare earth metal is required for multiple uses, a metal grade of below 0.70 g/g reduces the number of applications in which the product could be used, but also commercial value and subsequently the financial viability of the recovery process in its entirety. Therefore, it is necessary for the metal ion in the extractant to be beneficiated further by employing the use of a stripping section in the LLE column. As explained in Sections 5.4-5.6, the stripping solution suitable for application would be a nitric acid solution whose $[H^+]$ lies on the upper end of the experimentally tested boundary. The analysis of Figure 5.17 shows that the selectivity in this region for neodymium is low, enabling further purification via stripping. A nitric acid solution at a concentration of 2.9 M was selected as the stripping solution feed.

Similar to the process employed for the evaluation of the degree of recovery obtainable by a variation in the number of extraction stages, a column flow profile for the solvent free purity of neodymium obtainable by the stripping solution moving through the number of stripping stages was performed and the results plotted. Figure 5.20 below is a graphical representation of the solvent free purity of metal ions present in the stripping solution leaving each stage along with the solvent free purity of neodymium in the stripping solution leaving each stage. The results in Figure 5.20 below were obtained by a calculation carried out with organic and aqueous flow rates of 1 l/min.

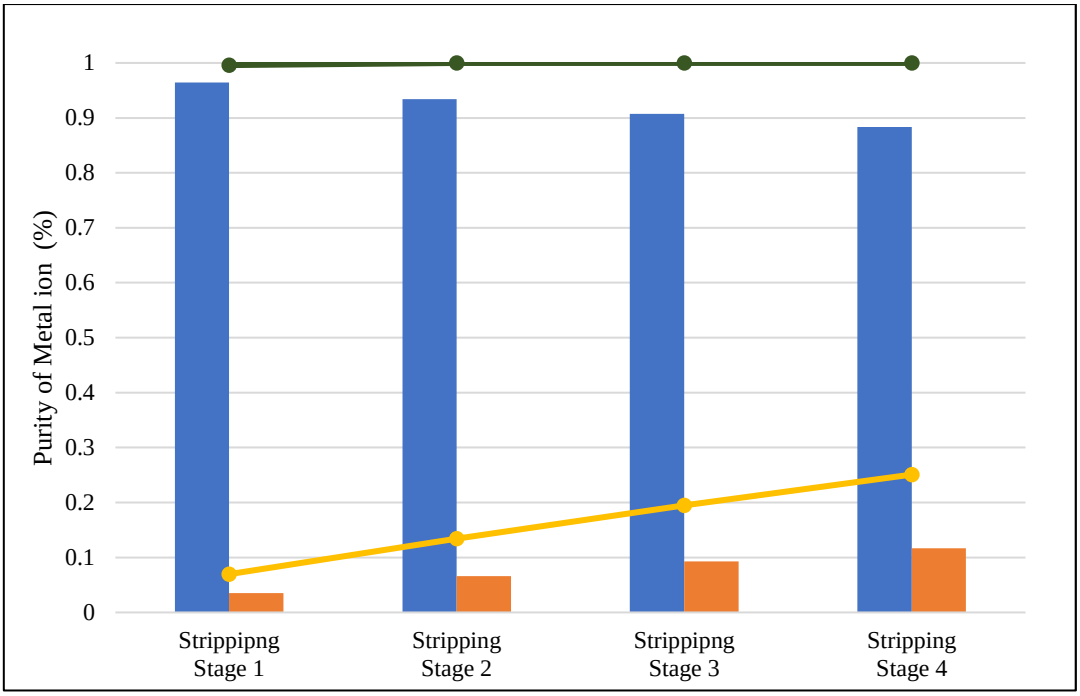

Figure 5.20 The solvent free purity of metal ion recovered in each extraction stage and the solvent free purity of neodymium in the organic extractant leaving each extraction stage. , Neodymium purity ; , Iron purity; , Iron extracted in the stripping solution and , Neodymium extracted in the stripping solution (All data shown on a solvent free basis).

Similar to the result obtained for the extraction stages of the LLE column it can be seen that after the first stripping stage the amount of neodymium recovered as well as its purity in the stripping solution decreases markedly. Similar to Figure 5.19, Figure 5.20 shows that the purity of iron in the stripping solution increases as the stripping solution moves through a greater number of equilibrium stages in the column. The sensitivity analysis carried out on the ratio of organic extractant to aqueous stripping solution flow rates was performed and the results are presented in Table 5.16 below.

Table 5.16 Sensitivity analysis for the effect of the extractant to aqueous feed flow rate ratios for a 5 stage stripping section in an LLE column

Organic Extractant to Aqueous Feed Ratio	0.05	0.10	0.20	0.33	1.00	2.00
Neodymium purity	0.9644	0.9642	0.9632	0.9606	0.8439	0.0275

In Table 5.16 the sensitivity analysis was conducted on the effect of the extractant to aqueous feed flow rate ratio on the solvent free purity of neodymium obtained in the extraction stages. Unlike the result demonstrated in Table 5.15, Table 5.16 shows that the ratio of the extractant to the aqueous feed flow rate has a significant impact on the solvent free neodymium purity with an increase in the aqueous solution feed rate correlating to an increase in the solvent free purity of neodymium obtained. By considering the solvent free purity of neodymium obtainable by a doubling of the aqueous feed flow rate or a halving of the extractant flow rate between the ratios of 0.10 and 0.05, the increase in purity is 0.02 %. This degree of neodymium beneficiation gained by the variation in flowrates is modest when compared to the variation in the relative amount of solution that must be employed to realise this increase. Therefore, any further decrease in the ratio of the extractant to the aqueous feed flow rate yields unfeasible results when considering the cost and practical implications of the change. The size of the column must also be considered in the selection of a flow rate ratio as the purity of the products and column size must be weighed against one another as detailed by Gruber and Carsky (2020). In a production environment wherein the rate of production is amongst the chief considerations the choice of the flow rate ratio becomes more significant.

5.7.4 Modelling Results

To understand the effect of the following parameters: the number of extraction stages, the number of stripping stages, the organic extractant to aqueous feed ratio (extraction stages) and the organic extractant to aqueous stripping solution ratio, regression analyses on the data presented above were performed. To simplify the regression analyses it was decided that organic extractant to aqueous feed ratio over the extraction stages was of lesser significance. The three remaining parameters were then analysed. The regression analysis is undertaken to gain macroscopic insight into the effect of the above-mentioned parameters on the solvent free neodymium purity obtained. Table 5.17 below shows the regression parameters obtained for the regression in linear to quartic forms. Where quadratic, cubic and quartic forms are regression models with include parameters for the independent variables raised to the 2, 3 and 4^{th} exponent respectively (see Section 2.3.3).

Table 5.17 Table of the multivariable linear regression parameters for the purity of neodymium obtainable in an LLE column

Parameter	Linear	Quadratic	Cubic	Quartic
Multiple R	0.453	0.803	0.803	0.816
R^2	0.205	0.645	0.645	0.666
Adjusted R^2	0.086	0.520	0.344	0.208
Standard Error	0.182	0.132	0.132	0.132
Number Observations	24	24	24	24

An analysis of Table 5.17 revealed that, of the tested macroscopic fitting models, the cubic would yield the best fit to the data for a holistic macroscopic analysis. The R^2 of 0.645 yields the best fit for the data while simultaneously maintaining the greatest value of adjusted R^2 indicating the least amount of superfluous information fed into the regression analysis.

The neodymium data presented above, and the analysis thereof would realise its greatest potential once tested in LLE extraction equipment. There is no case-study or actual plant to which the results of the LLE system modelled above can be compared. However, to consider the applicability of the above proposed process, it is useful to compare the results that can be obtained from the calculation to the work of Gruber and Carsky (2020) under similar conditions. The work of Gruber and Carsky (2020) investigated NdFeB magnets dissolved in 2 M H_2SO_4 which were subjected to extraction with 1.20 M HDEHP in n-dodecane (extractant to feed flow ratio of 3.2). A subsequent stripping step using 4.00 M H_2SO_4 solution was employed. After the second extraction the purity of neodymium achieved was 0.7451. Adjusting the simulation discussed above to similar flowrate ratios, a neodymium purity of 0.9641 was obtained.

The neodymium purity obtained in the model produced by the calculation detailed in Section 5.7.2 differs by 21.90% from that obtained in the investigation by Gruber and Casrsky (2020). The neodymium purity obtained in this study is greater. This difference can be explained by the fact that the study undertaken by Gruber and Carsky (2020) utilised an aqueous feed solution derived from the dissolution of NdFeB magnets. Solutions produced from the dissolution of magnets contain a greater number of chemical species than those used in the calculations in the model employed in this work (see). The degree of competitive complexation is increased in the study undertaken by Gruber and Carsky (2020) due to the number of metal ion species present in the separation unit. Furthermore, the study undertaken by Gruber and Carsky (2020) was not designed to maximise the purity of neodymium as was

the objective of the modelling in this work. The study by Gruber and Carsky (2020) was set to optimise the purity of didymoxide, which is a mixture of praseodymium and neodymium. The difference in the objectives of this study and that of Gruber and Carsky (2020) has a bearing on the purity of the product obtained as the separation of the similar REEs, praseodymium and neodymium, is complicated by their similar thermophysical properties. Although it is not explicitly mentioned in the investigation by Gruber and Carsky (2020) it is conceivable that separation of praseodymium from neodymium was not investigated due to the complexities it presents and the large volumes of chemicals which would be necessary to effect such a separation. The comparison of the purities obtained above must be viewed as a preliminary estimate and can be used as the basis for the exploration of a more rigorous design and investigation.

Chapter 6:Conclusions

The accuracy of the results produced by the experimental method used in this study was confirmed by the evaluation of the distribution coefficient of europium. The gradient evaluated from trendline fitted to the data obtained as a result of this work (-2.328) was found to be comparable (within 10%) to the gradients of the trendlines fitted to the data presented in the literature.

For the test system using yttrium as the metal ion, it was found that the exponential relationship between the distribution coefficient and aqueous $[H^+]$ (0.2- 3.0 M) is not valid for all aqueous concentrations when yttrium is extracted with 1.0 M HDEHP in n-dodecane. A saturation of the organic extractant phase with Y^{3+} occurs at a $[H^+] \approx 1.0$ M and $D_Y \approx 70$. The existence of a saturated region ($[H^+] < 1.0$) and a non-saturated region ($[H^+] > 1.0$) demonstrates that at H^+ concentrations greater than ≈ 1 highly favourable interactions between the extractant and the metal cation are pronounced.

The measurement of the distribution coefficients of neodymium in liquid-liquid extraction systems where the aqueous phase was composed of water and nitric acid concentrations of ≈0.1 – 2.0 M and the organic phase was composed of HDEHP in n-dodecane was accomplished. The distribution coefficient of neodymium was found to be inversely proportional to the concentration of the H^+ ion in the aqueous phase.

The distribution behaviour of neodymium in nitric acid aqueous phases (≈0.1 - 2.9 M) was measured and the distribution coefficient calculated; the solutions were contacted with organic solutions of 0.1, 0.5 and 1.0 M HDEHP in n-dodecane.

The distribution coefficient data measured for neodymium extracted with 0.1 M HDEHP could not be fitted to a trendline due to a high degree of scatter.

The 0.5 and 1.0 M HDEHP extractant in n-dodecane distribution coefficient data was fitted successfully to linearized data with a coefficient of determination values of 0.9507 and 0.9528.

For the systems in which the extractant species was dosed with ILs , $BMImNTf_2$ was tested as the ionic liquid (at concentrations of 0.019 and 0.19 M respectively in 0.5 M HDEHP solution). The $BMImNTf_2$ addition was found to increase the distribution coefficient proportionally its concentration; the values of the gradient and intercept of the distribution coefficient at the nitric

acid [H^+] = 1 for the 0, 0.019 and 0.19 M BMImNTf$_2$ extractants being -2.29, 0.09; -2.79, 0.13 and -3.39, 0.04 respectively. It was also found that the increase in the distribution coefficient of neodymium is proportional to the increase in the concentration of the ionic liquid BMImNTf$_2$ in the extractant when contacted with an aqueous phase with nitric acid concentrations lower than 0.6024 M. It was concluded that the affinity of the extractant for the metal ion increases proportionally to the concentration of the ionic liquid.

The effect of adding the ionic liquid tributylphosphonium methyl sulfate at concentrations 0.01, 0.10 and 0.25 to a 0.50 M HDEHP in n-dodecane extractant was investigated. The data for the systems was fitted to trendlines yielding coefficient of determination values of 0.970, 0.9526 and 0.8559 for each added tributylphosphonium methyl sulfate concentration (0.01, 0.10 and 0.25 M respectively). The trendline gradients ($\partial(ln(D))/\partial(ln([H^+])$) and distribution coefficients for each tributylphosphonium methyl sulfate concentration doped extractant at nitric acid [H^+] = 1.00 M were -2.95 and 0.03, -2.42 and 0.09 as well as -1.84 and 0.20 respectively. The increase in the ionic liquid doping levels correlated to an increase in the distribution coefficient. However the distribution coefficient trend line for aqueous solution extracted with 0.5 M HDEHP in n-dodecane correlated with the 0.10 M ionic liquid concentration to a degree of 95 %. From the data presented in this study it can be concluded that the addition of ionic liquids to the extractant solution can result in either a decrease or an increase in the distribution coefficient as compared to the use of an extractant solution without an ionic liquid species.

From the separation of neodymium from iron using a LLE separation column with a 0.50 M HDEHP in n-dodecane extractant, the results showed that a neodymium purity of 0.9644 could be obtained. This result was shown to be achievable in a separation column with 5 extraction stages with an organic phase to aqueous solution ratio of 0.05 and a stripping section of 5 stripping stages with an organic phase to aqueous solution ratio of 0.05.

Chapter 7:Recommendations

The results obtained in this work provide a strong foundation for the study of the recovery of neodymium from nitric acid solutions using HDEHP as the primary extracting species. However, the following is recommended:

1. To further the applicability of this data for the recycling of NdFeB magnets, a testing of the original pre-COVID scope of this work is recommended. This refers to the evaluation of the distribution coefficient between an organic extractant phase of HDEHP in n-dodecane and a nitric acid based aqueous phase formulated by the crushing and dissolution of waste NdFeB magnets.
2. That further studies be carried out, quantifying the distribution coefficient for the binary combinations of an HDEHP and ionic liquid organic extractant solution contacted with water, aqueous H^+ and the metal ion. Thereafter, the number of constituents in the aqueous phase should be increased one at a time in varying combinations to thoroughly document the effects of competitive complexation. This study should be followed by the derivation of a robust thermodynamic or mathematical model that will more aptly describe the complexation behaviour.
3. That kinetic studies on the distribution coefficient be carried out to introduce an additional parameter through which the chemical mechanisms of competitive complexation can be further understood.
4. To increase the amount of data that can be generated within a reasonable time period, and in turn the level of understanding that can be gained into the behaviour of metal ions in LLE systems, it is recommended that additional equilibrium cells be added to the current experimental equipment.
5. The data generated in the laboratory scale equilibrium cells be used as a basis for measuring the performance of an HDEHP extractant when contacted with a nitric acid aqueous solution in a pilot scale LLE extraction column. This would assist in further quantifying the nuances in the extraction efficiency in the different modes of separation.
6. That further studies be undertaken to investigate solvents for REE-containing raw materials to mitigate the environmental risk that the use of nitric acid and sulphuric acid poses, either by investigating improved methods of materials handling or investigating alternative solvents.

7. That a study investigating the effect of altering the relative quantities of the organic and aqueous solvent be commissioned to further understanding of these parameters' contribution to the distribution coefficient.

References

Ahmad, Z., 2003. The properties and application of scandium-reinforced aluminium. *JOM*, 55(2), pp.35-39.

Alonso, E., Sherman, A., Wallington, T., Everson, M., Field, F., Roth, R. and Kirchain, R. (2012). Correction to Evaluating Rare Earth Element Availability: A Case with Revolutionary Demand from Clean Technologies. *Environmental Science & Technology*, 46(8), pp.4684-4684.

Atwood, D., 2013. *The Rare Earth Elements*. New York: Wiley.

Baba, Y., Kubota, F., Kamiya, N. and Goto, M. (2011). Recent Advances in Extraction and Separation of Rare-Earth Metals Using Ionic Liquids. *Journal of Chemical Engineering of Japan*, 44(10), pp.679-685.

Baba, Y., Kubota, F., Kamiya, N. and Goto, M., 2011. Recent Advances in Extraction and Separation of Rare-Earth Metals Using Ionic Liquids. *Journal of Chemical Engineering of Japan*, 44(10), pp.679-685.

Balaram, V., 2019. Rare earth elements: A review of applications, occurrence, exploration, analysis, recycling, and environmental impact. *Geoscience Frontiers*, 10(4), pp.1285-1303.

Balomenos, E., Giannopoulou, I., Gerogiorgis, D., Panias, D. and Paspaliaris, I., 2013. Resource-Efficient and Economically Viable Pyrometallurgical Processing of Industrial Ferrous By-products. *Waste and Biomass Valorizsation*, 5(3), pp.333-342.

Bauer, D.J., 1966. Extraction and separation of selected lanthanides with a tertiary amine. *US Bureau of Mines*, R.I., pp.6809.

Bian, Z., Wang, Y., Zhang, X., Li, T., Grundy, S., Yang, Q. and Cheng, R., 2020. A Review of Environment Effects on Nitrate Accumulation in Leafy Vegetables Grown in Controlled Environments. *Foods*, 9(6), pp.732.

Binnemans, K., Jones, P., Blanpain, B., Van Gerven, T., Yang, Y., Walton, A. and Buchert, M., 2013. Recycling of rare earths: a critical review. *Journal of Cleaner Production*, 51, pp.1-22.

Bipm Joint Committee for Guides in Metrology, 2008. Evaluation of measurement data – Guide to the expression of uncertainty in measurement JCGM 100:2008 (GUM 1995 with minor corrections). Paris, France: BIPM

Borra, C., Pontikes, Y., Binnemans, K. and Van Gerven, T., 2015. Leaching of rare earths from bauxite residue (red mud). *Minerals Engineering*, 76, pp.20-27.

Bridgemohan, S., Moodley R., 2021. Urban mining of rare earth elements from rare earth magnets – alternative solvents for extraction. ENCH4LA Laboratory /Industry Final Year Project Report, University of KwaZulu-Natal, Durban, South Africa (Unpublished)

Carrington, D., 2019. Phosphate fertiliser 'crisis' threatens world food supply. *The Guardian*, [online] Available at: <https://www.theguardian.com/environment/2019/sep/06/phosphate-fertiliser-crisis-threatens-world-food-supply> [Accessed 18 August 2020].

Cevasco, G. and Chiappe, C., 2014. Are ionic liquids a proper solution to current environmental challenges?. *Green Chemistry*, 16(5), pp.2375.

Chemicalbook.com. 2020. *BIS(2,4,4-Trimethylpentyl)Dithiophosphinic Acid | 107667-02-7*. [online] Available at: <https://www.chemicalbook.com/ChemicalProductProperty_EN_CB8436386.htm> [Accessed 25 July 2020].

Chen, Z., 2010. Global rare earth resources and scenarios of future rare earth industry. *Journal of Rare Earths*, 29(1), pp.1-6.

Chi, L. and Tian, J., 2007. Review of weathered rare earth ore. *Journal of Chinese Rare Earth ore*, 25(6), pp.641-652.

Cocalia, V., Jensen, M., Holbrey, J., Spear, S., Stepinski, D. and Rogers, R., 2005. Identical extraction behavior and coordination of trivalent or hexavalent f-element cations using ionic liquid and molecular solvents. *Dalton Transactions*, (11), pp.1966.

Coey, J., 2012. Permanent magnets: Plugging the gap. *Scripta Materialia*, 67(6), pp.524-529.

Cossu, R., 2013. The urban mining concept. *Waste Management*, [online] 33(3), pp.497-498. Available at: <https://doi.org/10.1016/j.wasman.2013.01.010>.

Date, A. and Gray, A., 1989. *Applications Of Inductively Coupled Plasma Mass Spectrometry*. 17th ed. London, UK.

Davris, P., Balomenos, E., Panias, D. and Paspaliaris, I., 2016. Selective leaching of rare earth elements from bauxite residue (red mud), using a functionalizsed hydrophobic ionic liquid. *Hydrometallurgy*, 164, pp.125-135.

Doyle, F., 1986. Solvent extraction. Principles and applications to process metallurgy, part 1. *International Journal of Mineral Processing*, 16(3-4), pp.299-300.

Doyle, F., Benz, M., Shei, M., Bao, J., Ku, D. and Zhen, H., 2000. Direct production of mixed, rare earth oxide feed for high energy-product magnets. *Rare Earths and Actinides: Science, Technology and Applications*, 4, pp.31-44.

Dupont, D. and Binnemans, K., 2015. Rare-earth recycling using a functionalizsed ionic liquid for the selective dissolution and revalorizsation of Y2O3: Eu3+ from lamp phosphor waste. *Green Chemistry*, 17(2), pp.856-868.

Ekberg, C., Englund, S., Persson, I., 2012. The tetrad effect in the lanthanoid series — experiment and explanation. Glob. J. Inorg. Chem. 3 (11), pp. 1–4

European Commission, 2011. Critical metals in strategic energy technologies. (Available at), http://setis.ec.europa.eu/system/files/CriticalMetalsinStrategicEnergyTechnologiesdef.pdf (Sept. 2014).

European Commission, 2014. Critical raw materials for EU. Report of the Ad-hoc Working Group on Defining Critical Raw Materials (Available at: http://ec.europa.eu/ enterprise/policies/raw-materials/files/docs/report-b_en.pdf Sept. 2014).

Faustino, M., Marques, J., Monteiro, L., Stellato, T., Soares, S., Silva, T., da Silva, D., Pires, M. and Cotrim, M., 2016. Uncertainty estimation in the determination of metals in superficial water by ICP-OES. *Journal of Physics: Conference Series*, 733, p.012032.

Fleischer, M., 1954. The abundance and distribution of the chemical elements in the earth's crust. *Journal of Chemical Education*, 31(9), pp.446.

Foskor.co.za. 2020. *Foskor - Home*. [online] Available at: <http://foskor.co.za/SitePages/Home.aspx> [Accessed 18 August 2020].

Geist, A., Nitsch, W. and Kim, J., 1999. On the kinetics of rare-earth extraction into D2EHPA. *Chemical Engineering Science*, 54(12), pp.1903-1907.

Gergoric, M., Barrier, A. and Retegan, T., 2018. Recovery of Rare-Earth Elements from Neodymium Magnet Waste Using Glycolic, Maleic, and Ascorbic Acids Followed by Solvent Extraction. *Journal of Sustainable Metallurgy*, 5(1), pp.85-96.

Gruber, V. and Carsky, M., 2020. New technology for lanthanide recovery from spent Nd-Fe-B magnets. *South African Journal of Chemical Engineering*, 33, pp.35-38.

Haque, N., Hughes, A., Lim, S. and Vernon, C. 2014. Rare Earth Elements: Overview of Mining, Mineralogy, Uses, Sustainability and Environmental Impact. *Resources*, 3(4), pp.614-635.

Hexion, 2015. Hexion Versatic Acid [Material and Safety Data Sheet], Hexion, accessed 29 September 2021, https://www.hexion.com/CustomServices/PDFDownloader.aspx?type=tds&pid=4cf78a2c-5814-6fe3-ae8a-ff0300fcd525

Hino, A., Nishihama, S., Hirai, T. and Komasawa, I., 1997. Practical study of liquid-liquid extraction process for separation of rare earth elements with bis(2-ethylhexyl) phosphinic acid. *Journal of Chemical Engineering of Japan*, 30(6), pp.1040-1046.

Hirayama, N., Okamura, H., Kidani, K. and Imura, H., 2008. Ionic Liquid Synergistic Cation-Exchange System for the Selective Extraction of Lanthanum(III) Using 2-Thenoyltrifluoroacetone and 18-Crown-6. *Analytical Sciences*, 24(6), pp.697-699.

Hogberg, S., Holboll, J., Mijatovic, N., Jensen, B. and Bendixen, F., 2017. Direct Reuse of Rare Earth Permanent Magnets—Coating Integrity. *IEEE Transactions on Magnetics*, 53(4), pp.1-9.

Huang, X., Dong, J., Wang, L., Feng, Z., Xue, Q. and Meng, X., 2017. Selective recovery of rare earth elements from ion-adsorption rare earth element ores by stepwise extraction with HEH(EHP) and HDEHP. *Green Chemistry*, 19(5), pp.1345-1352.

Huang, X., Dong, J., Wang, L., Feng, Z., Xue, Q. and Meng, X., 2017. Selective recovery of rare earth elements from ion-adsorption rare earth element ores by stepwise extraction with HEH(EHP) and HDEHP. *Green Chemistry*, 19(5), pp.1345-1352.

Institute for Applied Technology, 2012. *Recycling Critical Raw Materials From Waste Electronic Equipment*. Darmstadt: Institute for Applied Technology.

Jensen, M., Neuefeind, J., Beitz, J., Skanthakumar, S. and Soderholm, L., 2003. Mechanisms of Metal Ion Transfer into Room-Temperature Ionic Liquids: The Role of Anion Exchange. *Journal of the American Chemical Society*, 125(50), pp.15466-15473.

Jones, A., Wall, F. and Williams, C., 1996. Rare Earth Minerals. Chemistry, Origin and Ore Deposits. *Mineralogical Magazine*, 60(402), pp.853-853.

Jordens, A., Cheng, Y. and Waters, K., 2013. A review of the beneficiation of rare earth element bearing minerals. *Minerals Engineering*, 41, pp.97-114.

Kilbourn, B., 1993. A lanthanide lanthology. *Applied Catalysis A: General*, [online] 115(1). Available at: <: http://www.phy.davidson.edu/fachome/dmb/RESolGelGlass/Lanthology/Lanthology_A-L.pdf>.

King, H., 2020. *REE - Rare Earth Elements - Metals, Minerals, Mining, Uses*. [online] Geology.com. Available at: <https://geology.com/articles/rare-earth-elements/> [Accessed 22 April 2020].

Kislik, V., 2002. Competetive Complexation/Solvation Theory of solvent extraction. II. Solvent extraction of metals by acidic extractants. *Separation Science and Technology*, 37(11), pp.2623-2657.

Kolarik, Z., 2013. Ionic Liquids: How Far Do they Extend the Potential of Solvent Extraction of f-Elements?. *Solvent Extraction and Ion Exchange*, 31(1), pp.24-60.

Korkisch, J., 1969. *Modern Methods For The Separation Of Rarer Metal Ions*. 1st ed. Pergamon Press, pp.20-26.

Korpusov, A.V., Danilov, N.A., Krylov, Yu. S., Korpusova, R.D., Drygin, A.I., Shvartsman, V.Y., 1974. Investigation of rare earth elements extraction with different carboxylic acids, In:

Proceedings of International Solvent Extraction Conference (ISEC 74), vol. II, Lyon, pp.1109–1120

Kozonoi, N. and Ikeda, Y., 2007. Extraction Mechanism of Metal Ion from Aqueous Solution to the Hydrophobic Ionic Liquid, 1-Butyl-3-methylimidazolium Nonafluorobutanesulfonate. *Monatshefte für Chemie - Chemical Monthly*, 138(11), pp.1145-1151.

Krishnamurthy, N. and Gupta, C., 2016. *Extractive Metallurgy of Rare Earths*. Boca Raton: CRC Press/Taylor & Francis Group.

Kubota, F, Koyanagi, Y, Nakashima, K, Shimojo, K, Kamiya, N & Goto, M 2008, 'Extraction of lanthanide ions with an organophosphorous extractant into ionic liquids', *Solvent Extraction Research and Development*, vol. 15, pp. 81-87.

Lahiri, S., Nayak, D., Nandy, M. and Das, N., 1998. Separation of carrier free lutetium produced in proton activated ytterbium with HDEHP. *Applied Radiation and Isotopes*, 49(8), pp.911-913.

Lahiri, S., Nayak, D., Nandy, M. and Das, N., 1998. Separation of carrier free lutetium produced in proton activated ytterbium with HDEHP. *Applied Radiation and Isotopes*, 49(8), pp.911-913.

Li, D., Wang, Z. and Chen, Z., 1988. Study on extraction separation of rare earths, cerium(IV), scandium and thorium by P507. *Acta Chimica Sinica*, 46(5), pp.492-495.

Liu, J., Vora, P. and Walmer, M., 2008. Overview of Recent Progress in Sm-Co Based Magnets. *Journal of Iron and Steel Research, International*, 13, pp.319-323.

Liu, Z. and Li, H., 2015. Metallurgical process for valuable elements recovery from red mud—A review. *Hydrometallurgy*, 155, pp.29-43.

Lu, J., Wei, Z., Li, D., Ma, G., Jiang, Z., 1998. Recovery of Ce (IV) and Th (IV) from rare earths (III) with Cyanex 923. *Hydrometallurgy* 50, pp.77–87.

Ma, E., Yan, X., Long, H. and Yuan, C., 2003. Chemistry of lanthanides extraction by 2-ethylhexylphosphonic acid mono-2-ethylhexylester. *Science in China Series B: Chemistry*, 5(3), pp.565-573.

Mallah, M., Shemirani, F. and Maragheh, M., 2009. Ionic Liquids for Simultaneous Preconcentration of Some Lanthanoids Using Dispersive Liquid−Liquid Microextraction Technique in Uranium Dioxide Powder. *Environmental Science & Technology*, 43(6), pp.1947-1951.

Mallah, M., Shemirani, F., Ghannadi Maragheh, M. and Jamali, M., 2010. Evaluation of synergism in dispersive liquid–liquid microextraction for simultaneous preconcentration of some lanthanoids. *Journal of Molecular Liquids*, 151(2-3), pp.122-124.

McLennan, S., 1994. Rare earth element geochemistry and the “"tetrad”" effect. *Geochimica et Cosmochimica Acta*, 58(9), pp.2025-2033.

Meyer, L., Bras, B., 2011. Rare earth metal recycling. *IEEE International Symposium on Sustainable Systems and Technology (ISSST)*, pp.1–6.

Millsaps, L. (2018). *Rare earth magnet recycling is a grind, but new process takes a simpler approach*. [online] Phys.org. Available at: https://phys.org/news/2018-04-rare-earth-magnet-recycling-simpler.html [Accessed 6 Feb. 2020].

Molbase.com. 2020. *Versatic 10 Acid_Molbase*. [online] Available at: <http://www.molbase.com/en/name-VERSATIC%2010%20ACID.html> [Accessed 12 August 2020].

Nair, S. and Smutz, M., 1967. Recovery of lanthanum from didymium chloride with Di(2-ethylhexyl)-phosphoric acid as solvent. *Journal of Inorganic and Nuclear Chemistry*, 29(7), pp.1787-1797.

Nakashima, K., Kubota, F., Maruyama, T. and Goto, M., 2003. Ionic Liquids as a Novel Solvent for Lanthanide Extraction. *Analytical Sciences*, 19(8), pp.1097-1098.

Nakashima, K., Kubota, F., Maruyama, T. and Goto, M., 2005. Feasibility of Ionic Liquids as Alternative Separation Media for Industrial Solvent Extraction Processes. *Industrial & Engineering Chemistry Research*, 44(12), pp.4368-4372.

Nash, K., 1993. A Review of the Basic Chemistry and Recent Developments in Trivalent f-Elements Separations. *Solvent Extraction and Ion Exchange*, 11(4), pp.729-768.

Nayak, P., Kumaresan, R., Venkatesan, K., Antony, M. and Vasudeva Rao, P., 2014. Extraction Behavior of Am(III) and Eu(III) from Nitric Acid Medium in Tetraoctyldiglycolamide-Bis(2-Ethylhexyl)Phosphoric Acid Solution. *Separation Science and Technology*, 49(8), pp.1186-1191.

National Center for Biotechnology Information. PubChem Compound Summary for CID 9275, Bis(2-ethylhexyl) hydrogen phosphate. https://pubchem.ncbi.nlm.nih.gov/compound/Bis_2-ethylhexyl_-hydrogen-phosphate. Accessed May 20, 2022.Nilsson, M. and Nash, K., 2007. Review Article: A Review of the Development and Operational Characteristics of the TALSPEAK Process. *Solvent Extraction and Ion Exchange*, 25(6), pp.665-701.

Ochsenkühn-Petropulu, M., Lyberopulu, T., Ochsenkühn, K. and Parissakis, G., 1996. Recovery of lanthanides and yttrium from red mud by selective leaching. *Analytica Chimica Acta*, 319(1-2), pp.249-254.

Okamura, H., Hirayama, N., Morita, K., Shimojo, K., Naganawa, H. and Imura, H., 2010. Synergistic Effect of 18-Crown-6 Derivatives on Chelate Extraction of Lanthanoids(III) into an Ionic Liquid with 2-Thenoyltrifluoroacetone. *Analytical Sciences*, 26(5), pp.607-611.

Peppard, D. and Wason, G., 1961. Liquid-liquid extraction of trivalent rare earths using acidic phosphonates as extractant. *Rare Earth Research*, pp.37-50.

Peppard, D., Driscoll, W., Sironen, S. and Mason, G., 1953. Study of the solvent extraction of the transition elements. *Journal of Physical Chemistry*, pp.334-343.

Peppard, D., Mason, G. and Lewey, S., 1969. A tetrad effect in the liquid-liquid extraction ordering of lanthanides(III). *Journal of Inorganic and Nuclear Chemistry*, 31(7), pp.2271-2272.

Peppard, D., Mason, G., Driscoll, W. and Sironen, R., 1958. Acidic esters of orthophosphoric acid as selective extractants for metallic cations—tracer studies. *Journal of Inorganic and Nuclear Chemistry*, 7(3), pp.276-285.

Peppard, D., Mason, G., Maier, J. and Driscoll, W., 1957a. Fractional extraction of the lanthanides as their di-alkyl orthophosphates. *Journal of Inorganic and Nuclear Chemistry*, 4(5-6), pp.334-343.

Peppard, D.F., Driscoll, W.J., Sironen, R.J., McCarty, S., 1957b. Nonmonotonic ordering of lanthanides in tributyl phosphate-nitric acid extraction system. *Journal of Inorganic & Nuclear Chemistry* 4, pp.326–333.

Pesavento, M., Alberti, G. and Biesuz, R., 2009. Analytical methods for determination of free metal ion concentration, labile species fraction and metal complexation capacity of environmental waters: A review. *Analytica Chimica Acta*, 631(2), pp.129-141.

Preston, J. and du Preez, A., 1996. The separation of europium from a middle rare earth concentrate by combined chemical reduction, precipitation and solvent-extraction methods. *Journal of Chemical Technology & Biotechnology*, 65(1), pp.93-101.

Bis(2-ethylhexyl)-hydrogen-phosphate, Pubchem.ncbi.nlm.nih.gov. 2021. *Bis(2-ethylhexyl) hydrogen phosphate*. [online] Available at: <https://pubchem.ncbi.nlm.nih.gov/compound/Bis_2-ethylhexyl_-hydrogen-phosphate#section=3D-Conformer> [Accessed 12 May 2021].

Qi, D., 2018. *Hydrometallurgy Of Rare Earths Separation And Extraction*. 1st ed. Elsevier, pp.187-389.

Rabie, K., 2007. A group separation and purification of Sm, Eu and Gd from Egyptian beach monazite mineral using solvent extraction. *Hydrometallurgy*, 85(2-4), pp.81-86.

Ranganathan, S., Gribskov, M., Nakai, K. and Schönbach, C., 2019. *Encyclopedia of bioinformatics and computational biology*. 1st ed. Amsterdam: Elsevier Inc, pp.722-727.

Raposo, C., Windmöller, C. and Durão Júnior, W., 2003. Mercury speciation in fluorescent lamps by thermal release analysis. *Waste Management*, 23(10), pp.879-886.

Rathilal, S., 2010. *Modelling of a Vibrating-Plate Extraction Column*. Ph.D. University of KwaZulu-Natal.

Reddy, B., Kumar, B. and Radhika, S., 2009. Solid-Liquid Extraction of Terbium from Phosphoric Acid Medium using Bifunctional Phosphinic Acid Resin, Tulsion CH-96. *Solvent Extraction and Ion Exchange*, 27(5-6), pp.695-711.

Reddy, M., Rao, P. and Damodarm, A., 1995. Liquid-liquid extraction processes for the separation and purification of rare earths. *Mineral Processing and Extractive Metallurgy Review*, 12, pp.91-113.

Rey, J., Dourdain, S., Dufrêche, J., Berthon, L., Muller, J., Pellet-Rostaing, S. and Zemb, T., 2016. Thermodynamic Description of Synergy in Solvent Extraction: I. Enthalpy of Mixing at the Origin of Synergistic Aggregation. *Langmuir*, 32(49), pp.13095-13105.

Rey, J., Dourdain, S., Dufrêche, J., Berthon, L., Muller, J., Pellet-Rostaing, S. and Zemb, T., 2016. Thermodynamic Description of Synergy in Solvent Extraction: I. Enthalpy of Mixing at the Origin of Synergistic Aggregation. *Langmuir*, 32(49), pp.13095-13105.

Rice, A.C., Stone, C.A., 1962. Amines in liquid–liquid extraction of rare earth elements. *US Bureau of Mines* R.I., pp.5923

Rio Tinto Alcan International Ltd, 1989. *Recovery Of Rare Earth Elements From Sulphurous Acid Solution By Solvent Extraction*. US5015447A.

Ronda, C., Jüstel, T. and Nikol, H., 1998. Rare earth phosphors: fundamentals and applications. *Journal of Alloys and Compounds*, 275-277, pp.669-676.

Rösslein, M., (2014). Calculation of Measurement Uncertainty: An Example for Titration. White Paper. Greifensee, Switzerland: Mettle

Santhi, P., Reddy, M., Ramamohan, T. and Damodaran, A., 1991. Liquid-liquid extraction of yttrium (III) with mixtures of organophosphorus extractants: theoretical analysis of extraction behaviour. *Hydrometallurgy*, 27(2), pp.169-177.

Sato, T., 1989. Liquid-liquid extraction of rare-earth elements from aqueous acid solutions by acid organophosphorus compounds. *Hydrometallurgy*, 22(1-2), pp.121-140.

Sherrington, L., 1983. Commercial process for rare earths and thorium. *Handbook of Solvent Extraction*. Willey Interscience, New York, pp. 17.

Shimojo, K., Kurahashi, K. and Naganawa, H., 2008. Extraction behavior of lanthanides using a diglycolamide derivative TODGA in ionic liquids. *Dalton Transactions*, (37), pp.5083.

Shimojo, K., Naganawa, H., Kubota, F. and Goto, M., 2006. Solvent Extraction of Lanthanides into an Ionic Liquid ContainingN,N,N′,N′-Tetrakis(2-pyridylmethyl)ethylenediamine. *Chemistry Letters*, 35(5), pp.484-485.

Sigmaaldrich.com. 2020a. *Bis(2-Ethylhexyl) Phosphate*. [online] Available at: <https://www.sigmaaldrich.com/catalog/product/aldrich/237825?lang=en&region=ZA&gclid=CjwKCAjwps75BRAcEiwAEiACMV7b0Faa4V72t4fu3URI5DloVh_vj_bIS57Bc2QkcEXeLvuHRvKzGhoCvjYQAvD_BwE> [Accessed 12 August 2020].

Sigmaaldrich.com. 2020b. *Trioctylphosphine Oxide*. [online] Available at: <https://www.sigmaaldrich.com/catalog/product/aldrich/223301?lang=en&region=ZA> [Accessed 25 July 2020].

Sigmaaldrich.com. 2020c. *Adogen® 464*. [online] Available at: <https://www.sigmaaldrich.com/catalog/product/aldrich/856576?lang=en&region=ZA> [Accessed 25 July 2020].

Špadina, M., Bohinc, K., Zemb, T. and Dufrêche, J., 2019. Colloidal Model for the Prediction of the Extraction of Rare Earths Assisted by the Acidic Extractant. *Langmuir*, 35(8), pp.3215-3230.

Statista., 2022. *Neodymium oxide price globally 2009-2030 | Statista*. [online] Available at: https://www.statista.com/statistics/450152/global-reo-neodymium-oxide-price-forecast/ [Accessed 6 Jan. 2022].

Stoy, L., Diaz, V. and Huang, C., 2021. Preferential Recovery of Rare-Earth Elements from Coal Fly Ash Using a Recyclable Ionic Liquid. *Environmental Science & Technology*, 55(13), pp.9209-9220.

Suárez, C., Ahumada, E., Orellana, F., Hein, H., Cote, G. and Lizama, H., 2002. Extraction of iron(III) from acidic sulfate solutions with bis(2-ethylhexyl)phosphoric acid in PENRECO® 170 ES, a new friendly diluent. *Journal of Chemical Technology & Biotechnology*, 77(2), pp.183-189.

Sun, X., Ji, Y., Chen, J. and Ma, J., 2009. Solvent impregnated resin prepared using task-specific ionic liquids for rare earth separation. *Journal of Rare Earths*, 27(6), pp.932-936.

Sun, X., Luo, H. and Dai, S., 2013. Mechanistic investigation of solvent extraction based on anion-functionalized ionic liquids for selective separation of rare-earth ions. *Dalton Transactions*, 42(23), pp.8270.

Sun, X., Luo, H. and Dai, S., 2013. Mechanistic investigation of solvent extraction based on anion-functionalized ionic liquids for selective separation of rare-earth ions. *Dalton Transactions*, 42(23), pp.8270.

Sun, X., Wu, D., Chen, J. and Li, D., 2007. Separation of scandium(III) from lanthanides(III) with room temperature ionic liquid based extraction containing Cyanex 925. *Journal of Chemical Technology & Biotechnology*, 82(3), pp.267-272.

Suzuki, Y., Nagayama, T., Sekine, M., Mizuno, M. and Yamaguchi, K., 1986. Proceedings of the seventeenth rare earth research conference — part 1 precipitation incidence of the lanthanoid(III) hydroxides. *Journal of the Less Common Metals*, 126, pp.351-356.

Takayama, R., Ooe, K., Yahagi, W., Fujisawa, H., Komori, Y., Kikunanga, H., Yoshimura, T., Takahashi, N., Takahisa, k., Haba, H., Kudou, Y., Ezaki, Y., Toyoshima, A., Asai, M., Nagame, Y., Saito, T., Mitsugashira, T. and Shinohara, A., 2011. Solvent extraction of trivalent actinides with di(2-ethylhexyl) phosphoric acid. *Radiochimica Acta*, 1, pp.157-160.

Tanaka, M., Oki, T., Koyama, K., Narita, H. and Oishi, T., 2013. Recycling of Rare Earths from Scrap. *Including Actinides*, pp.159-211.

TCI Chemical, 2020. *Naphthenic Acid Price, Buy Naphthenic Acid - Chemicalbook*. [online] Chemicalbook.com. Available at: <https://www.chemicalbook.com/Price/NAPHTHENIC-ACID.htm> [Accessed 25 July 2020].

Thermofisher.com. n.d. *Comparison Of ICP-OES And ICP-MS For Trace Element Analysis | Thermo Fisher Scientific - UK*. [online] Available at: <https://www.thermofisher.com/za/en/home/industrial/environmental/environmental-learning-center/contaminant-analysis-information/metal-analysis/comparison-icp-oes-icp-ms-trace-element-analysis.html#:~:text=ICP%2DOES%20is%20mainly%20used,%2C%20soil%2C%20and%20solid%20waste.&text=ICP%2DMS%2C%20on%20the%20other,samples%20with%20low%20regulatory%20limits.> [Accessed 24 August 2020].

Thompson, M. and Walsh, J., 1989. *Handbook Of Inductively Coupled Plasma Spectrometry*. 2nd ed. Springer U.S.

Tian, G., Li, J. and Hua, Y., 2010. Application of ionic liquids in hydrometallurgy of nonferrous metals. *Transactions of Nonferrous Metals Society of China*, 20(3), pp.513-520.

Tkac, P., Vandegrift, G., Lumetta, G. and Gelis, A., 2012. Study of the Interaction between HDEHP and CMPO and Its Effect on the Extraction of Selected Lanthanides. *Industrial & Engineering Chemistry Research*, 51(31), pp.10433-10444.

Tkac, P., Vandegrift, G., Lumetta, G. and Gelis, A., 2012. Study of the Interaction between HDEHP and CMPO and Its Effect on the Extraction of Selected Lanthanides. *Industrial & Engineering Chemistry Research*, 51(31), pp.10433-10444.

Tse, P.K., 2011. China's rare earth industry, Open-file report 2011-1042, U.S.S Department of the Interior/U.S.S Geological Survey

Tunsu, C., Petranikova, M., Gergoric, M., Ekberg, C. and Retegan, T., 2015. Reclaiming rare earth elements from end-of-life products: A review of the perspectives for urban mining using hydrometallurgical unit operations. *Hydrometallurgy*, [online] Available at: <, http://dx.doi.org/10.1016/j.hydromet.2015.06.007> [Accessed 4 May 2020].

Turanov, A., Karandashev, V. and Baulin, V., 2008. Effect of ionic liquids on the extraction of rare-earth elements by bidentate neutral organophosphorus compounds from chloride solutions. *Russian Journal of Inorganic Chemistry*, 53(6), pp.970-975.

Tyler, G., 1992. AA or ICP - Which do you choose?. *Chemistry in Australia*, 59(4), pp.150-152.

U.S. Department of Energy, 1963. *Naphthenic Acid Solvent Extraction Of Rare-Earth Sulfates*. Washington: US Department of the Interior.

USGS, 2002. Rare earth elements — critical resources for high technology. (Available at), http://pubs.usgs.gov/fs/2002/fs087-02/ (Sept. 2014).

Wang, W., Pranolo, Y. and Cheng, C., 2011. Metallurgical processes for scandium recovery from various resources: A review. *Hydrometallurgy*, 108(1-2), pp.100-108.

Williams, A., Ellison, S., Berglund, M., Haesselbarth, W., Hedegaard, K., Kaarls, R., Mnsson, M., Rösslein, M., Stephany, R., Veen, A., Wegscheider, W., Wiel, H., Wood, R., Rong, P., Salit, M., Squirrell, A., Yasuda, K., Johnson, R., Lee, J., Mowrey, D., Regge, P., Fajgelj, A. and Galsworthy, D., 2000. *Quantifying uncertainty in analytical measurement*. London: Eurachem.

Williams-Wynn, M., Naidoo, P. and Ramjugernath, D., 2020. The distribution coefficients of Y^{3+} and Eu^{3+} between HNO3 and HDEHP. *Minerals Engineering*, 153, pp.106285.

Xie, F., Zhang, T., Dreisinger, D. and Doyle, F., 2014. A critical review on solvent extraction of rare earths from aqueous solutions. *Minerals Engineering*, 56, pp.10-28.

Xie, M., 2020. *Cyanex 302 Cas:132767-86-3 - Buy Cyanex 302 Product On Alibaba.Com*. [online] www.alibaba.com. Available at: <https://www.alibaba.com/product-detail/Cyanex-302-Cas-132767-86-3_60493010559.html> [Accessed 25 July 2020].

Xiong, Y., Wang, X. and Li, D., 2005. Synergistic Extraction and Separation of Heavy Lanthanide by Mixtures of Bis(2,4,4-trimethylpentyl)phosphinic Acid and 2-Ethylhexyl Phosphinic Acid Mono-2-Ethylhexyl Ester. *Separation Science and Technology*, 40(11), pp.2325-2336.

Xu, S., Simm, R., White, R. and Robinson, E., 1995. Prediction of P- and S- wave logs for seismic modeling. *SEG Technical Program Expanded Abstracts 1995*.

Xu, Y., Chumbley, L. and Laabs, F., 2000. Liquid metal extraction of Nd from NdFeB magnet scrap. *Journal of Materials Research*, 15(11), pp.2296-2304.

Yang, F., Kubota, F., Baba, Y., Kamiya, N. and Goto, M., 2013. Selective extraction and recovery of rare earth metals from phosphor powders in waste fluorescent lamps using an ionic liquid system. *Journal of Hazardous Materials*, 254-255, pp.79-88.

Yang, F., Kubota, F., Baba, Y., Kamiya, N. and Goto, M., 2013. Selective extraction and recovery of rare earth metals from phosphor powders in waste fluorescent lamps using an ionic liquid system. *Journal of Hazardous Materials*, 254-255, pp.79-88.

Yoon, H., Kim, C., Chung, K., Lee, J., Shin, S., Lee, S., Joe, A., Lee, S. and Yoo, S., 2014. Leaching kinetics of neodymium in sulfuric acid of rare earth elements (REE) slag concentrated

by pyrometallurgy from magnetite ore. *Korean Journal of Chemical Engineering*, 31(10), pp.1766-1772.

Yoon, S., Lee, J., Tajima, H., Yamasaki, A., Kiyono, F., Nakazato, T. and Tao, H., 2010. Extraction of lanthanide ions from aqueous solution by bis(2-ethylhexyl)phosphoric acid with room-temperature ionic liquids. *Journal of Industrial and Engineering Chemistry*, 16(3), pp.350-354.

Yu, T., Olsson, E., Lian, G., Liu, L., Huo, F., Zhang, X. and Cai, Q., 2021. Prediction of the Liquid–Liquid Extraction Properties of Imidazolium-Based Ionic Liquids for the Extraction of Aromatics from Aliphatics. *Journal of Chemical Information and Modeling*, 61(7), pp.3376-3385.

Zhang, Y., Li, J., Huang, X., Wang, C., Zhu, Z. and Zhang, G., 2008. Synergistic extraction of rare earths by mixture of HDEHP and HEH/EHP in sulfuric acid medium. *Journal of Rare Earths*, 26(5), pp.688-692.

Zhao, Q., Li, Y., Kuang, S., Zhang, Z., Bian, X. and Liao, W., 2019. Synergistic extraction of heavy rare earths by mixture of α-aminophosphonic acid HEHAMP and HEHEHP. *Journal of Rare Earths*, 37(4), pp.422-428.Ahmad, Z., 2003. The properties and application of scandium-reinforced aluminum. *JOM*, 55(2), pp.35-39.

Zheng, D., Gray, N. and Stevens, G., 1991. Comparison of Naphthenic Acid, Versatic Acid and D2EHPA for the Separation of Rare Earths. *Solvent Extraction and Ion Exchange*, 9(1), pp.85-102.

Zhou, B., Li, Z. and Chen, C., 2017. Global Potential of Rare Earth Resources and Rare Earth Demand from Clean Technologies. *Minerals*, 7(11), pp.203.

Zuo, Y., Chen, J. and Li, D., 2008. Reversed micellar solubilization extraction and separation of thorium(IV) from rare earth(III) by primary amine N1923 in ionic liquid. *Separation and Purification Technology*, 63(3), pp.684-690.

Zuo, Y., Liu, Y., Chen, J. and Li, D., 2008a. The Separation of Cerium(IV) from Nitric Acid Solutions Containing Thorium(IV) and Lanthanides(III) Using Pure [C8mim]PF6as Extracting Phase. *Industrial & Engineering Chemistry Research*, 47(7), pp.2349-2355.

Zuo, Y., Liu, Y., Chen, J. and Li, D., 2009. Extraction and recovery of cerium(IV) along with fluorine(I) from bastnasite leaching liquor by DEHEHP in [C8mim]PF6. *Journal of Chemical Technology & Biotechnology*, 84(7), pp.949-956.

Appendices

Appendix A: Additional Information

A.1 Review of Experimental Methods Reported in Literature

Rey *et al., (*2016) discusses a system in which a DMDOHEMA and HDEDP mixture is used as the extractant. Five samples of known concentrations were prepared with analytical grade dodecane as a solvent. These were contacted to aqueous solutions composed of 50 $^{mmol}/_{L}$ of europium nitrate in 1 $^{mol}/_{L}$ of nitric acid, obtained by dissolution of $Eu(NO_3)_3 \cdot 6H_2O$ salts (Rey *et al.*, 2016). To study the effects of synergy the ratio, the DMDOHEMA concentration is varied up to 100% (Rey *et al.*, 2016). To determine the Critical Aggregate Concentration (CAC), the ranges of the molar concentrations (DMDOHEMA + HDEHP) were varied between 5.1×10^{-3} and 0.6 $^{mol}/_{L}$. Extractions were performed in test tubes by contacting the aqueous and organic phases for 1 hour at room temperature to allow the transfer phase equilibrium to be reached (Rey *et al.*, 2016).

The europium in the aqueous solution was analysed using the Inductively Coupled Plasma Atomic Emission Spectrophotometry (ICP-OES, Spectro Arcos) (Rey *et al.*, 2016). The aqueous solution was analysed before and after the extraction had taken place. The extraction of water was quantified by coulometry and the nitric acid titrated by potentiometry with NaOH solution of 0.1$^{mol}/_{L}$. The electrospray ionisation mass spectroscopy measurements were recorded in the positive ionisation mode using a Bruker microTOFII equipped with an electrospray ionisation source and a time-of-flight analyser (Rey *et al.*, 2016). The experimental conditions can be found in Rey *et al., (*2016). The Quadruple Time of flight spectroscope (QTOF) was calibrated using an Agilent (G2421A) ES-TOF tuning solution. Fragmentation mass spectra were obtained from collision-induced dissociation with nitrogen. A syringe infusion pump (Cole Palmer) delivered samples at 180 $^{\mu L}/_{h}$ to the electrospray source. The organic phases were diluted to concentrations of the order 1×10^{-4} in methanol prior to analysis. The organic and aqueous phase densities were measured with a high-precision thermostated density analyser based on an oscillatory fork (Rey *et al.*, 2016).

Takayama *et al., (*2011) discusses the extraction of Am, Cm, Cf and Fm using HDEHP in benzene. The HDEHP used for the study is of 99% purity. The rare earths were supplied as 10 ppm standard solutions. The other chemicals used were high purity grades. The preparation of the aqueous solutions was carried out by evaporating the standard solutions to dryness in PFA beakers, the residues were subsequently dissolved in HNO_3 (Takayama *et al.*, 2011). The organic phases used were of concentrations varying between 0.08–1.0 M HDEHP in benzene. Six millilitres of each phase were mixed in a polypropylene tube then shaken in an incubator at 31±1°C for a period of 10 min (Takayama, 2011).

Subsequent to centrifuging the mixture to induce phase separation, an aliquot of 5ml (organic phase) was placed in a different test tube (Takayama *et al.*, 2011). This aliquot was mixed with 5ml of 10M HNO_3 to back-extract Ln(III) into the nitric acid solution. Thereafter 4mL of the aqueous phase and the organic phase were evaporated to dryness in PFA beakers and the residues dissolved in 5% HNO_3. The pH of the equilibrated aqueous phase was measured by titration with 0.1 or 0.025M NaOH (Takayama *et al.*, 2011). The distribution ratios were thereafter calculated by measuring the concentrations of the Ln(III) metals in the aqueous and organic phases by ICP-MS (Agilent 7500s) alongside the calibration curve method. ^{139}Ce and ^{152}Eu tracers were used to confirm the extraction behaviour of the Ln(III) by comparison with the results of the ICP-MS measurements (Takayama *et al.*, 2011).

Nayak *et al., (*2014) investigated the extraction behaviour of Am (III) and Eu(III) from Nitric acid medium. The chemicals used were of analytical grade; Eu (III) was purchased as a tracer. The Am(III) used in the running of the experiments was purchased as Am_2O_3 and dissolved in nitric acid. The HDEHP used was purchased, and the TODGA was synthesised. An equilibration tube of 5 mL capacity containing 1 mL of both organic and aqueous phase was equilibrated in a constant temperature water bath (298 K). The organic phases used were blends of TODGA, HDEHP, and TODGA-HDEHP in n-dodecane. The aqueous phase was composed of various concentrations of nitric acid laced with ^{241}Am(III) or $^{(152+154)}$Eu(III) tracer. After equilibration, the radioactivity of ^{241}Am(III) and $^{(152+154)}$Eu(III) in the organic and aqueous phases was measured using a well-type NaI(Tl) detector. The distribution ratio (D_M) of the metal ions was then determined.

In the study conducted by Wlliams-Wynn *et al., (*2020) the distribution co-efficient measurements, describing the concentrations of yttrium and europium in the aqueous and organic phases were performed by the use of jacketed liquid-liquid equilibrium cells. The

stirring mechanism was coated with PTFE to withstand the pressures of mineral acid-organic solvent mixtures. The jacket of the cell is filled with water, while the internal void of the cell (40ml) contained the mixture which was to be studied. The temperature of the water passing through the cell jacket was maintained using a Polyscience® temperature controller (model 7306A12E, stability of 0.01 K). The Liquid-Liquid Extraction (LLE) cell was placed upon a magnetic stirrer plate (FMH Instruments, Model STR-M). The PTFE-coated stirrer bar (12 mm length, 4.5 mm OD) was placed in the cell, enabling agitation of the contents within the cell.

The temperature inside the cell was monitored by the use of a Pt100 temperature probe (WIKA Instruments, model TF45 class A) and a Shinko Digital Indicating Controller (Shinko DIC, model ACS-13A Series 1/16 DIN) was used to monitor the temperature measured by the probe. A mass balance, (Mettler Toledo, model AB204-S) with an uncertainty of 0.001 g, was used for the formation of the liquid phases and the recording of mass measurements. The concentration of hydronium ions within the aqueous phase was determined by the use of back titration by NaOH solution with phenolphthalein indicator. The concentrations of the metal ions within the aqueous phase were determined by the use of a Perkin Elmer OptimaTM 8300 ICP-OES (Inductively coupled plasma optical emission spectrometer). The conditions of the atmosphere were measured by the use of an internal barometer of a high-pressure calibrator (Mensor, model CPC 8000, uncertainty of 0.005 kPa or 0.01% of the full range). All equipment was calibrated accordingly (Williams-Wynn *et al.*, 2020).

Solutions of known concentrations of yttrium or europium in nitric acid were synthesised by digestion. The mass of acid required for the digestion and production of these solutions was calculated prior to formulation (Williams-Wynn *et al.*, 2020). Approximately 0.05 g of rare earth oxide was digested in 0.5 - 8 g of 55 wt. % nitric acid. Subsequent to digestion, the aqueous solution was then diluted to the correct H + ion concentration (0.24-4M) by the addition of distilled water. The organic solvent (HDEHP in n-nonane or n-dodecane) was prepared by the dilution of a known mass of HDEHP, in a volumetric flask. Once these organic and aqueous phases had been prepared, 3-4g of each phase was added to the LLE cells by the use of a syringe. Agitation was carried out for 12 hours at a temperature of 298.2K. After the 12 hours of agitation, 8 the mixture was allowed to separate for 8 hours. The NaOH titration solution was prepared by the dissolution of NaOH pellets in

a volume of distilled water. The concentration of the NaOH solution was tested by back-titration against a potassium hydrogen phthalate (KHP) standard solution.

As the ICP-OES was not capable of ionising organic material, the concentration of the metals in the aqueous phase was analysed in the study. A material balance calculation was thereafter used to calculate the concentration of the metals in the organic phase. The LLE samples collected were further diluted by mass, using the mass balance, to ensure that the concentrations fell within the ranges of the ICP-OES calibration curves (Williams-Wynn *et al.*, 2020).

In the system described by Davris *et al., (*2016) the viscosity measurements were conducted with a Brookfield viscometer supported by a Brookfield Thermosel accessory. Mineralogical characterisations were made by a Bruker D8 centre X-beam diffractometer. The particle size measurements were achieved by the use of a Malvern Laser particle size analyser. Infrared measurements directed with a Perkin Elmer FTIR range 100. 1 H NMR studies contacted with a Varian V300 MHz spectrometer utilising DMSO-d6 as a solvent at 25 °C (Davris *et al*., 2016). The metals in the solution were measured utilising ICP-MS and AAS. Calcium content was determined in a solid sample with XRF. Atmospheric leaching is carried out in a small reactor that includes a temperature controller, mechanical stirrer and a vapour condenser. Pressure leaching is carried out in a titanium autoclave reactor. The acquired solution was thereafter diluted for chemical analysis (Davris *et al.*, 2016).

Preston and du Preez (1996) described a continuous solvent extraction process for the separation of the 'middle' REEs (Sm, Eu, Gd, and Tb) as well as the light rare earth fractions (La, Ce, Pr, and Nd) from a nitrate feed. The 'middle' REEs were first subjected to extraction in a 15% v/v of HDEHP in Shellsol AB using an 8 stage counter-current circuit, succeeded by scrubbing with 1 mol/L HNO_3 in 2–4 stages, and thereafter stripping with 1.5 mol/L HCl in 6–8 stages. Residual REEs still present in the organic phase were recovered by the use of a secondary stripping circuit employing 2.5 mol/L HCl in 4 stages. A processing amount in excess of 1000 L of feed liquor was processed in two continuous counter-current trials operating over 630 hours. The recoveries of the 'middle' REEs in the strip liquors were relatively high (95–100%), whereas losses of the light REEs were below 4%. HDEHP has also been successfully used to separate Sm, Eu, and Gd from the other rare earths in a mixed nitrate-chloride leachate from monazite (Xie *et al.*, 2014; Rabie, 2007).

HDEHP can be used in the extraction of REEs at low pH values. However, the stripping of the loaded metals becomes difficult as the equilibrium lies firmly in favour of absorption. Therefore, a range of alternative acidic organophosphorus extractants have been studied for REE solvent extraction. It has been reported that DS5834 (Zeneca Specialties, with a formulation similar to M2EHPA, mono-2-ethylhexyl phosphoric acid) could extract Ga, In, Sm, and Gd from acidic media, but this alternative was found to be lacking selectivity for Sm and Gd,and showed little efficacy in the separation of these metals (Xie *et al.*, 2014). HEHEHP, available on the open market named as PC-88A, has experienced keen interest from REE separation researchers because REEs can be stripped from it at lower acidities than from HDEHP (Reddy *et al.*, 1995).

A few di-alkyl phosphinic acids have been reviewed for possible use in REE separation, although only Cyanex 272 (bis(2,4,4-trimethylpentyl)phosphinic acid) has been used commercially (Xie *et al.*, 2014). The extraction selectivity of DCHPA was found to be inferior to that of other di-alkyl phosphinic acids where La, Pr, Eu, Ho and Yb in chloroform solutions containing dicyclohexylphosphinic acid (DCHPA) were concerned. This could be attributed to the steric hindrance caused by the DCHPA cyclohexyl groups in the process of chelate formation (Xie *et al.*, 2014).

Solvation Extraction

Thorium Limited a UK based company used TBP to separate light rare earths in nitrate media by batch processing under total reflux (Xie *et al.*, 2014). Upon achieving steady-state operation, the process was stopped, and samples of varying compositions were drawn from different stages. The use of batch processing is not only difficult to scale up but is also costly when compared to continuous processing (Xie *et al.*, 2014) The extraction of mixed REE oxides from calcium sulfate hemihydrate sludge generated from operations at Phalaborwa mines in South Africa were studied at pilot scale (Peppard *et al.*, 1996). It was shown that from a leach liquor consisting of 1.0M nitric acid and 0.5M calcium nitrate REEs could be effectively leached. The organic phase was then stripped with water to produce a solution of REE nitrates. This recovery of REE oxides was effected by the addition of oxalic acid and calcining the resulting precipitate (Xie *et al.*, 2014).

Synergistic Solvent Extraction

The result caused by the addition of a series of di-alkyl alkylphosphonates $(RO)_2RPO$, tri-alkyl phosphates $(RO)_3PO$, tri-alkylphosphine oxides R_3PO and alkyl di-alkylphosphinates $(RO)R_2PO$ on the extraction behaviour of the trivalent lanthanides and yttrium from chloride media by DIPSA (3,5-di-isopropylsalicylic acid) was documented. All mixtures displayed synergistic effects will varying levels of intensity (Preston and du Preez, 1994). In so far as the series of compounds possessing R = n-butyl, the synergistic effect was observed to increase in the following order: $(RO)_3PS < (RO)_3PO < (RO)_2RPO < (RO)R_2PO < R_3PO$. Blends of N, N′ -Diisopropylcarbodiimide (DIPSA) and tri-isobutyl phosphine oxide (TIBPO) yielded marginal improvements on the separation factors between light and middle lanthanides ($\beta_{Sm/Nd} = 3.0$) than when compared with Versatic 10 acid alone ($\beta_{Sm/Nd} = 2.6$). The authors suggested that the extracted REE complexes existed in the form of LnA_3L_2 (wherein HA denotes a carboxylic acid and L represents the neutral organophosphorous compound). They also suggested that the synergism was a result of the replacement of all or some of the undissociated carboxylic acid (Xie *et al.*, 2014).

Xiong *et al.*, (2005) investigated binary acid extractant systems for the extraction of Yb^{3+} from chloride solutions using Cyanex 272, P507 (HEHEHP), and their blends in n-heptane. The extraction of Yb^{3+} was found to be higher when the blend is used when compared with Cyanex272 or P507 alone. Synergistic effects were observed when the separation of Yb/Tm and Lu/Yb was studied (Xie *et al.*, 2014). An investigation of the extraction of trivalent La, Nd, Sm, and Gd from sulfate media by a mixture of HDEHP and HEHEHP was studied by (Zhang *et al.*, 2008). Synergistic effects were observed the extraction of the four REEs under conditions at which the is pH = 2.0. The separation of Sm and Nd was significantly increased using a blend of HDEHP (40% v/v) and HEHEHP (60% v/v) (Xie *et al.*, 2014).

A.2 Solutions from recycled materials

Large amounts of REE waste ends its life in landfills as the large-scale recovery of many REEs is scarce (Meyer and Bras, 2011). Some of the areas of concern in the recovery of REEs via urban mining and the conventional production chain of REEs are the same. The pre-emanent drawbacks of urban mining relate to collection and dismantling requirements, difficult separation by conventional milling operations, matrix heterogeneity and, sometimes, low REEs content (Institute for Applied Technology, 2012).

REEs in recycled materials are present in matrices alongside many other contaminants, some of which pose serious environmental concerns. The isolation of the REE presents challenges to the economic feasibility for processing certain streams. It can be deduced that these difficulties are amongst the reasons that has resulted in the relatively large body of research in which the REE is obtained and studied as ion in solution or as a high purity REE oxide (Tunsu *et al.*, 2014). Yang *et al., (*2013), Raposo *et al., (*2003), Huang *et al., (*2017), Davris *et al., (*2016) as well as Xu *et al., (*2000) have investigated the recovery of the REE from waste materials as well as the subsequent beneficiation steps.

One of the examples of environmentally hazardous components occurring alongside the desired REE is mercury in the phosphors powder of spent fluorescent lamps (Raposo *et al.*, 2003; Tunsu *et al.*, 2014). The decontamination processes undertaken in cases such as these become mandatory. Leaching REEs as a method of pre-treatment demands the use of concentrated acids and bases at elevated temperatures in to achieve satisfactory leaching efficiencies. Although the hurdles to be overcome in the recycling process of REEs can be significant, it must be noted that in some cases; the virgin mining of REEs can pose challenges of a similar nature, if not greater (Tunsu *et al.*, 2014). The most important aspect in favour of urban mining is the relatively high content of REEs in certain products compared to natural deposits.

Appendix B: Temperature Probe Calibration

The temperature of the water bath as shown in Figure 4.1 is controlled by temperature controller (Vivo Itherm, Class 1). This was monitored by the use of a Pt100 temperature sensor. This sensor was calibrated to obtain the temperature using a WIKA CTH6500 liquid calibration bath. Figure C.1 below shows the relation between the Reference Sensor Temperature and the Pt100 sensor using 5 equidistant points, repeated 4 times. These points extend 10 K on either end of the 298 K operating point.

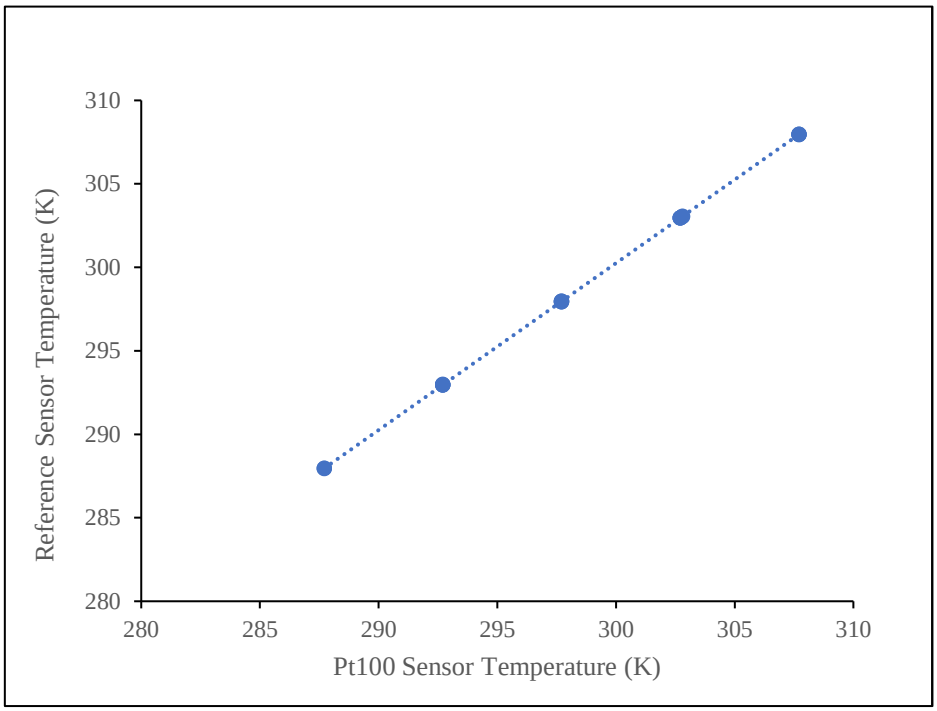

Figure B. 1 Calibration chart for temperature probe Pt 100 using WIKA CTH6500 liquid calibration bath

Figure B.1 above shows the scatter of the reference temperature probe with respect to the Pt100 sensor. The chart shows a consistent reading with a constant □T at the single decimal point significance of 0.3 K on which hysteresis has no discernible effect (Figure B.2).

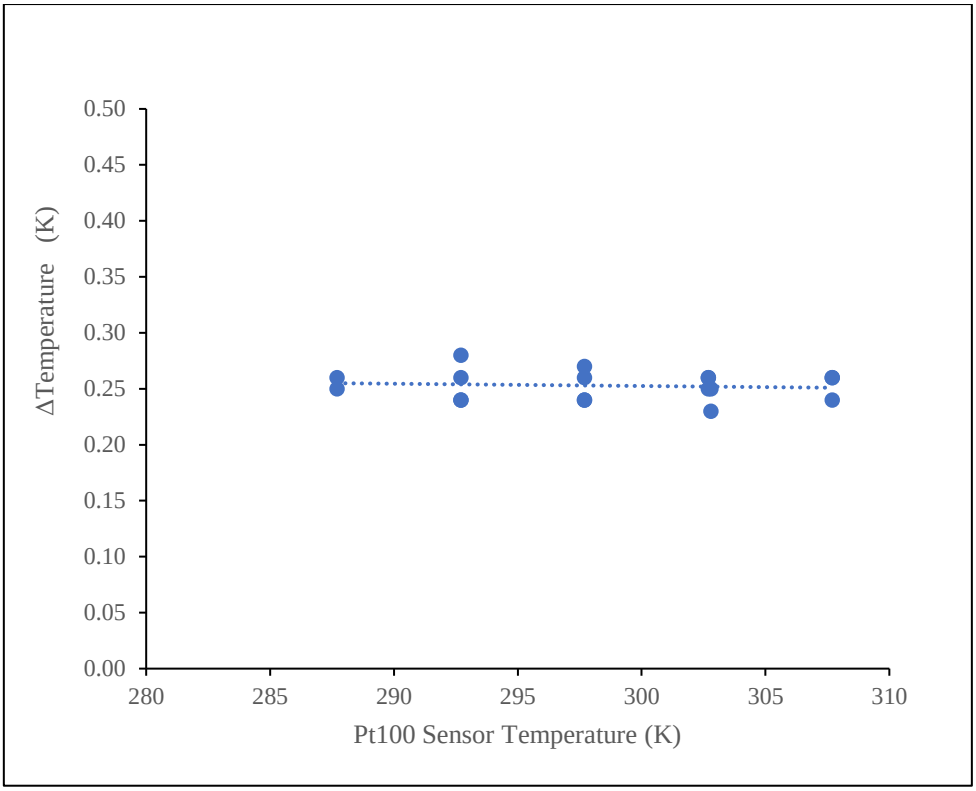

Figure B. 2 Plot of the temperature difference between the reference temperature sensor and the Pt100 temperature sensor (Δ Temperature) for tested points during the temperature sensor calibration

Appendix C: Experimental Uncertainty in Measurements

C.1 Distribution Coefficient Uncertainty

Figure C.1 below depicts the Ishakawa diagram, based on the work of Faustino *et al., (*2016), for the source's uncertainty inherent in the measurement of the concentrations of REEs by use of the ICP-OES analysis as detailed in Chapter 4 (see Section 4.4.6). Using the law of propagation of uncertainty the different sources described in the diagram were combined adhering to the Guide to the Expression of Uncertainty in Measurement (GUM) (BIPM Joint Committee for Guides in Metrology, 2008). As the distribution coefficient is given by the quotient of terms on a mass basis (see Section 2.3.1) the contributions of uncertainty are expressed on a mass basis to simplify the uncertainty computations.

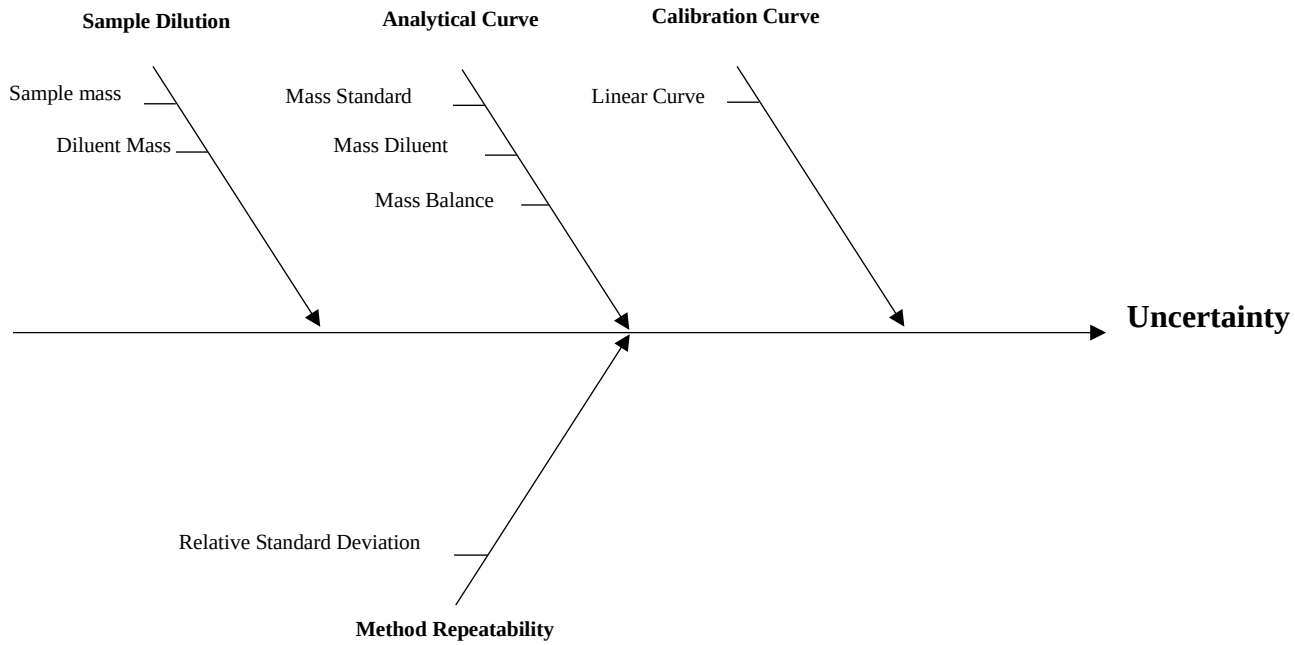

Figure C. 1 Ishikawa diagram for the evaluation of ICP-OES measured data uncertainties

C.1.1 Sample dilution Uncertainty

To minimize the number of variables needed for the analysis of the uncertainty due to the dilution of the samples, a mass basis was used. The contribution to this uncertainty being only the mass of the sample and the diluent. The uncertainty introduced to the value of the distribution coefficient due to the dilution of the sample, $u(C_{\text{sample dilution}})$, is described by the following equation:

$$u(C_{\text{sample dilution}}) = \sqrt{\left(\frac{u(m_{bal})}{m_{\text{sample}}}\right)^2 + \left(\frac{u(m_{bal})}{m_{\text{diluted}}}\right)^2} \cdot C_{\text{sample}} \quad \text{(C.1)}$$

In this equation $u(m_{bal})$ is the stated manufacturer uncertainty for the mass balance, m_{sample} refers to the mass of the concentrated sample used for the dilution, and m_{diluted} is the mass of the diluted sample.

B.1.2 Analysis Uncertainty

To account for the uncertainty associated with the application of the ICP-OES calibration curve and its measured intensities, the uncertainties emanating from the preparation of the standards was used. The standards used were prepared on a mass basis, therefore the uncertainty associated with their preparation is influenced greatly by the uncertainty of the mass balance. The uncertainty in the concentration of the stock solution, $u(C_{stock})$ was dependent primarily on the uncertainty of the mass balance and the manufacturer stated purity of the REO used in the preparation of the standards. The equation describing this relationship is as follows:

$$u(C_{\text{stock}}) = \sqrt{\left(\frac{u(m_{bal})}{m_{\text{REO}}}\right)^2 + \left(\frac{u(m_{bal})}{m_{HNO_3}}\right)^2 + \left(\frac{u(m_{bal})}{m_{water}}\right)^2 + {X_{REO}}^2} \cdot C_{\text{stock}} \quad \text{(C.2)}$$

The mass of component i is denoted as m_i, and the purity of the REO is denoted X_{REO}. Pursuant to this, the uncertainty of the concentration of the standards, $C_{stand,k}$, prepared from the stock solution can be estimated using the following equation:

$$u(C_{\text{stand,k}}) = \sqrt{\left(\frac{u(m_{bal})}{m_{\text{Stand,k}}}\right)^2 + \left(\frac{u(m_{bal})}{m_{dil}}\right)^2 + \left(\frac{u(C_{\text{stock}})}{C_{Stand,k}}\right)^2} \cdot C_{\text{stand,k}} \quad \text{(C.3)}$$

B.1.3 Calibration Curve uncertainty

The determination of the uncertainty due to the use of the calibration curve fitted to the standards was carried out using the equation by Ellison and Williams (2012). It is presented below:

$$u(C_{\text{calib}}) = \frac{S}{B_1}\sqrt{\frac{1}{p} + \frac{1}{n} + \frac{(C_{\text{sample}} - \bar{C})^2}{\sum_1^n (C_l - \bar{C})^2}} \quad \text{(C.4)}$$

Use in the case of curve fitting by least squares linear regression S represents the standard deviation, B_1 represents the slope of the calibration curve, p represents the number of replicated measurements used to determine C_{sample}, and n representing the number of samples used to determine the point. In the case of a single measurement being used (ie. n=1) equation 5.4 is then reduced to the following form:

$$u(C_{calib}) = \frac{S}{B_1}\sqrt{\frac{1}{p} + 2} \tag{C.5}$$

B.1.4 Repeatability Uncertainty

When the mean of multiple measurements made under the same physical and chemical conditions is reported, there exists uncertainty emanating from this repetition. This is termed a type B uncertainty. This uncertainty can be evaluated from the relative standard deviation of the measured data and is described in the equation presented below:

$$u(C_{repeat}) = \frac{a}{\sqrt{3 \cdot n}} \tag{C.6}$$

In equation B.6 a is defined as the range of the data.

Once the uncertainties as described by equations C.1 - C.6 are collated by the law of propagation of uncertainties a coverage factor of k = 2 (for a 95% confidence interval) was applied to estimate the combined expanded uncertainties.

C.2 Acid Concentration Uncertainty

The uncertainty in the concentration of the H^+ ion was also estimated using the GUM standards. The components contributing to the overall uncertainty are displayed in figure C.2 (Ishakawa diagram) below:

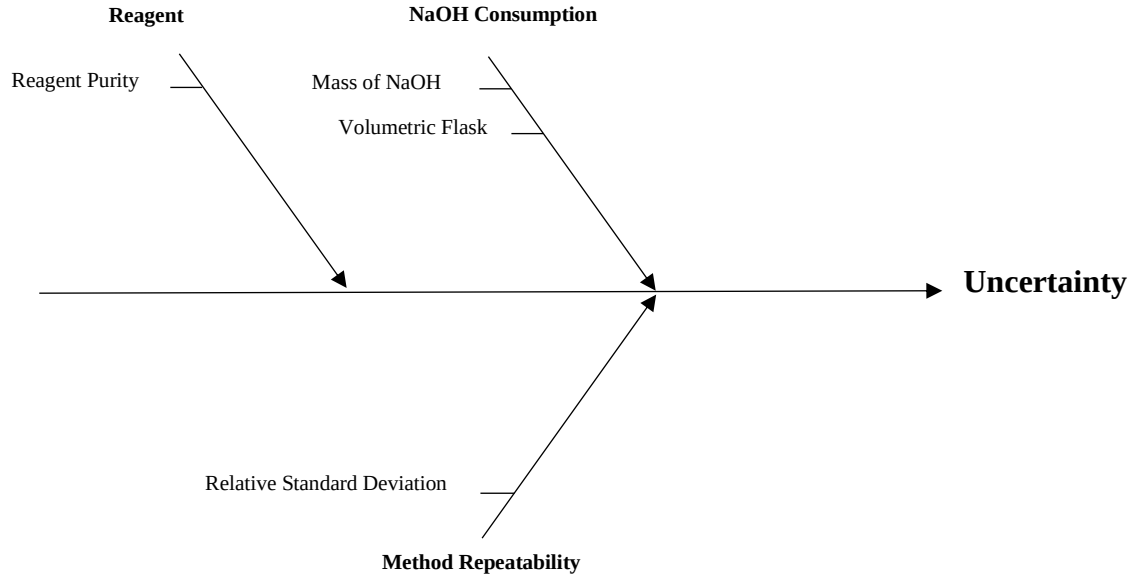

Figure C. 2 Ishikawa diagram for the evaluation of [H^+] data uncertainties

B.2.1 Repeatability Uncertainty

As mentioned in Section 4.4 and 5.1 repetition of measurements introduce uncertainty which was accounted for in the concentration of the H^+ ion by the following equation:

$$u\left(H^+_{repeat}\right) = \frac{a}{\sqrt{3 \cdot n}} \qquad (C.7)$$

a, represents the range of [H^+] and n represents the number of titrations.

B.2.2 Purities Uncertainty

The contribution of the purities of the reagents to the overall uncertainty can be classified as a Type B uncertainty.

B.2.3 Solution Concentration Uncertainty

The uncertainty in the concentration of the NaOH solution can be calculated using the following equation:

$$u(C_{soln}) = \sqrt{\left(\frac{u(m_{bal})}{m_{NaOH}}\right)^2 + \left(\frac{u(V_{flask})}{V_{soln}}\right)^2} \cdot C_{soln} \quad \text{(C.8)}$$

B.2.3 NaOH consumption Uncertainty

Rösslein (2014) described a procedure for the evaluation of the uncertainty for the consumption of NaOH in an equivalence point, $V_{eq,T}$, titration. This uncertainty is an amalgamation of uncertainties emanating from the calibration of the burette and the temperature at which the titration is carried out. The uncertainty contribution from the calibration of the burette can be described as a triangular distribution and can be evaluated by the quotient of the limit of the burette to $\sqrt{6}$. The temperature uncertainty contribution is reliant on the coefficient of thermal expansion of the solution and can be evaluated from equation C.9 below.

$$u\left(C_{V_{eq,T}}\right) = \frac{Vb_{soln}(|20°C - T_{soln}|)}{\sqrt{3}} \quad \text{(C.9)}$$

Using the law of propagation of uncertainty, the combined $[H^+]$ uncertainty can be calculated using equation B.10 below.

$$u([H^+]) = \sqrt{u\left([H^+]_{repeat}\right)^2 + u(C_{soln})^2 + u\left(C_{V_{eq,T}}\right)^2} \quad \text{(C.10)}$$